
Effects of HT-ATES on the subsurface - the NIOO case study

An evaluation of the effects of a HT-ATES system (45 °C) on the subsurface

Prepared by: Peter Oerlemans, NIOO-KNAW, IF Technology
Benno Drijver, IF Technology

Checked by: Petra van den Berg, NIOO-KNAW

Approved by: Holger Cremer, TNO, HEATSTORE coordinator

Please cite this report as: Oerlemans, P.J.A. & Drijver, B. 2021: Effects of HT-ATES on the subsurface - the NIOO case study, GEO THERMICA – ERA NET Cofund Geothermal. 78 pp.

This report is published as part of HEATSTORE project deliverable number D5.2

TNO innovation
for life



storengy



KWR



u^b



HEATSTORE (170153-4401) is one of nine projects under the GEO THERMICA – ERA NET Cofund aimed at accelerating the uptake of geothermal energy by 1) advancing and integrating different types of underground thermal energy storage (UTES) in the energy system, 2) providing a means to maximise geothermal heat production and optimise the business case of geothermal heat production doublets, 3) addressing technical, economic, environmental, regulatory and policy aspects that are necessary to support efficient and cost-effective deployment of UTES technologies in Europe.

This project has been subsidized through the ERANET cofund GEO THERMICA (Project n. 731117), from the European Commission, RVO (the Netherlands), DETEC (Switzerland), FZJ-PtJ (Germany), ADEME (France), EUDP (Denmark), Rannis (Iceland), VEA (Belgium), FRCT (Portugal), and MINECO (Spain).



About HEATSTORE

High Temperature Underground Thermal Energy Storage

The heating and cooling sector is vitally important for the transition to a low-carbon and sustainable energy system. Heating and cooling is responsible for half of all consumed final energy in Europe. The vast majority – 85% - of the demand is fulfilled by fossil fuels, most notably natural gas. Low carbon heat sources (e.g. geothermal, biomass, solar and waste-heat) need to be deployed and heat storage plays a pivotal role in this development. Storage provides the flexibility to manage the variations in supply and demand of heat at different scales, but especially the seasonal dips and peaks in heat demand. Underground Thermal Energy Storage (UTES) technologies need to be further developed and need to become an integral component in the future energy system infrastructure to meet variations in both the availability and demand of energy.

The main objectives of the HEATSTORE project are to lower the cost, reduce risks, improve the performance of high temperature (~25°C to ~90°C) underground thermal energy storage (HT-UTES) technologies and to optimize heat network demand side management (DSM). This is primarily achieved by 6 new demonstration pilots and 8 case studies of existing systems with distinct configurations of heat sources, heat storage and heat utilization. This will advance the commercial viability of HT-UTES technologies and, through an optimized balance between supply, transport, storage and demand, enable that geothermal energy production can reach its maximum deployment potential in the European energy transition.

Furthermore, HEATSTORE also learns from existing UTES facilities and geothermal pilot sites from which the design, operating and monitoring information will be made available to the project by consortium partners.

HEATSTORE is one of nine projects under the GEO THERMICA – ERA NET Cofund and has the objective of accelerating the uptake of geothermal energy by 1) advancing and integrating different types of underground thermal energy storage (UTES) in the energy system, 2) providing a means to maximize geothermal heat production and optimize the business case of geothermal heat production doublets, 3) addressing technical, economic, environmental, regulatory and policy aspects that are necessary to support efficient and cost-effective deployment of UTES technologies in Europe. The three-year project will stimulate a fast-track market uptake in Europe, promoting development from demonstration phase to commercial deployment within 2 to 5 years, and provide an outlook for utilization potential towards 2030 and 2050.

The 23 contributing partners from 9 countries in HEATSTORE have complementary expertise and roles. The consortium is composed of a mix of scientific research institutes and private companies. The industrial participation is considered a very strong and relevant advantage which is instrumental for success. The combination of leading European research institutes together with small, medium and large industrial enterprises, will ensure that the tested technologies can be brought to market and valorised by the relevant stakeholders.

Document Change Record

This section shows the historical versions, with a short description of the updates.

Version	Short description of change
2020.12.21	First draft
2021.08.12	Second draft
2021.09.03	Final draft
2021.10.08	Final version
2021.10.25	Final edited version

Table of Content

About HEATSTORE	3
1 Introduction.....	7
1.1 NIOO: The Netherlands Institute of Ecology.....	7
1.2 Geothermica HEATSTORE	7
1.3 Problem statement.....	7
1.4 Reading guide.....	8
2 Legal framework for the NIOO HT-ATES	9
2.1 The ambition for sustainable heating.....	9
2.2 Licensing conditions: The Water Law	9
2.3 Estimated subsurface properties at NIOO in 2009	10
2.4 The NIOO HT-ATES permit	11
3 NIOO HT-ATES system: well locations and monitoring setup.....	12
4 Monitoring activities at NIOO	15
4.1 Monitoring program.....	15
4.1.1 Flow parameters	15
4.1.2 Temperature	15
4.1.3 Groundwater composition.....	15
4.2 Monitoring procedures	16
4.3 Additional monitoring activities.....	17
4.4 Monitoring results.....	17
5 Hydrogeological setting.....	18
5.1 Sources of information	18
5.2 Lithology.....	18
5.3 Flow properties.....	21
5.4 Regional groundwater flow regime	22
6 Hydrothermal evaluation.....	25
6.1 Results and Discussion.....	25
6.1.1 Temperatures at well screen depth	25
6.1.2 Temperatures above storage depth.....	25
6.2 Conclusions.....	30
7 Chemical evaluation of the groundwater composition	32
7.1 Chloride concentrations	32
7.1.1 Reference measurements	32
7.1.2 Regular chloride measurement results 2010 - 2020.....	32
7.2 Other chemical parameters.....	38
7.2.1 Mixing.....	38
7.2.2 Mineral equilibria: calcite precipitation and silicate dissolution.....	39
7.2.3 Organic carbon mobilization	41
7.2.4 Arsenic mobilization	42
8 Microbiology	44
8.1 Regular measurements.....	44
8.2 Additional microbial analysis in 2019	44
8.2.1 Background: ATP and DNA-analysis.....	45
8.2.2 Methods: NGS, qPCR and ATP measurements at NIOO	45
8.2.3 Results.....	46
8.2.4 Discussion.....	47
8.3 Additional microbial analysis in 2021	48
8.3.1 Methods	48
8.3.2 Results	49
8.3.3 Discussion.....	50
9 Modelling heat and solute transport.....	53
9.1 Introduction	53
9.2 Methods	53
9.2.1 HST3D Software.....	53
9.2.2 Model input parameters	53

9.3	Results and discussion	54
9.3.1	Chloride concentrations	54
9.3.2	Temperature distribution	56
10	Conclusions and recommendations	59
10.1	Conclusions	59
10.2	Recommendations	63
11	References	65
12	Appendix	66

1 Introduction

1.1 NIOO: The Netherlands Institute of Ecology

The Netherlands Institute of Ecology (NIOO) is a scientific research institute within the Royal Netherlands Academy of Arts & Sciences (KNAW). NIOO's mission is to carry out ground-breaking fundamental and strategic ecological research in terrestrial and aquatic ecosystems, and make its ecological knowledge available to science and society. In 2011, NIOO moved to a new building near the Wageningen University & Research campus. The features of the NIOO building and facilities find root in the 'Cradle to Cradle' philosophy that holds the ambition to close as many different cycles (energy, water, nutrients) as possible. In this ambition, NIOO has developed into an institute where unconventional applications have been realized and monitored to demonstrate the potential of innovation in creating a more sustainable planet. It has realized several systems that contribute to closing the energy cycle (heating and cooling of the building). First of all, NIOO invested in a state of the art building climate control system that enables heat and cold to be continuously exchanged between the different facilities to minimize the overall heat or cold demand. Also, an ATES systems is used for storage of low temperature heat and cold, to exploit the seasonal variation in availability and demand for heat and cold. Additionally, NIOO integrated a HT-ATES system into the heating system, enabling solar heat to be stored in groundwater (at max. 45 °C) during summer, for direct use (i.e. without a heat pump) in winter. The temperatures and groundwater composition in and around this system have been intensively monitored for the last ten years, offering a unique opportunity to evaluate the effects of HT-ATES on the subsurface.

1.2 Geothermica HEATSTORE

HEATSTORE is an international research program that focusses on the development and integration of thermal energy storage techniques into the future energy system infrastructure, in order to balance variations in the availability and demand of energy. The objective of the consortium of 24 partners from 9 European countries is to improve the performance, reduce the risk and lower the cost of High Temperature (25 °C – 90 °C) Underground Thermal Energy Storage (HT-UTES) techniques, of which Thermal Energy Storage in abandoned Mines (MTES), in Pits (PTES) and in Aquifers (ATES) are examples. This is achieved by 6 new demonstration projects and the evaluation of 8 existing systems with distinct configurations. HEATSTORE contributes to the GEO THERMICA program objective of accelerating the uptake of geothermal energy by advancing storage techniques, improving geothermal doublet business cases and addressing technical, economic, environmental, regulatory and policy aspects involved in HT-UTES. Having the longest running monitoring program (10 years), NIOO is a valuable partner of the consortium, serving as one of the HT-ATES case studies. Contributing to Work Package 5 of HEATSTORE, this report describes the NIOO HT-ATES system and evaluates the data acquired in order to contribute to a further understanding of the effects and impact of HT-ATES on the subsurface. The lessons learned during the course of the NIOO evaluation provided valuable insights that were directly utilized for the permitting procedure, monitoring setup and monitoring plan of the Dutch HT-ATES demonstration project within HEATSTORE at ECW in Middenmeer, which has been developed between 2018 and 2021.

1.3 Problem statement

Although the Dutch law provides a legal framework for the permission and realization of HT-ATES systems, the permitting procedures are often of long duration, complex and with no certainty of the outcome. This is related to the uncertainties on the scale and impact of HT-ATES systems on groundwater quality. Increasing temperatures influence (the rate of) (bio)chemical processes in the subsurface, which in turn may change groundwater composition. But, since the original groundwater and geochemical composition of the subsurface is often uncertain, it remains challenging to quantitatively assess the effects on groundwater composition, which contributes to the complexity of the permitting procedure. These complexities in turn generate risks for investors and users, which then hinders the large-scale implementation of HT-ATES in the Netherlands. Therefore, to promote HT-ATES and to benefit from its CO₂ emission reduction potential, it is important to obtain more insight in the thermal, chemical and microbiological effects of HT-ATES on the surrounding subsurface.

This study offers an evaluation of the NIOO HT-ATES pilot project that started in 2010 and is still in operation. The 10-year series of thermal, geochemical and microbiological data provide the opportunity to evaluate the processes that occur and to compare the results from the field with findings from literature and

laboratory experiments. The aim of this report is to provide a better understanding of the processes and risks of the NIOO HT-ATES system, which then contributes to improved insights in HT-ATES effects on the subsurface in general.

1.4 Reading guide

Chapter 2 covers the current legal framework for HT-ATES systems. The well locations and monitoring setup are shown in chapter 3, followed by a description of the monitoring activities that were performed over the last decade in chapter 4. The hydrogeological setting around the HT-ATES system is reported in chapter 5, followed by an evaluation of the thermal effects in chapter 6, the chemical effects in chapter 7 and the microbial effects in chapter 8. The 9th chapter comprises a numerical model study in which the 3D distribution of heat and chloride resulting from the HT-ATES operation is visualized and compared to the field measurements. The report ends with the conclusions and recommendations that follow from this HT-ATES case study in chapter 10.

2 Legal framework for the NIOO HT-ATES

2.1 The ambition for sustainable heating

With the HT-ATES system, NIOO has combined the ambition to close the energy cycle with a field scale experiment to develop the understanding of the impact of this technology on the subsurface. In summer, solar collectors create surplus heat which is supplied to the groundwater by a heat exchanger and subsequently stored in the HT-ATES system at a maximum temperature of 45 °C. Additionally, surplus high temperature heat from the NIOO research facilities (offices, laboratories, greenhouses) is stored in the HT-ATES. During winter, part of the heat is recovered from the storage and directly transferred to the local heating network which connect the NIOO facilities, without the use of a heat pump (resulting in highly energy efficient heating). The cooled water is reinjected in the 'cold' well of the HT-ATES system, with an injection temperature of about 26 °C. The storage and subsequent recovery of solar and surplus heat results in a significant reduction of fossil energy consumption in the heating system of the building, hence in a reduction of the CO₂-emission.

In the shallow part of the Dutch subsurface (0 – 500 meters below ground surface, mbgs), natural groundwater temperatures in the Netherlands generally range between 10 and 20 °C. This means that the storage of heat at 45 °C will cause local heating of the subsurface.

2.2 Licensing conditions: The Water Law

In the Netherlands, according to the 'Water Law' (Dutch: Waterwet), the Provinces are the governmental bodies that hold authority to issue permits on ATES systems up to 500 mbgs. The law and its subordinate regulations state that the injection of high temperature water (>25 °C) and the net addition of heat to the subsurface can only be permitted under the condition that this is not in conflict with the interest of the protection of the subsurface, and that it contributes to an effective application of ATES. In practice this means that the province assesses the effects and may issue a permit for HT-ATES when no other interests are negatively affected. The NIOO HT-ATES system was permitted by the Province of Gelderland by assigning the project a 'pilot' status, and under the condition that extensive temperature and groundwater monitoring was performed during the course of operation to track the temperature and groundwater compositional changes around the system.

2.3 Estimated subsurface properties at NIOO in 2009

During the permitting procedure in 2009, there was little field data of the subsurface at the NIOO site. A scheme of the lithology as expected in 2009 is shown in Figure 2-1 (IF Technology, 2009a).

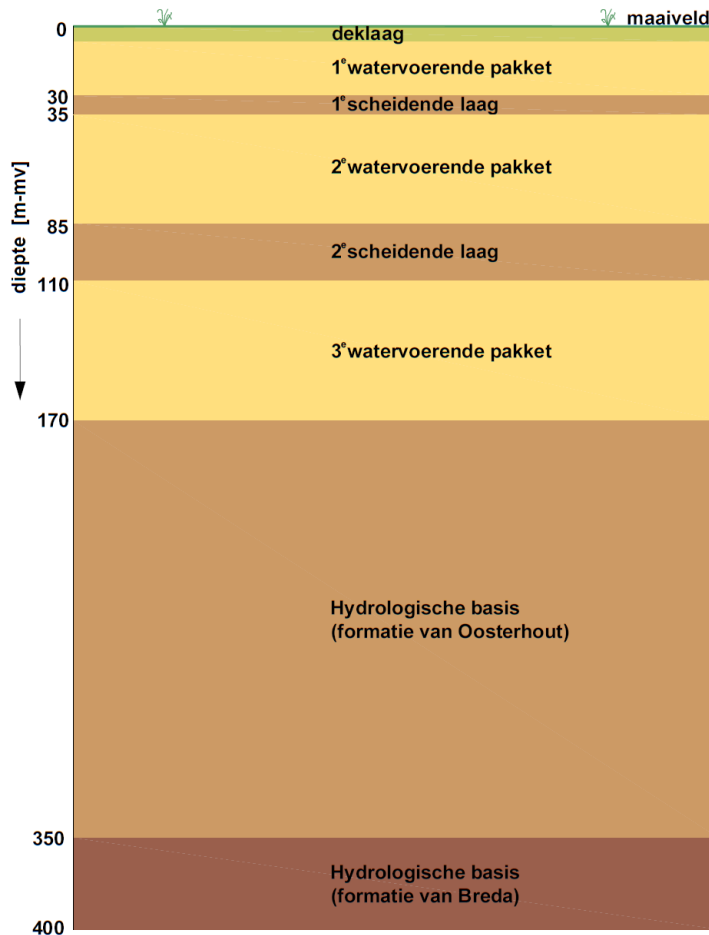


Figure 2-1 | Expected lithology at NIOO based on the data available in 2009. Yellowish layers represent aquifers and light brown/dark brown layers represent layers that have low hydraulic conductivities.

The 3rd aquifer (110 – 170 mbgs, '3^e watervoerende pakket' in Figure 2-1) holds high quality fresh groundwater from which drinking water is produced (about 7.5km downstream of NIOO). Large scale degradation of the groundwater quality of this aquifer is not acceptable. The fresh-brackish water interface (> 150 mg Cl/L) water was expected to be located around 200 mbgs. In 2009 it was known that buoyancy flow had a considerable negative impact on the thermal recovery efficiency. It was hence preferable to store the heat in a layer with low vertical hydraulic conductivity to limit buoyancy flow effects. Therefore, it was advised to place the well screens in the fine sands of the Oosterhout Formation (upper 'Hydrologische Basis' in Figure 2.1), with well screens between 220 – 295 mbgs.

2.4 The NIOO HT-ATES permit

The operational limits for which the permit of the HT-ATES system was granted are shown in Table 2-1 (Provincie Gelderland, 2010).

Table 2-1 | Operational limits for the HT-ATES system

Parameter	Unit	Summer heat storage	Winter heat recovery	Yearly total
Flow rate	m ³ /h	60	60	-
Average pumped volume per season	m ³	70.000	45.000	115.000
Maximum pumped volume per season	m ³	105.000	105.000	210.000
Maximum infiltration temperature	°C	45	26	-
Average pumped energy per year	MWht/yr	1.283	578	705

The main concern about the HT-ATES application was its potential effect on the groundwater quality of the 3rd aquifer, either by displacement of brackish water towards this aquifer or by the temperature-related effects on it. The storage of heat in the hydrological base was permitted under the condition that extra monitoring activities were carried out on a regular basis. The obtained field data was meant to provide insight in the effects of the HT-ATES system and to allow for the assessment of risks and intervention options when negative effects on other interests would become unacceptable. Additionally, such a monitoring program was meant to provide insights and new experience in HT-ATES related effects on groundwater composition. Based on these considerations, a monitoring well system configuration was set up and included in the permit.

3 NIOO HT-ATES system: well locations and monitoring setup

As can be seen from Figure 3-1 both a ‘regular’ ATES system (injection temperatures < 25 °C) and a High Temperature ATES system (temperatures > 25 °C) were realized at NIOO:

- The ATES system has well screens in the 2nd aquifer at 54 – 83 mbgs
- The HT-ATES system has well screens in the hydrological base at 220 – 295 mbgs.

Both systems have been in continuous operation since 2010.

This research focusses on the HT-ATES system and the monitoring well. These wells were drilled in June – July 2010. No test drilling was performed for the HT-ATES system because of financial considerations.

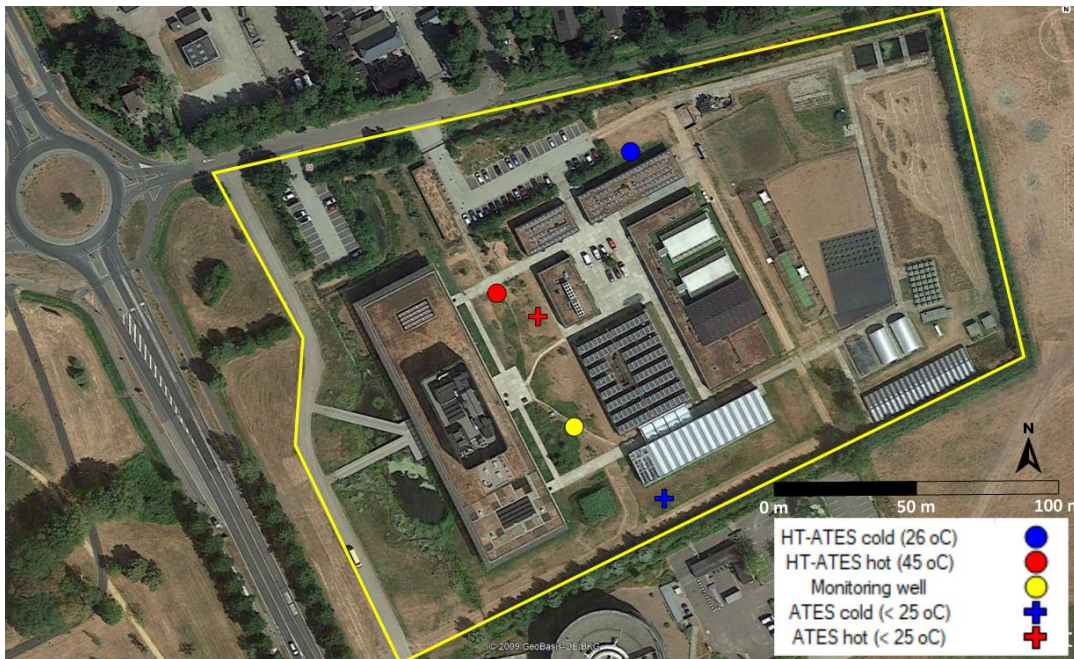


Figure 3-1 | A bird’s-eye view of the NIOO terrain with the hot, cold and monitoring well of the HT-ATES system shown as a red, blue and yellow dot respectively. The locations of the regular ATES wells (< 25 °C) are indicated with crosses.

The HT-ATES system comprises a hot well and a ‘cold’ well, that were placed ~70m apart. Note that the well of a HT-ATES doublet system with the lowest injection temperature is typically referred to as the ‘cold’ well, even though the storage temperature is relatively high compared to the natural groundwater temperature and the temperature of the regular ATES systems. At approximately 56 m south of the hot HT-ATES well, there is a third well location, referred to as the ‘monitoring well’ (see Figure 2.2) to monitor thermal and groundwater composition effects. No water can be injected or extracted through the monitoring well (except for sampling of the groundwater), as it is simply a group of four piezometers, each with 2m-long well screens at different depths. The specifications of the three wells are shown in Table 3-1.

Table 3-1 | Well configuration of the HT-ATES doublet.

Well type	Well code	Well location in RD-coordinates (m)	Maximum injection temperature [°C]	Depth interval of well screen [mbgs]	Screen length [m]
Hot well	W	X: 174.533 Y: 444.365	45	220 – 283	63
Cold well	K	X: 174.581 Y: 444.416	26	220 - 295	75
Monitoring well	MP	X: 174.560 Y: 444.316	-	-	-

Piezometers were installed in the boreholes of the hot and cold wells too, at similar depths as the piezometers of the monitoring well. This is in accordance with the targeted monitoring locations as assigned in the permit. A top view of the well and the piezometers adjacent to it is shown in Figure 3-2.



Figure 3-2 | Top view of the hot well of the HT-ATES system, accompanied by four smaller piezometers (blue), which all reach to different depths.

Each piezometer is a small tube (diameter 40 - 63 mm) that is installed in a borehole, with perforations at the bottom of the tube through which groundwater can enter. With this setup, temperature and groundwater composition can be monitored at four different depths for three locations. The depths of the perforations of the piezometers are specified in Table 3-2.

Table 3-2 | Specifications of the piezometers installed at the hot well (prefix 'W'), cold well (prefix 'K') and monitoring well (prefix 'MP'). F1 to F4 refer to the piezometer screen numbers, with higher numbers referring to deeper piezometers.

Piezometer code	Perforation depth (mbgs)	Piezometer code	Perforation depth (mbgs)	Piezometer code	Perforation depth (mbgs)
W-F1	170-172	K-F1	170-172	MP-F1	170-172
W-F2	193-195	K-F2	193-195	MP-F2	193-195
W-F3	220-222	K-F3	220-222	MP-F3	220-222
W-F4	280-282	K-F4	293-295	MP-F4	285-287

Figure 3-3 shows a schematization of the well and piezometer configuration lithology, projected on the lithology as expected in 2009. This setup allows for monitoring of the effects of the heat storage and possible propagation towards the overlying 3rd aquifer.

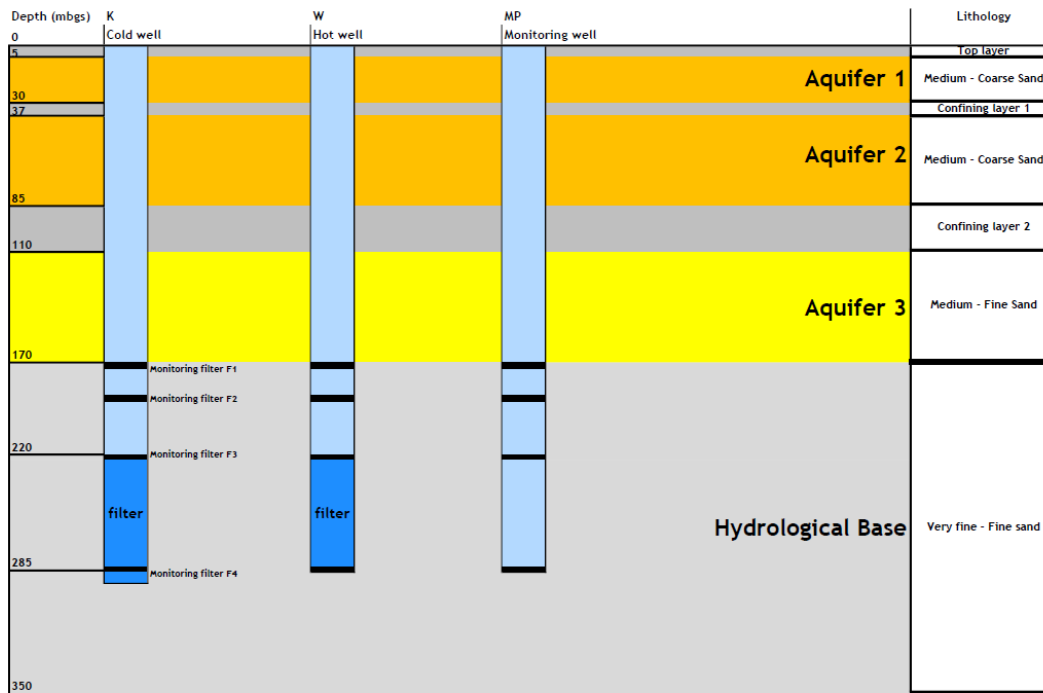


Figure 3-3 | Schematized cross-section of the expected lithology in 2009 and the well configurations of the NIOO HT-ATES system. Well screens of the doublet are indicated in dark blue. The piezometer screens are located between the well screens and the bottom of aquifer 3, to track if HT-ATES induced effects propagate upwards to the 3rd aquifer. Note that no distinct confining layer overlies the heat storage depth interval.

4 Monitoring activities at NIOO

4.1 Monitoring program

The HT-ATES permit of 2009 prescribes the monitoring activities that have to be carried out at the HT-ATES system (hot, cold HT-ATES well and monitoring well). The monitoring parameters as well as the frequency of monitoring are described here.

4.1.1 Flow parameters

The volumes and temperatures of the produced and injected groundwater, along with the well pressures, have been registered since the start of operation with a frequency of 8 minutes. With these parameters, the energy that is infiltrated and produced by the HT-ATES system can be calculated. The pressure monitoring of the well system allows for evaluation of the well performance.

4.1.2 Temperature

In accordance with the permit, temperature profiles with 5 m interval were obtained at the hot, cold and monitoring wells, at the following moments:

- before the HT-ATES system becomes operational (reference measurement)
- at the end of each summer
- at the end of each winter

4.1.3 Groundwater composition

Reference measurements

The permit of 2009 prescribes that a reference measurement had to be performed by sampling all the piezometers, before the system became operational. The samples were analyzed for all parameters in Table 4-1.

Regular measurements

In accordance with the permit of 2009, regular measurements were performed on the groundwater composition.

At the end of each summer and at the end of each winter, groundwater samples were acquired from piezometers W-F2, W-F3, W-F4, K-F2, K-F3 and K-F4 for chloride concentration analysis.

Additionally, at the end of summer, groundwater samples were obtained from W-F3. At the end of winter, samples are taken from K-F3. Note that the F3 piezometer screens are located at the same depth as the top of the well screens of the warm and cold wells. These samples were analyzed on an extensive set of chemical and microbiological parameters (as can be seen in the left hand side column of Table 4-1), to investigate the temperature effects on the groundwater composition near the well screens.

In 2021, an updated permit was granted by the province, allowing for a less extensive set of monitoring parameters to be measured from 2021 onwards (Provincie Gelderland, 2021). This adjustment of the monitoring requirements was based on an analysis of the monitoring results of the previous years and the additional measurements performed within the HEATSTORE framework.

Table 4-1 | The parameters that are analyzed on a regular basis are shown on the left side ('Regular analyses'). For the reference analyses an extra set of chemical parameters was analyzed on top of the 'Regular analyses' parameters. These additional chemical species are shown on the right hand side of the table ('Additional reference analyses'). cfu = 'colony forming units'.

Regular analyses				Additional reference analyses			
Parameter name	symbol	Parameter type	Unit	Parameter name	symbol	Parameter type	Unit
Electroconductivity	EC	Field	µS/cm	Arsenic	As	Chemical	mg/l
pH	pH	Field	pH	Bicarbonate	HCO ₃ ⁻	Chemical	µg/l
Oxygen	O ₂	Field	mg/l	Nickel	Ni	Chemical	µg/l
Chloride	Cl	Chemical	mg/l	Zink	Zn	Chemical	µg/l
Calcium	Ca	Chemical	µg/l	Aluminum	Al	Chemical	µg/l
Dissolved Organic Carbon	DOC	Chemical	mg/l	Ammonium	NH ₄ ⁺	Chemical	mgN/l
Boron	B	Chemical	µg/l	Assimilable Organic Carbon	AOC	Chemical	µg/l
Bromide	Br	Chemical	mg/l	Cadmium	Cd	Chemical	µg/l
Iron	Fe	Chemical	µg/l	Chromium	Cr	Chemical	µg/l
Iodide	I	Chemical	mg/l	Potassium	K	Chemical	µg/l
Magnesium	Mg	Chemical	µg/l	Copper	Cu	Chemical	µg/l
Manganese	Mn	Chemical	µg/l	Quicksilver	Hg	Chemical	µg/l
Methane	CH ₄	Chemical	µg/l	Lead	Pb	Chemical	µg/l
Sodium	Na	Chemical	mg/l	Nitrate	NO ₃ ⁻	Chemical	mg/l
Ortho-Phosphate	PO ₄ ³⁻	Chemical	mgP/l	Nitrite	NO ₂ ⁻	Chemical	mg/l
Silicon	Si	Chemical	µg/l	Color measurement		General	mg Pt / l
Sulphate	SO ₄ ²⁻	Chemical	mg/l				
Sulfide	S ²⁻	Chemical	mg/l				
Tin	Sn	Chemical	µg/l				
Aeromonas		Microbiological	cfu/100ml				
Coliforms 37 °C		Microbiological	cfu/100ml				
Escherichia coli 44 °C		Microbiological	cfu/100ml				
Enterococcus		Microbiological	cfu/100ml				
Bacterial count 22 °C		Microbiological	cfu/ml				
Bacterial count 25 °C		Microbiological	cfu/ml				
Bacterial count 37 °C		Microbiological	cfu/ml				
Sulphite-Reducing Clostridia		Microbiological	cfu/100ml				

4.2 Monitoring procedures

Temperature

The temperature in the borehole of the hot, cold and monitoring well was measured by descending a temperature probe into the deepest piezometer (W-F4, K-F4 and MP-F4 respectively), resulting in a 5 m interval temperature profile for that well. Within the probe, the electrical resistance of a piece of metal is measured at different depths and from this data, temperature can be calculated.

From spring 2014 onwards, temperature registration in the hot well shifted to W-F3 instead of W-F4, because the probe got stuck in W-F4. No further investigation has been performed on the cause of this, but one can hypothesize that the relatively high temperatures near the hot well (up to 45 °C) may have played a role. The piezometer is made of PVC which is sensitive to plastic deformation at temperatures of about 45 °C and higher.

Sampling of groundwater

Groundwater samples were taken by extracting groundwater from the piezometers. The piezometers (approximately Ø63 mm) were pumped until at least three times their well volume was discharged. Using this protocol, a representative sample was taken of the groundwater from the depth of the piezometer screen. The samples were analyzed by a certified laboratory. Samples taken for microbiological analysis were cooled during transport and analyzed within 24 hours after sampling.

4.3 Additional monitoring activities

In addition to the monitoring activities prescribed in the permit, measurements were performed on additional parameters within the HEATSTORE program:

In November – December 2018:

- Concentrations of nickel and zinc at W-F3 and K-F3
- All parameters in Table 4-1, with the exception of EC, O₂(g), iodide, *Aeromonas*, Coliforms, *Enterococcus* and *E.Coli* were measured at MP-F2, MP-F3, MP-F4, W-F2 and K-F3.
- Temperature logs in the hot, cold and monitoring wells.

May 2019 and November 2020:

- Arsenic concentrations at F2, F3 and F4 of the hot and cold well.

4.4 Monitoring results

Data on the heat injection and recovery is obtained by the high-frequency registration of the building climate control system (well flow rates, injection/production temperatures and pressures in the wells). The monthly injected water volumes into the hot and cold wells are shown in Figure 4-1 with the corresponding injection temperatures.

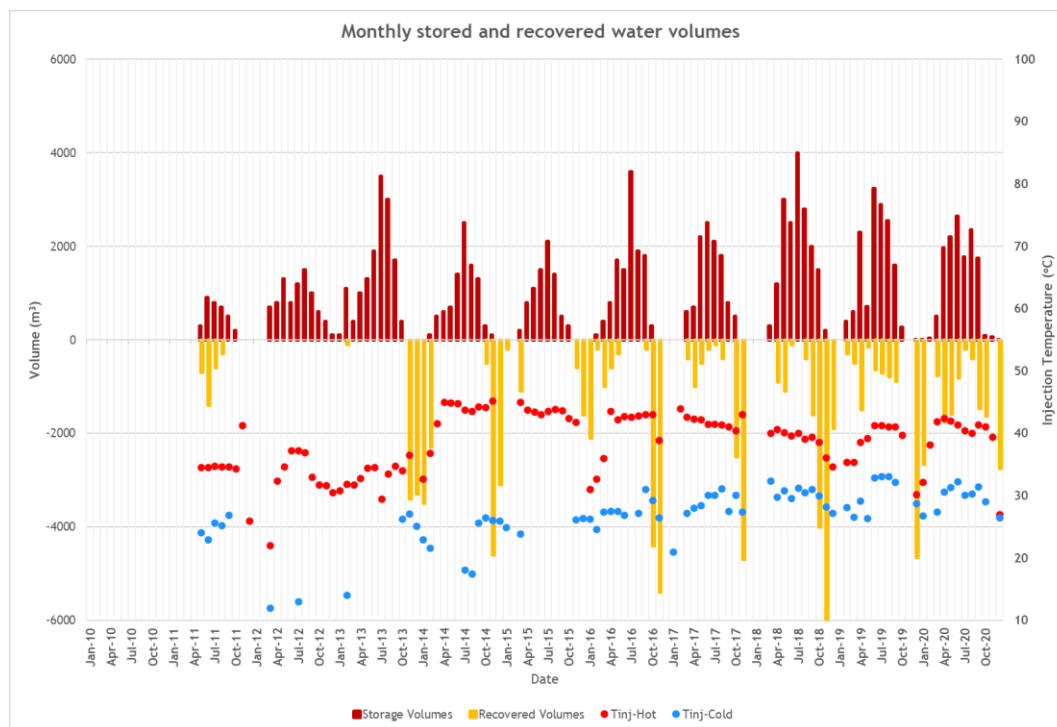


Figure 4-1. Stored (red) and recovered (yellow) water volumes at the hot well. Note that during storage of heat, water is produced from the cold well and injected in the hot well. During recovery of heat, the water flows in opposite direction.

The monitoring efforts in the field have resulted in a unique data series on temperature and the hydrochemical/microbiological effects on the subsurface. This data is presented and discussed in the chapters below.

5 Hydrogeological setting

This section describes the hydrogeological setting at NIOO. This includes the lithology, hydrogeological properties of the subsurface layers and the regional groundwater flow regime in various aquifers. This setting offers the subsurface framework from which the thermal, chemical and microbiological changes can be explained.

5.1 Sources of information

The hydrogeological setting as reported in this section is based on the following sources of information:

- Borehole logs of the hot, cold and monitoring well (drilled in June – July 2010)
- Well production tests of the ATES and HT-ATES wells
- Report of IF Technology on the flowmeter log (or: flowmeter measurement) along the well screens of the HT-ATES system performed at 20 September 2010, and the grainsize distribution analysis by Fugro of 2012 (reference 26.940/57517/PM, (IF Technology, 2012)).
- Memo of IF Technology on the well stimulation (October 18, 2010, reference 22.857/57517/RH, (IF Technology, 2010))
- Reference report on the NIOO HT-ATES system (June 28th, 2011, reference 24.714/57517/MH, (IF Technology, 2011)).
- Monitoring reports of IF Technology on the NIOO HT-ATES measurements (2012 – 2020):
 - 2012 (IF Technology, 2013)
 - 2013 (IF Technology, 2014)
 - 2014 (IF Technology, 2015)
 - 2015 (IF Technology, 2016)
 - 2016 (IF Technology, 2017)
 - 2017 (IF Technology, 2018)
 - 2018 (IF Technology, 2019)
 - 2019 (IF Technology, 2020)
 - 2020 (IF Technology, 2021)
- REGIS II database for hydraulic head contour lines in aquifer 1, 2 and 3 (TNO, 2020).

Table 5-1 shows the information that can be derived from these information sources

Table 5-1 | References for the hydrogeological setting at NIOO

Source	Provides information on
Borehole logs (cold, hot, monitoring well)	Lithology, grainsizes, geological formation boundaries
Well production tests of the hot and cold wells of both the HT-ATES and the ATES systems	Transmissivity and hydraulic conductivity along well screen, well performance
Flow log	Flow distribution along well screens, well performance
Analysis of the grainsize distribution along the filters of the HT-ATES wells	Flow distribution along well screens, sand production risk, geological formation boundary identification
REGIS II database	Hydraulic head contour line distribution

The hydrogeological setting as interpreted from these data sources is described below.

5.2 Lithology

The lithology at the NIOO site, as derived from the borehole logs of the hot (BAM, 2010b), cold (BAM, 2010a) and monitoring wells (GEBO, 2010), is shown in Figure 5-1.

The boreholes of the hot and cold wells were drilled by reverse-rotary drilling, whereas the monitoring well was drilled using the rotary drilling technique. It is assumed that lithology can be more accurately described by using the reverse-rotary drilling technique, which is why the lithology at NIOO is mainly interpreted from the hot and cold well borehole logs. In Figure 5-1, the lithology at the HT-ATES system of NIOO is

presented. The depth ranges and the information in the 'Geology' columns are derived from the borehole logs. The 'Hydrological unit' names assigned to the layers found at NIOO are in line with the classification of aquifers and aquitards found in the region. The 'flow properties' are derived from various sources (see section 5.3).

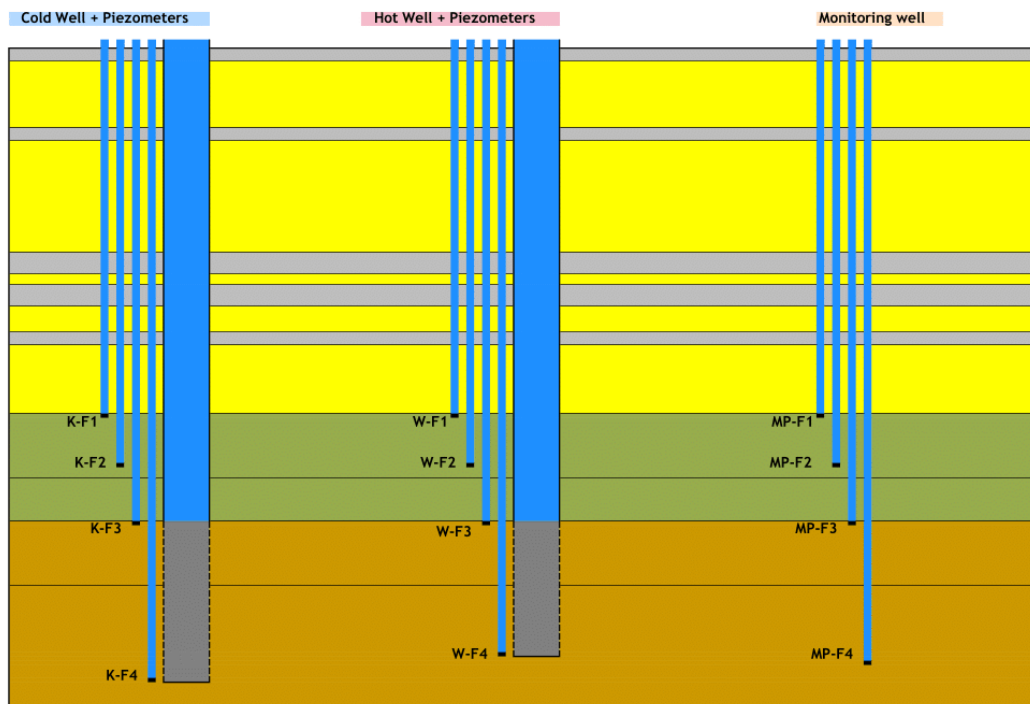
The lithology found at NIOO up to 170 mbgs is similar to the expected lithology at 2009 (see Figure 2-1). The first aquifer consists of glacial deposits of the Drenthe Formation. The second aquifer contains relatively coarse sands deposited in a fluvial environment and is classified as the Peize/Waalre Formation. The bottom part of the 2nd aquitard and the 3rd aquifer are part of the marine Maassluis Formation, which contains shell material. Little information on the deeper regions was available in 2009, except that it consisted of relatively fine grained sediments from the Oosterhout and Breda Formations, which is why the subsurface below 170 mbgs was classified as 'hydrological base'. The Hydrological base is a term used in the Netherlands for the layers with relatively low hydraulic conductivity that make up the lower limit of the shallower hydrogeological system, where the bulk of groundwater transportation occurs. Heat storage at NIOO was planned in the hydrological base to limit heat losses caused by buoyancy-driven upward flow. The borehole logs of the wells have shown the properties of this hydrological base in greater detail, showing that grainsizes decrease from fine sand at 170 mbgs to very fine sand and silt at 307 mbgs.

Maassluis and Oosterhout Formation boundary

In the DINOLoket Nomenclator (TNO, 2013), the character of the boundary between the Maassluis and Oosterhout formation is described as either sharp (involving a dark grey to brown clay layer) or gradual. In case of a gradual boundary, the transition to Oosterhout is characterized by a change in the shell characteristics, as well as the incoming presence of glauconite, which is typically absent in Maassluis Fm. Around 170 mbgs at NIOO, the color changes from grey to dark grey and green, which suggests an increase in glauconite content, and the shell characteristics change too. This agrees with the transition description, so that the Maassluis – Oosterhout boundary was set at 170 mbgs for the NIOO site. This depth coincides with the expected lower boundary of the 3rd aquifer which holds high quality groundwater.

The lower boundary of the Oosterhout Fm, i.e. with the Breda Fm, is characterized by an increasing glauconite content and a decrease of shell content with depth. These characteristics were found in the borehole log descriptions of NIOO around 250 mbgs, hence the boundary between the Oosterhout Fm and Breda Fm at the NIOO site was set at 250 mbgs. This agrees with the depth of the boundary as shown in the REGIS geohydrological model (TNO, 2013) which indicates the boundary depth at around 240 mbgs.

Moreover, the flowmeter log of 2010 showed that in the hot well, practically all water is injected in the upper part of the well screen (220 – 250 mbgs) although screen was placed up to 283 mbgs. This suggests that the permeability in the depth range of the upper part of the well screen (Oosterhout Fm) is much higher than in the depth range of the lower part of the well screen (Breda Fm). The Breda Fm is a complex formation with low permeability, so the flowmeter log results are in support of the boundary definition at 250 mbgs.



Clay to silt
Silt to very fine sand M < 125
Very fine to medium sand M < 200
Medium to coarse sand M < 400

(Monitoring) Well Casing
Hot/Cold Well Filter
Piezometer Well Filter

Depth (mbgs)	Thickness (m)	Geology			Hydrogeology	
		Dominant grain size	Details	Formation name	Flow properties	Hydrogeol. unit
0	6	Fine sand and clay	Light brown	Holocene	kv = 0.05 m/d	Top aquitard
6	31	Fine to coarse sand	Grey to rusty brown	Drente	kh = 20 m/d	1st Aquifer
37	6	Clay	Grey	Drente	kv = 0.01 m/d	1st Aquitard
43	52	Medium to coarse sand	Grey, locally very coarse	Peize/Waalre	kh = 53 m/d	2nd Aquifer
95	10	Clay with silt and medium	Grey	Peize/Waalre	kv = 0.1 m/d	2nd Aquitard
105	5	Medium sand	Grey, locally coarse	Peize/Waalre		
110	10	Silt and clay	Grey	Maassluis	kh = 20 m/d	3rd Aquifer
120	12	Medium sand	Grey, shell grit	Maassluis		
132	6	Clay	Grey	Maassluis	kv = 0.01 m/d	3rd Aquifer
138	35	Fine to medium sand	Grey, shell grit	Maassluis	kh = 10 m/d	
170	27	Fine sand	Greenish, silty, brown shell debris	Oosterhout	kh = 8 m/d	Hydrological base
200	20	Fine and very fine sand	Greenish, silty, shell grit	Oosterhout	kh = 5 m/d	
220	30	Very fine sand	Greenish, silty, shell grit	Oosterhout	kh = 2.4 m/d	
250	57	Very fine sand and silt	Dark green, dark grey, shell grit, clay	Breda	kh = 0.4 m/d	
307						

Figure 5-1. The lithology at NIOO as interpret by the borehole log data. Hydrogeological properties of the layers are shown in the right hand side of the figure.

5.3 Flow properties

The flow properties of the layers are shown in the ‘flow properties’ column in Figure 5-1. The deduction of these properties is discussed in this section.

1st aquifer

The flow properties from the first aquifer were derived from grainsize information from the borehole logs of the ATES and HT-ATES wells, using Shepherd’s method (Shepherd, 1989) and DINOloket information (TNO, 2013), resulting in a hydraulic conductivity estimation of about 15 m/d.

2nd aquifer

The regular ATES system that is installed between 60 and 83 mbgs at NIOO enables a relatively accurate assessment of the flow properties of the 2nd aquifer. The results of the pumping tests carried out after installation and development of the well are shown in Table 5-2. The corrected hydraulic conductivity (k) values indicate that the average hydraulic conductivity of the 2nd aquifer is approximately 53 m/d.

Table 5-2 | Well testing results of the warm and cold ATES well (<25 °C) and the hydraulic conductivity (k) of the 2nd aquifer as derived from these results. The head drop is the drop in hydraulic head in a monitoring well that is placed at well screen depth, to exclude non-linear skin effects on the head.

Well	Well screen length (m)	Flow rate (m3/h)	Drawdown (m)	Specific Capacity (m3/h/m)	Estimated k (m/d)
ATES-W Q25%	29	22.5	0.34	66.2	52
ATES-W Q50%	29	45	0.67	67.2	53
ATES-W Q75%	29	67.5	1.02	66.2	52
ATES-W Q100%	29	90	1.39	64.7	51
ATES-K Q25%	28	22.5	0.34	66.2	54
ATES-K Q50%	28	45	0.65	69.2	56
ATES-K Q75%	28	67.5	1.01	66.8	54
ATES-K Q100%	28	90	1.36	66.2	54

3rd aquifer

The flow properties from the third aquifer were derived from grainsize information from the borehole logs of the HT-ATES wells, using Shepherd’s method (Shepherd, 1989) and DINOloket information, resulting in a hydraulic conductivity estimation of about 10 m/d.

Hydrological base

The flow properties of the hydrological base, at the depth interval where no well screen was placed, i.e. 170 – 220 mbgs, were derived from grainsize information from the borehole logs of the HT-ATES wells, using Shepherd’s method (Shepherd, 1989) and DINOloket information, resulting in a hydraulic conductivity estimation of about 8 m/d and 5 m/d for the intervals 170 – 200 and 200 – 220 mbgs respectively.

HT storage aquifer

The flow properties at the depth of the well screens of the heat storage were deduced from a combination of grainsize information, pumping tests, flowmeter tests in the HT-ATES wells and specific capacity information during operation. The flow properties in this depth interval are not as homogeneous as expected in the design phase. The bottom part of the well screen is located in the Breda Fm, which is a complex formation with poor flow properties and is hence not suitable for heat storage.

A flow test was performed in the hot well in 2010 and showed that approximately 85% of the extracted water was produced from the upper 30 m of the well screen, in the depth range 220 – 250 mbgs, leaving only 15% of the water to be produced from the bottom 33 m of the well screen (250 – 283 mbgs) (IF Technology, 2012). IF Technology used drawdown data from the hot, cold and monitoring well, obtained during the flowmeter log activities (IF Technology, 2012), to calibrate a MLU model (Hemker & Randall, 2010), and found a transmissivity (KD) of 85 m²/d for the depth interval of the well screen. Using this transmissivity value and assuming that the flowmeter log accurately represents the distribution of the transmissivity along the well

screen, the hydraulic conductivities along the hot well screen were calculated to be 2.4 m/d for the upper part (220 – 250 mbgs, 30 m) and 0.4 m/d for the bottom part (250 – 283 mbgs, 33m) of the hot well. The hydraulic conductivity at the depth of the well screens, as derived from the pumping test data, is lower than the 3.4 m/d that was expected during the design phase in 2009 (IF Technology, 2009b)).

Anisotropy of hydraulic conductivity

The hydraulic conductivity is an anisotropic flow property, meaning that it is dependent of direction. In hydrology, the vertical anisotropy of a layer (simply referred to as ‘anisotropy’ here) is indicated as the ratio of horizontal (k_h) over vertical hydraulic conductivity (k_v). It remains challenging to deduce anisotropy ratios from unconsolidated materials in laboratory experiments because of their friable nature, resulting in scarce anisotropy data in the literature.

On a microscale, anisotropy ratios increase with increasing aspect ratios of the grains and increased degree of their alignment (Masad, Martys, & Muhunthan, 2000) (van den Berg, 2003). Highest anisotropy ratios (3 to 10) are hence associated with compacted silt-or clay sized materials that consist of aligned and platy particles (Bolton, Maltman, & Fisher, 2000). Using upscaling methods, Bierkens deduced anisotropy ratios up to 3.8 for fine and loamy sands. Typically, well sorted sand has lower anisotropy ratios (in the range of 1.1 to 1.3) compared to poorly sorted sand (Okagbue, 1995).

Besides these microscale grain characteristics, the presence of thin layers with low k_v values within a larger hydrological unit influences the effective k_v at macroscale. Typically, clay lenses or loamy sand layers within a larger sand formation dominantly control the k_v of the layer as a whole. Grain size analysis results are only representative for the local flow properties at sampling depth, so this analysis is only useful when sufficient samples are taken over a limited depth interval. Additionally, borehole data in the Netherlands report lithology at a 1 m interval, so that clay lenses of centimeter scale (which can have a large impact on the anisotropy value of an aquifer) are not distinguished. Furthermore, during rotary or reverse rotary drilling the clay lens is probably mixed up with the sand during drilling. This once again emphasizes that deducing anisotropy from field data is challenging.

The k_v for each hydrological unit in the NIOO lithology (Figure 5-1) is determined based on the interpreted k_h value and the applied anisotropy factor. For the 1st, 2nd and 3rd aquifer, an anisotropy factor of 2 is applied, related to the variety of grainsizes in each unit. The hydrological base consists of very fine to fine sands that are partly or dominantly silty, and contain shell debris and shell grit as well. It was hence concluded that the hydrological base is poorly sorted, which expectedly results in a relatively high anisotropy factor of 4. The anisotropy factors applied to the hydrological units from Figure 5-1 are shown in Table 5-3 below.

Table 5-3 | Flow properties of the hydrological units identified at the NIOO site.

Hydrogeological unit	Depth interval (mbgs)	Lithology	Depositional environment	K_h (m/d)	Anisotropy (-)	K_v (m/d)
1 st aquifer	6 - 37	Fine to coarse sand	Glacial	20	2	10
2 nd aquifer	43 – 95	Medium to coarse sand	Fluvial	53	2	26.5
3 rd aquifer	138 - 170	Fine to medium sand, shell grit	Marine	10	2	5
Hydrological base	170 – 200	Fine sand, silty, shell grit	Marine	8	4	2
	200 – 220	Fine and very fine sand, silty, shell grit	Marine	5	4	1.25
	220 – 250	Very fine sand, silty, shell grit	Marine	2.4	4	0.6
	250 -307	Very fine sand and silt, shell grit, clay	Marine	0.4	4	0.1

5.4 Regional groundwater flow regime

NIOO is situated North of the city of Wageningen and adjacent to the more elevated location of Wageningen-Hoog (“Wageningen-High”), which is part of the Veluwe, an end moraine formed in the Saalien glaciation. Because of its location, groundwater flow in the shallow aquifers is directed in west and southwest direction, as can be seen from the hydraulic head contour lines in Figure 5-2, for the 1st, 2nd and 3rd aquifer.

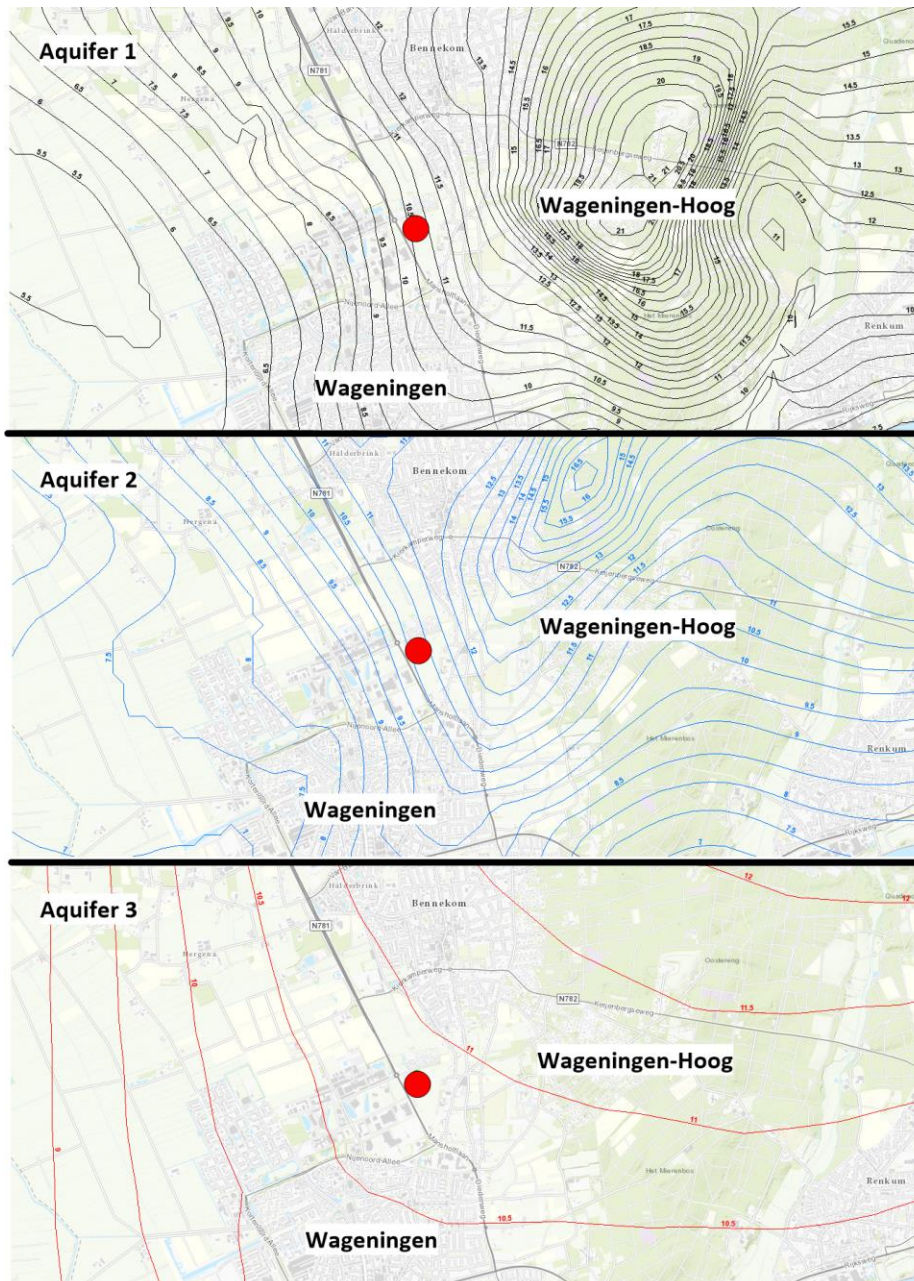


Figure 5-2. Hydraulic head contour lines of the 1st, 2nd and 3rd aquifer at NIOO (red). Hydraulic head units are in meters above NAP (Normaal Amsterdams Peil). Groundwater flow is directed from the Wageningen-Hoog hills (part of the Veluwe, a pushed morene) towards the lower regions in the west and southwest.

Based on the hydraulic head contour line pattern (Figure 5-2) and the horizontal hydraulic conductivity from Figure 5-1, the groundwater flow velocities can be calculated. The Darcy velocity was calculated using Darcy's law, which requires the hydraulic gradient (derived from the maps with the hydraulic head contour lines) and hydraulic conductivity values (as described before). The actual flow velocity in the aquifer was calculated using the Darcy velocity and an assumed porosity of 0.35. The resulting groundwater flow velocities (m/y) are presented in Table 5-4. The hydraulic head contour line pattern of the 3rd aquifer is used for the hydraulic base (in which the HT-ATES well screens are placed), since no such pattern is available for the hydrological base (storage depth). This is expected to be a reasonable assumption, since there is no clear aquitard between the hydraulic base and the third aquifer.

Table 5-4. Groundwater flow velocities for the 1st, 2nd and 3rd aquifer and the hydrological base.

Hydrogeological unit	Depth interval (mbgs)	Hydraulic gradient at NIOO (m/km)	Direction of groundwater flow	Horizontal hydraulic conductivity (m/d)	Groundwater flow velocity (m/y)
1 st aquifer	6 - 37	2.86	WSW	20	70
2 nd aquifer	43 – 95	2.86	SW	53	180
3 rd aquifer	138 - 170	0.33	SW	10	4.1
Hydrological base	220 - 250	0.33	SW	2.4	0.97
Hydrological base	250 - 295	0.33	SW	0.4	0.16

6 Hydrothermal evaluation

This section discusses the thermal effects of the HT-ATES system on the subsurface. The results of the temperature measurements acquired in the 2010 – 2020 period are presented and evaluated.

6.1 Results and Discussion

The temperature profiles of the cold, hot and monitoring wells are shown in Figure 6-1, Figure 6-2 and Figure 6-3 respectively. Each line represents a temperature profile taken at either spring or autumn. See legend for corresponding colors.

6.1.1 Temperatures at well screen depth

At the hot and the cold well, temperatures are highest at the depth interval that corresponds to the well screens. At the top of the well screen (220 – 250 mbgs), temperatures are significantly higher compared to the bottom part of the well screen (>250 mbgs), which is explained by the finding that over 85% of the storage volume is stored in the upper part of the well screen (see section 5.3) combined with the density driven flow that expectedly occurs around storage depth. Comparing temperatures at this depth interval with the flow and temperature registration data from the surface installation, it becomes clear that the temperatures measured at the piezometer are strongly related to the temperature of the water that has been injected/produced in the hours before the measurement was carried out. This explains the relatively high temperature at the cold well screen in the spring of 2018, because at the day of measurement (3rd of May), relatively warm water of approximately 32 °C was injected in the cold well, expectedly caused by an error in the flow distribution system. This shows that the temperatures measured in these piezometers are strongly dependent on the temperature of the water pumped in the days, if not hours, before measurement, especially when the well was used for injection (injection temperatures generally show much more variation than extraction temperatures).

In the bottom part of the cold well screen, temperatures are relatively high in the 280 – 285 mbgs depth interval (see Figure 6-1). The borehole logs show that the grainsizes are higher in this depth interval, which allows more water to be injected in this interval, increasing the temperatures.

6.1.2 Temperatures above storage depth

Temperatures above the cold well screen

Note that the cold well of the HT-ATES system is not located close to another well (see Figure 3-1), so that the temperatures at this well are probably not influenced by the other wells. In the 0 – 20 mbgs depth interval, all temperature profiles show high variety, which is caused by the yearly temperature variations at the ground surface. In the depth range 35 – 45 mbgs, the temperatures are higher compared to the over- and underlying meters of ground material. Borehole information shows that clay is present at this depth. The clay prevents the heat that was conducted from the well casing to the subsurface material from being carried away by groundwater flow. At depths where groundwater flow velocity is higher, the measured temperatures are consistently closer to the native groundwater temperature. This is visible especially at 30 – 35 mbgs and 60 – 75 mbgs, where, according to borehole information, very coarse sand is present, facilitating groundwater flow. The relatively high groundwater flow velocity leads to enhanced convective heat transport of heated water away from the well casing and, at the same time, inflow of relatively cold native groundwater. Section 5.4 showed that groundwater flow is exceptionally high in the 1st and 2nd aquifer (at least for Dutch standards), because of a steep hydraulic gradient combined with relatively high hydraulic conductivity values. In the 75 – 200 mbgs depth range, temperatures increase more gradually, with a gradient comparable to the native thermal gradient. From 200 to 220 mbgs, temperatures increase more rapidly towards the average injection temperature of 26 °C. This is caused by the relatively warm water (26 °C) that is stored at 220 mbgs: the heat is transported upwards by a combination of flow, diffusion, dispersion and thermal conduction. The borehole logs of the cold well show that the median grain size decreases from 200 µm at 170 – 200 mbgs to 150 µm at 200 – 220 mbgs. Groundwater flow velocity is lower in the 200 – 220 mbgs depth interval, which may explain why the temperature ‘kink’ at 200 mbgs has always been sharp over time.

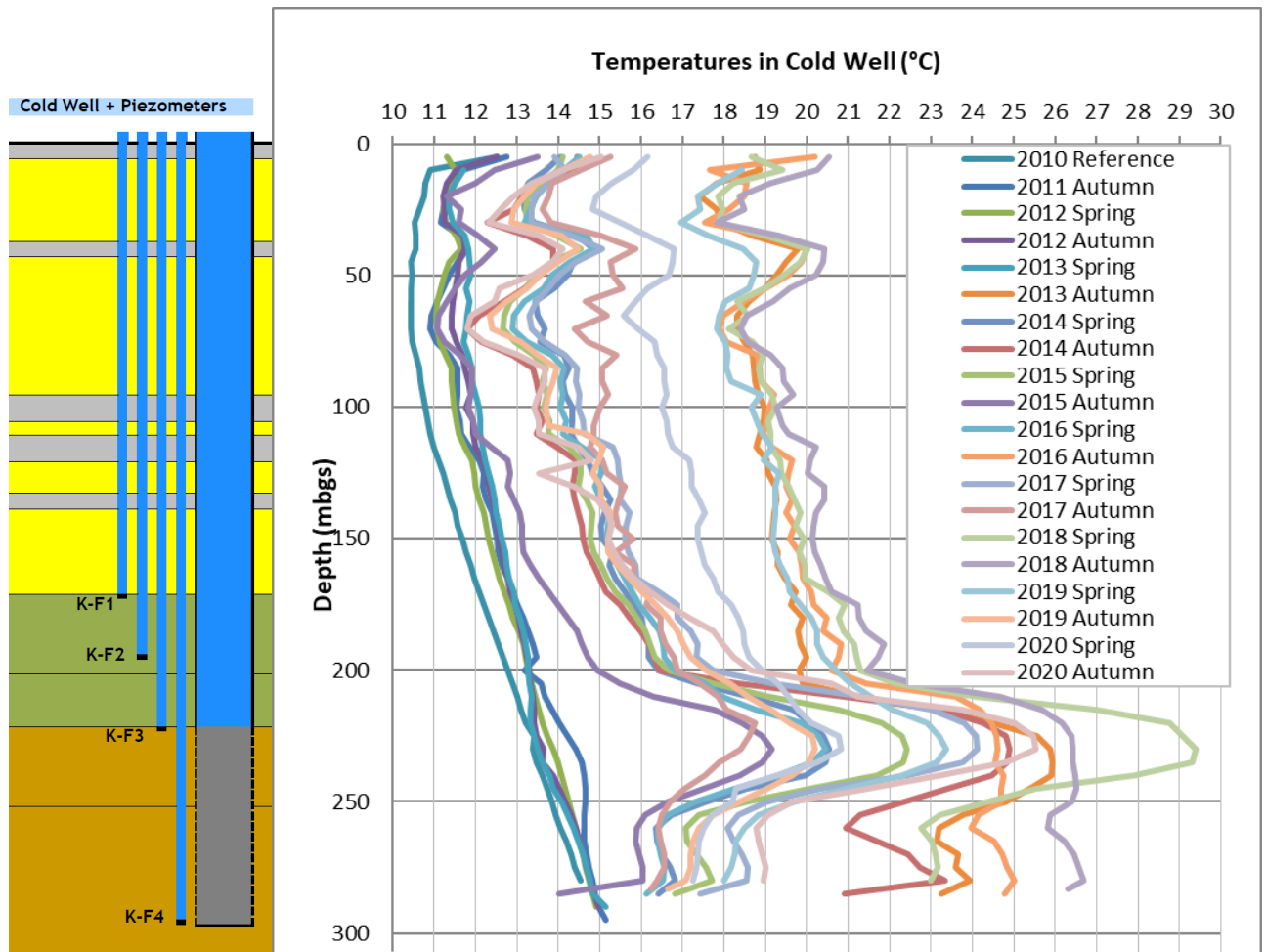


Figure 6-1 | Temperature profiles at the cold well, taken at K-F4 before operation (Reference 2010) and subsequently twice a year in spring and autumn. The lithology and well construction are indicated on the left hand side.

Temperatures above the well screen – Hot well

The temperature profile measurements for the hot well are shown in Figure 6-2. In the depth range 30 – 75 mbgs, the observations of the temperatures at the hot well are similar to those from the cold well, but more pronounced because of the larger differences with the original groundwater temperature. Considering each profile individually, temperatures show a dip around 30 mbgs, a peak around 40 mbgs and a dip again around 60 - 75 mbgs, related to the variety in groundwater flow velocity at different depths. Recall that groundwater flow velocity is high (for Dutch standards) particularly in the 1st and 2nd aquifer and very low in clay layers, which explains the sharp peak around 40 m depth.

The hot well of the HT-ATES system is located at around 15 m from the warm well of the regular ATES system (see Figure 3-1). Based on the flow and temperature registration data of the ATES system, the monthly average injection temperature of the warm ATES well during summer ranges between 13 and 17 °C. Based on the thermal radius of the warm well of the regular ATES system (<25 °C), influence on the HT-ATES well, at the well screen depth range of 54 – 83 mbgs is expected. However, at this depth, temperatures at the hot HT-ATES well are typically > 17 °C, because the thermal influence of the HT-ATES hot well casing controls the temperature in the piezometer. The effects of the ATES on the temperatures measured at the HT-ATES also depends on the size of the ATES storage at the time of measurement, hence on the time of year, and on the regional groundwater flow. But, no consistent distinction between temperatures in spring and autumn was observed between 54 and 83 mbgs at the hot HT-ATES well. This hints that heating by the well casing, as well as regional groundwater flow in the 2nd aquifer together have stronger control on the reigning temperatures at the hot HT-ATES well in the 2nd aquifer, than the warm well of the regular ATES system.

Additionally, the profiles consistently show distinctive dips towards the original groundwater temperature around 110 mbgs and peaks around 120 – 125 mbgs. Again, this can be explained by the information from the borehole log, showing a 6 m thick layer with very coarse sand between 106 – 112 mbgs overlying a 10 m thick layer of clay and silty to fine sand. This trend is not clearly observed in the cold HT-ATES well, expectedly because of the relatively limited temperature differences with the original groundwater or because of slight local differences in lithology.

Temperature profiles show subtle dips at the 150 – 155 mbgs interval. The borehole description, showing medium to coarse sand (260 µm) at 150 – 155 mbgs supports the hypothesis that groundwater flow effectively limits the temperatures by enhanced removal of heat (by convective heat transport) from this depth interval.

Below 155 mbgs, the temperature gradient changes into a relatively linear, but steeper temperature gradient, indicating that temperatures increase more rapidly in the 150 – 200 mbgs interval. The linearity of the gradient may partly be explained by the fact that the median grainsize is uniform (180 – 200 µm) at this depth, resulting in relatively uniform groundwater flow velocities. Note that the maximum temperature measured at 170 mbgs is 25 °C (autumn 2018).

In the depth interval 190 – 220 mbgs, all temperature profiles show clear kinks. Part of this may be explained by the fact that median grainsizes drop to 150 – 160 µm, resulting in temperature peaks, as is seen similarly at other depth intervals with low groundwater flow velocities. The strong increase in temperature with depth is explained by the fact that the thermal front of the stored heat is encountered in this interval. Heat moves upward by conduction and heats the layers overlying the storage layer. Additionally, upward heat transport is facilitated by upward flow of hot water (convection), because the layer overlying the storage layer is composed of (very) fine sands and is hence not completely 'confining'.

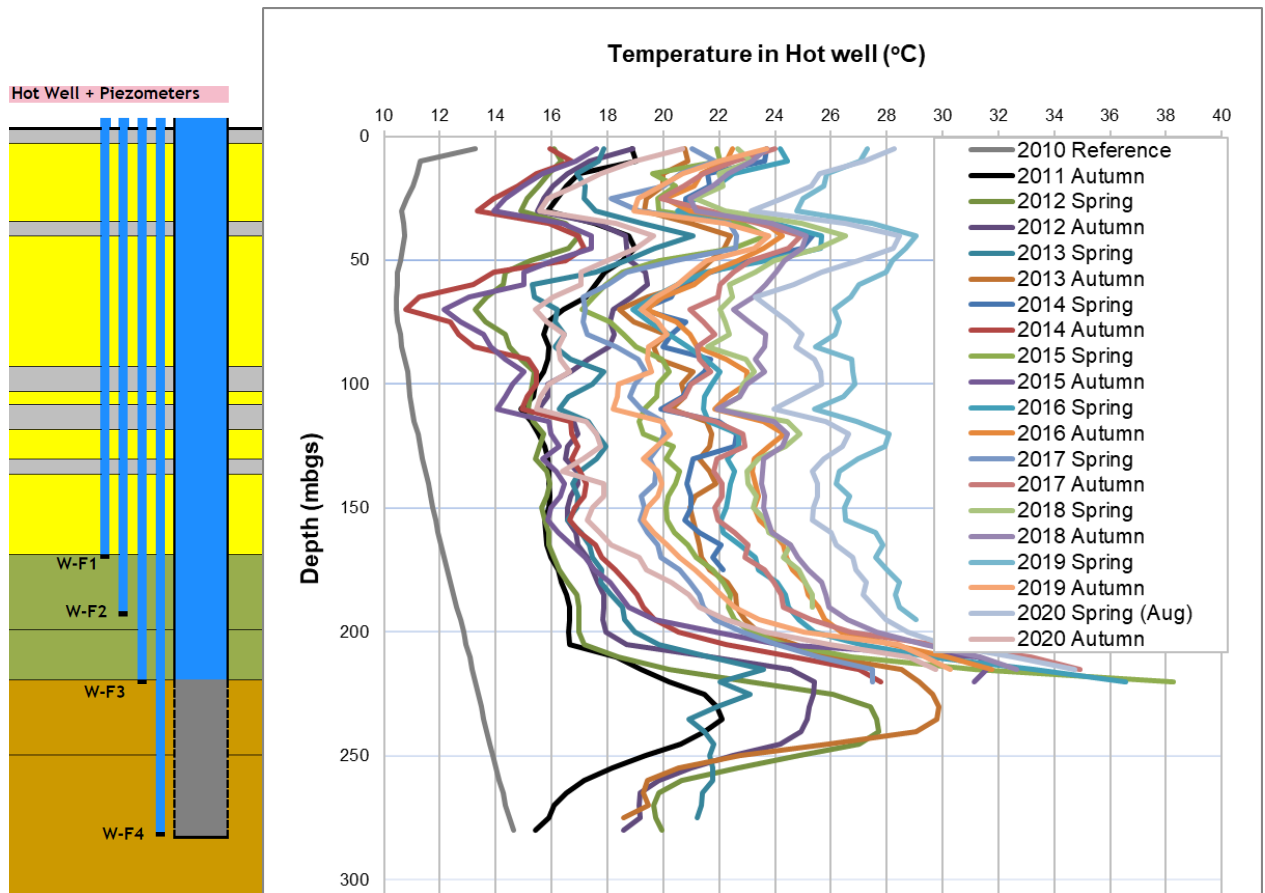


Figure 6-2 | Temperature profiles at the hot well, taken before operation (Reference 2010) and subsequently twice a year in spring and autumn. The lithology and well construction are indicated on the left hand side.

Temperatures in monitoring well

The monitoring well is located at a distance of 60 m and 100 m from the hot and the cold HT-ATES well, respectively. At the HT-ATES storage depth (220 – 295 mbgs), no significant thermal effects were observed (Figure 6-3). However, at the depth of the regular ATES system (well screens at depth interval 54 - 83 mbgs), thermal effects of both the warm and cold ATES wells were observed. The distance of the monitoring well to the hot and cold ATES well is approximately 45 and 42 m respectively. Compared to the natural temperature at ATES depth, the temperatures measured in the monitoring well are low in spring and high in autumn. This is explained by the size of the cold and warm bubble of the ATES system, as these are largest at the end of winter and summer, respectively. The temperature measurements show that water infiltrated at both the hot and cold ATES wells reach the monitoring well. Temperature minima and maxima are highest at 70 mbgs, which is the middle of the ATES well screen. The measured temperatures at the monitoring well are in line with the expectation based on the injection temperatures at the ATES system.

The temperature profiles of 2012, 2018 and 2019 show clear peaks at ATES depth. By looking at the pumping data of the ATES system, it becomes clear that a relatively large volume of water was infiltrated in the hot well, compared to the other years. Also, temperature measurement took place before considerable amounts of heat (hence warm water) was recovered from the ATES well. This means that the size of the hot storage was near its peak at the time of measurement. In the years 2013 – 2016, measurements took place after some heat was already recovered, so the size of the hot storage was smaller.

The peaks towards higher temperatures are larger than the dips towards lower temperatures. This is partly explained by the larger difference in average injection temperature relative to the original groundwater temperature at the warm well. Also, the southwest directed groundwater flow must be considered, as this facilitates transport of heat from the warm ATES well towards the monitoring well. It is noted that the borehole log of the warm ATES well shows coarse to very coarse sand (grainsizes 300 - 1400 μm) around 70 mbgs, whereas at the cold ATES well, the sand at this depth is less coarse (grainsizes 200 – 350 μm). This may contribute to the more pronounced temperature peaks in autumn, compared to the subtle dips in spring.

The maximum temperature measured at ATES depth is approximately 15 °C. The maximum temperature at the depth of HT-ATES is also 15 °C, but no significant variations have been observed over the last 9 years.

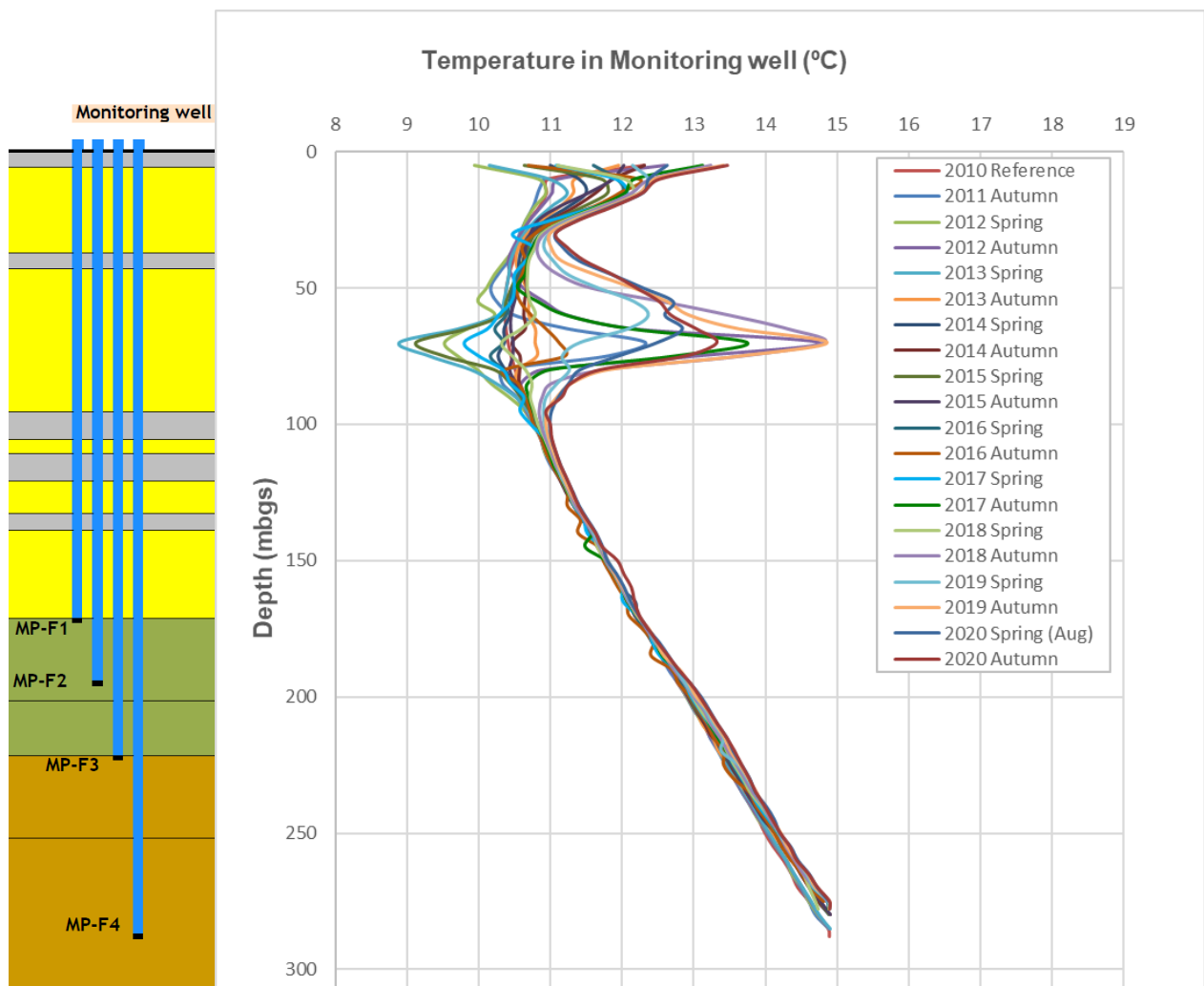


Figure 6-3 | Temperature profiles at the monitoring well, taken from MP-F4 before operation (Reference 2010) and subsequently twice a year in spring and autumn. The lithology and piezometer depths are indicated on the left hand side.

6.2 Conclusions

Temperature profiles were obtained by descending a probe in the piezometers that are installed in the gravel pack of the well, at approximately 20 cm from the well casing. The temperatures measured here are strongly controlled by the temperature of the water flowing through the well in the days (if not hours) before temperature measurements were performed, because of heat conduction. Sharp peaks and dips in the temperature profiles in the 20 – 200 mbgs depth interval were explained by the large variations in the horizontal groundwater flow velocity at different depths. Temperatures dipped in sandy layers with considerable groundwater flow, whereas they peaked in clay layers where the heat that has been conducted from the well casing largely remains in place because it is not transported away from the well by convective heat transport (groundwater flow).

Below 200 mbgs, the temperatures at both hot and cold wells increases more steeply with depth. This is an indication that this is the depth region which is thermally influenced by the water injected in the wells, as the injection temperature at the cold well (26 °C) and hot well (45 °C) are both higher compared to the natural temperature.

The monitoring well is located at approximately 60 m horizontal distance from the hot well. In the period 2010 – 2020, no significant changes in temperature were observed at the storage depth of the HT-ATES system (220 – 295). of the regular ATES system

At the depth of the regular ATES system (<25 °C), the temperatures in the monitoring well at 50 – 85 mbgs vary, depending on the time of year. Because of the relatively short distance between the monitoring well and the ATES wells (warm well at 45 m distance and cold well at 42 m) and the volumes of water that are pumped by the ATES system, the thermal influence of the regular ATES system is observed in the monitoring well.

7 Chemical evaluation of the groundwater composition

In this chapter, the groundwater analysis data acquired from the hot, cold and monitoring well is presented. Information on the hydrochemical composition of the groundwater was acquired by performing the monitoring activities as described in section 4. Specific assessment of these results are described below, for chloride and a number of other hydrochemical parameters.

7.1 Chloride concentrations

Since the main objective of the monitoring at NIOO was to track the displacement of the fresh-salt water interface, chloride was measured with a half-yearly frequency at piezometer F2, F3 and F4 of the hot and cold wells, resulting in an extensive chloride concentration dataset in time and space.

7.1.1 Reference measurements

In 2010, reference measurements of the chloride concentrations took place. However, groundwater taken at the cold, hot and monitoring well, from similar depth, showed considerable differences in chloride concentration, especially in the deepest piezometers (see Table 7-1). Therefore, an extra measurement was performed in 2018 at the monitoring well, where no considerable groundwater composition changes due to HT-ATES operation were expected. The results are shown in column '2018' of Table 7-1. Based on all reference measurements, it was concluded that the natural chloride concentrations at various depths was best represented by the 2010 reference measurement at the monitoring well (highlighted in green in Table 7-1).

These results show that fresh groundwater (32 mg Cl⁻/l) is present at the top of the well screens at 220 mbgs, while the groundwater at the bottom of the screens (283 – 295 mbgs) is saline: 3,800 mg Cl⁻/l. The fresh-brackish water interface is hence located somewhere between 220 – 285 mbgs, which means that it is located deeper than was expected during the permitting and designing phase, where it was assumed to be around 200 mbgs (see section 2.3).

Table 7-1 | Results of the reference measurements on chloride concentration, as performed in 2010, before the HT-ATES was taken into service. Chloride measurements at the monitoring well in 2018 are added, confirming that the groundwater at the monitoring well best represents native groundwater composition. n.a.: not available

Hot well	Depth (mbgs)	Concentration (mg/l)	Cold well	Depth (mbgs)	Concentration (mg/l)	Monitoring well	Depth (mbgs)	Concentration (mg/l)	
		2010		2010				2010	2018
W-F1	170-172	n.a.	K-F1	170-172	n.a.	MP-F1	170-172	7.3	n.a.
W-F2	193-195	20	K-F2	193-195	13	MP-F2	193-195	4.3	5.2
W-F3	220-222	30	K-F3	220-222	43	MP-F3	220-222	32	11
W-F4	280-282	610	K-F4	293-295	710	MP-F4	285-287	3,800	3,780

7.1.2 Regular chloride measurement results 2010 - 2020

Figure 7-1 shows the changes in chloride concentrations in piezometers K-F3 and W-F3 (top of well screens, 220 mbgs). The monthly cumulative net water displacement from cold to hot well is presented on the secondary y-axis.

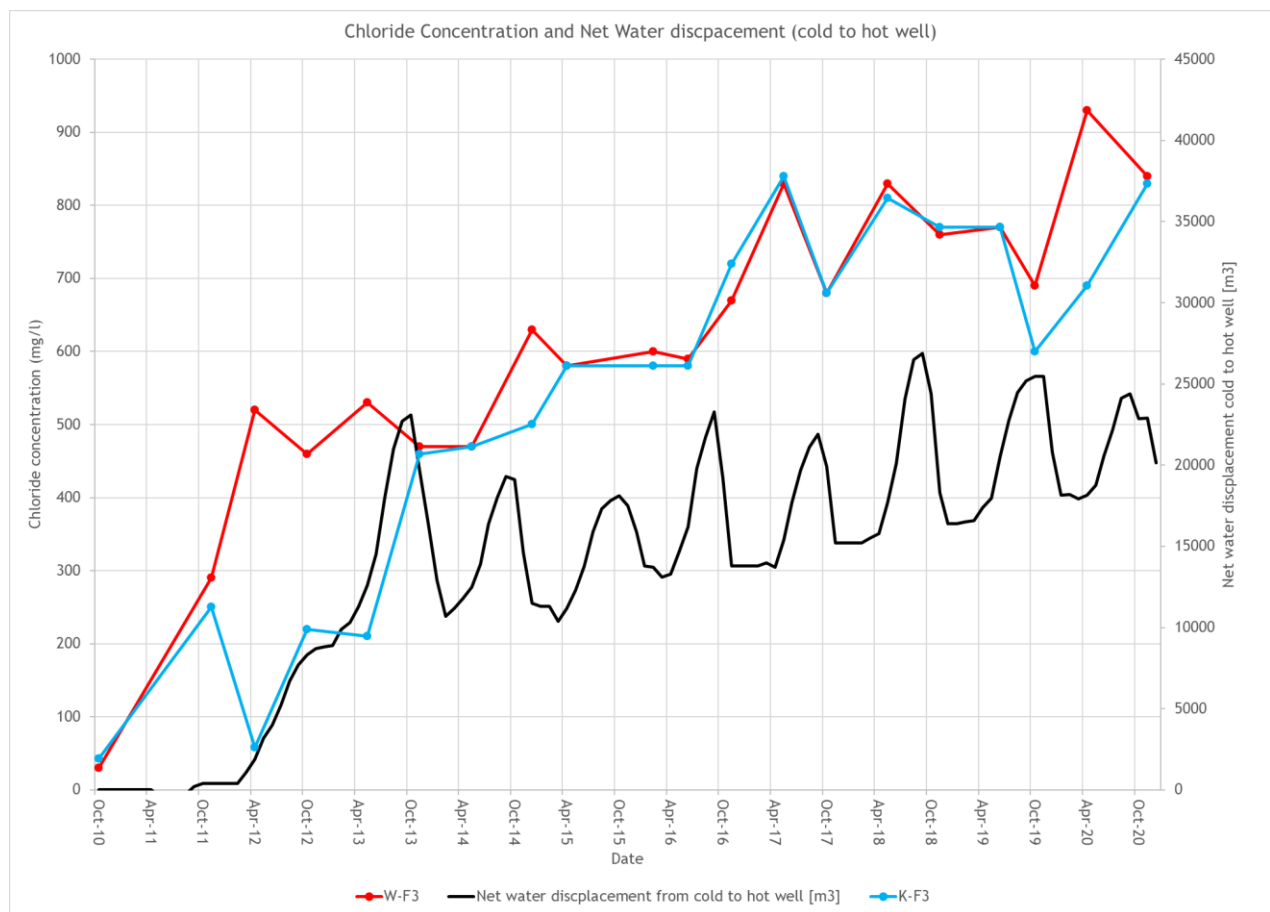


Figure 7-1 | Chloride concentrations in piezometers of the hot well (red) and the cold well (blue) plotted versus time. The secondary axis shows the net water displacement (black) from the cold to the hot well.

Mixing

The well screens of the hot and cold well of the HT-ATES system are placed between 220 – 295 mbgs. Table 7-1 showed that the groundwater at the top of the well screen is fresh (<150 mg Cl/l), while the groundwater at the bottom of the well screens is saline (>1,000 mg Cl/l). Upon groundwater production, saline groundwater from the bottom part of the well screen will thus be mixed with fresh water from the top of the screens. The mixed water (with a composition of about 500 mg Cl/l) is re-injected at the other well, causing chloride concentrations at the top of the injection well screen to increase, and at the bottom of the well screens to decrease, compared to their natural concentrations.

This is also visible in Figure 7-1. In the HT-ATES system, net water has been pumped from the cold to the hot well during the first years of operation (2010 – 2013). The mixed water is injected at the hot well, causing chloride concentrations at W-F3, at the top of the injection well screen, to increase. In this period, no considerable water volumes have been pumped back from the hot well to the cold well, explaining why the concentrations at W-F3 remain higher than K-F3. Only after a considerable water volume is pumped back from the hot well to the cold well (November 2013 – February 2014), the concentration at K-F3 is increased. As from November 2013, concentrations at the top of both the cold well screen (K-F3) and the hot well screen (W-F3) remain similar, as the mixed water is pumped between the two wells.

Mixing ratio upper – bottom part of well screens

In the hydrogeological evaluation it was explained that about 85% of the water flowing into the hot well is produced from the top 30 m of the well screen, leaving only 15% of the groundwater to be produced from the bottom part of the wells. The ratio of water produced from the top/bottom of the well screen controls the composition of the groundwater that is injected in the other well. In Figure 7-2, the chloride concentration trend is visualized again, but now the natural chloride concentrations at the top and bottom of the well screens are indicated as well (brown dashed lines). It shows that the mixed water composition is closer to

the natural groundwater at the top part of the well screens, since the majority of the groundwater is pumped from this depth. Mixing 85% of native groundwater from the top of the well screens (35 mg Cl/l) with 15% of native groundwater at the bottom of the filters (3,800 mg Cl/l), suggests that the mixed water should have a chloride concentration of about 600 mg/l. This is in line with the measured range.

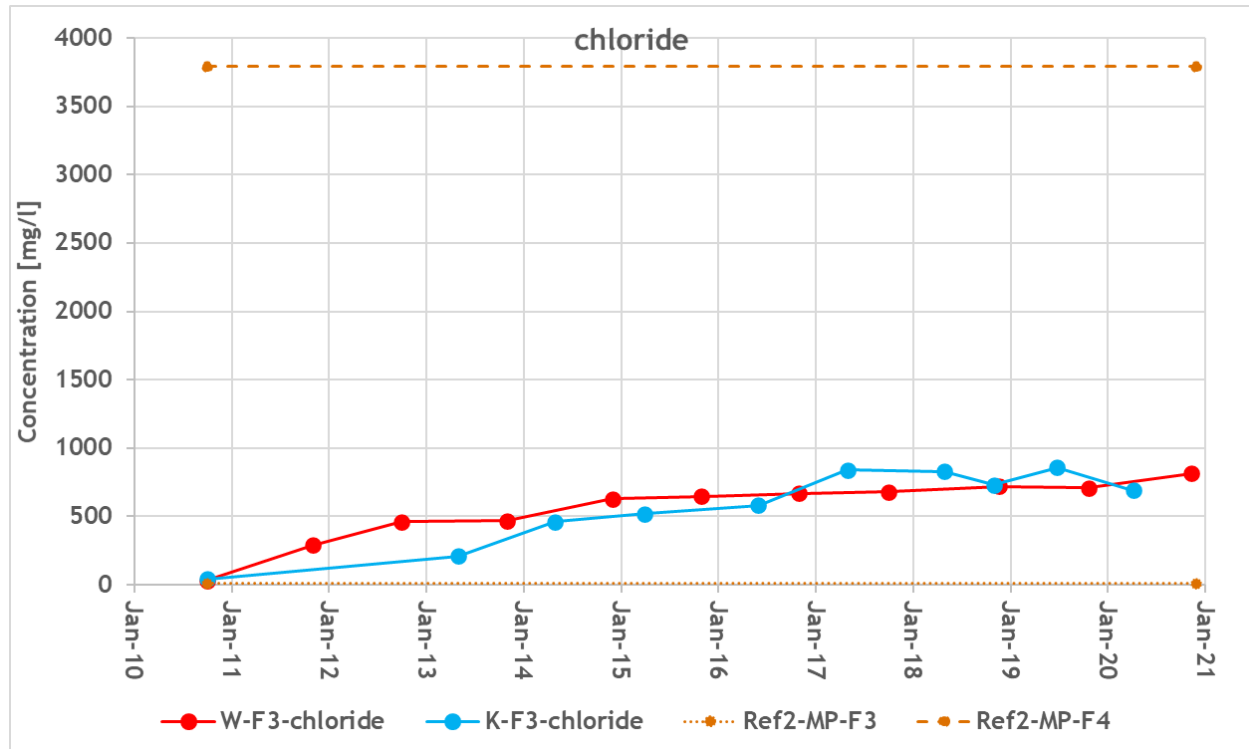


Figure 7-2. Reference concentrations are shown in brown, for the top of the storage depth (220 mbgs, 'Ref2-MP-F3') and the bottom of the storage depth (285 mbgs, 'Ref2-MP-F4'). The chloride concentrations at the top of the hot well ('W-F3') and at the top of the cold well ('K-F3') are shown in red and blue respectively.

Chloride concentration profile along well screens

From the period of 2010 – 2013, net water was pumped from the cold to the hot well. It is assumed that natural groundwater has flown horizontally towards the producing cold well during this period. Before the groundwater passes through the well screens, it must enter the borehole and pass the piezometers of K-F3 and K-F4. Expectedly, the most natural groundwater is found at these piezometer filters after a long period of water production at the well.

In 2012 and 2013, relatively high chloride concentrations of about 4,800 mg/l have been measured at K-F4 twice, suggesting that, at a depth of 295 mbgs, natural chloride concentrations are in this range.

The observations presented above support that chloride concentrations are about 35 mg/l at the top of the well screen (W-F3, 220 mbgs), 3,800 mg/l at MP-F4 (285 mbgs) and 4,800 mg/l at K-F4 (295 mbgs). When the chloride concentration gradient between K-F4 and MP-F4 is extrapolated linearly, the 35 mg/l concentration is expected at approximately 247 mbgs. This means that the fresh-brackish water interface (150 mg Cl/l) is located around 250 mbgs, i.e. at the Oosterhout – Breda Fm transition.

Based on this interpretation, the original chloride concentration gradient as shown in Figure 7-3 was estimated for NIOO.

Based on the observations and inter/extrapolations, the original chloride concentration gradient as shown in Figure 7-3 was estimated for NIOO.

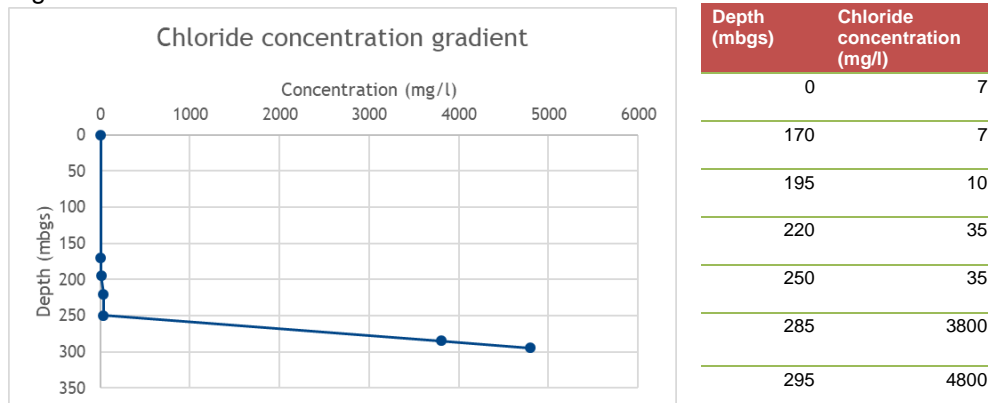


Figure 7-3 | Original chloride concentration profile with depth at NIOO, as interpret from the measurements.

The flow measurement in the hot well showed that 85% of the water was produced from the top part of the well screen (220 – 250 mbgs) and 15% in the bottom part (250 – 283 mbgs). A slightly different ratio should apply for the cold well, because the filter length of the bottom part of the cold well screen (250 – 295 mbgs) is about $1\frac{1}{3}$ as long as the bottom part of the hot well screen. For the cold well screen then, about 20% is produced from the bottom part (250 – 295 mbgs), leaving 80% for the top part (220 – 250 mbgs). Using this ratio, one can calculate the average concentration of the mixed water, which is injected into the hot well. For this calculation, it was assumed that the average chloride concentration along the bottom part of the cold well screen (250 – 295 mbgs) was about 2,400 mg/l (the average of 35 mg/l and 2,400 mg/l).

Top of cold well screen: 80% of water with average concentration of 35 mg Cl/l

Bottom of cold well screen: 20% of water with average concentration of 2,400 mg Cl/l

Mixture: 100% of water with average concentration of 508 mg Cl/l

The calculated average chloride concentration of the mixture produced from the cold well, deduced from the 2010 – 2013 period, agrees well with the concentration found at W-F3 in the same period (see Figure 7-1). This supports the suggested original chloride concentration profile as shown in Figure 7-3.

After 2013, the chloride concentration shows a slight increase after each cycle. This may be explained by the fact that each year, a net water volume is pumped from the cold to the hot well, combined with the position of the cold well screen as it reaches 12 m deeper than the hot well screen. This allows for natural, deep and saline groundwater from the bottom of the cold well to be produced at the cold well at each cycle. Hence, the chloride concentrations at the top of the hot well screen is slowly but steadily increased. This may cause the chloride concentrations of the mixed water to increase over time, meaning that the concentrations in and around the hot well may increase with it.

Chloride concentration measurements at shallower depth

The aim of the chloride measurements was to track whether the 3rd aquifer was experiencing salinization because of the HT-ATES operation. To this end, piezometers were installed at the bottom of the 3rd aquifer (F1, 170 mbgs), at the top of the HT-ATES well screens (F3, 220 mbgs) and in between (F2, 195 mbgs). See also Figure 5-1. In 2010, only one measurement was taken at the bottom of the 3rd aquifer (170 mbgs), at MP-F1, showing a chloride concentration of only 7.3 mg/l. In 2010 – 2019, no measurements at W-F1 or K-F1 were performed because of clogged piezometers, but these were cleaned in 2020. In April 2020, chloride concentrations at W-F1 and K-F1 were measured at 5.4 and 6.2 mg/l respectively, showing that no effects of the HT-ATES on the bottom of the 3rd aquifer were observed (yet).

Chloride was also measured at piezometers K-F2 and W-F2, located at a depth of 195 mbgs between the well screens (220 mbgs) and the 3rd aquifer (170 mbgs). The chloride concentrations at K-F2 and W-F2 are shown in Figure 7-4 together with the net pumped groundwater volume from cold to hot well.

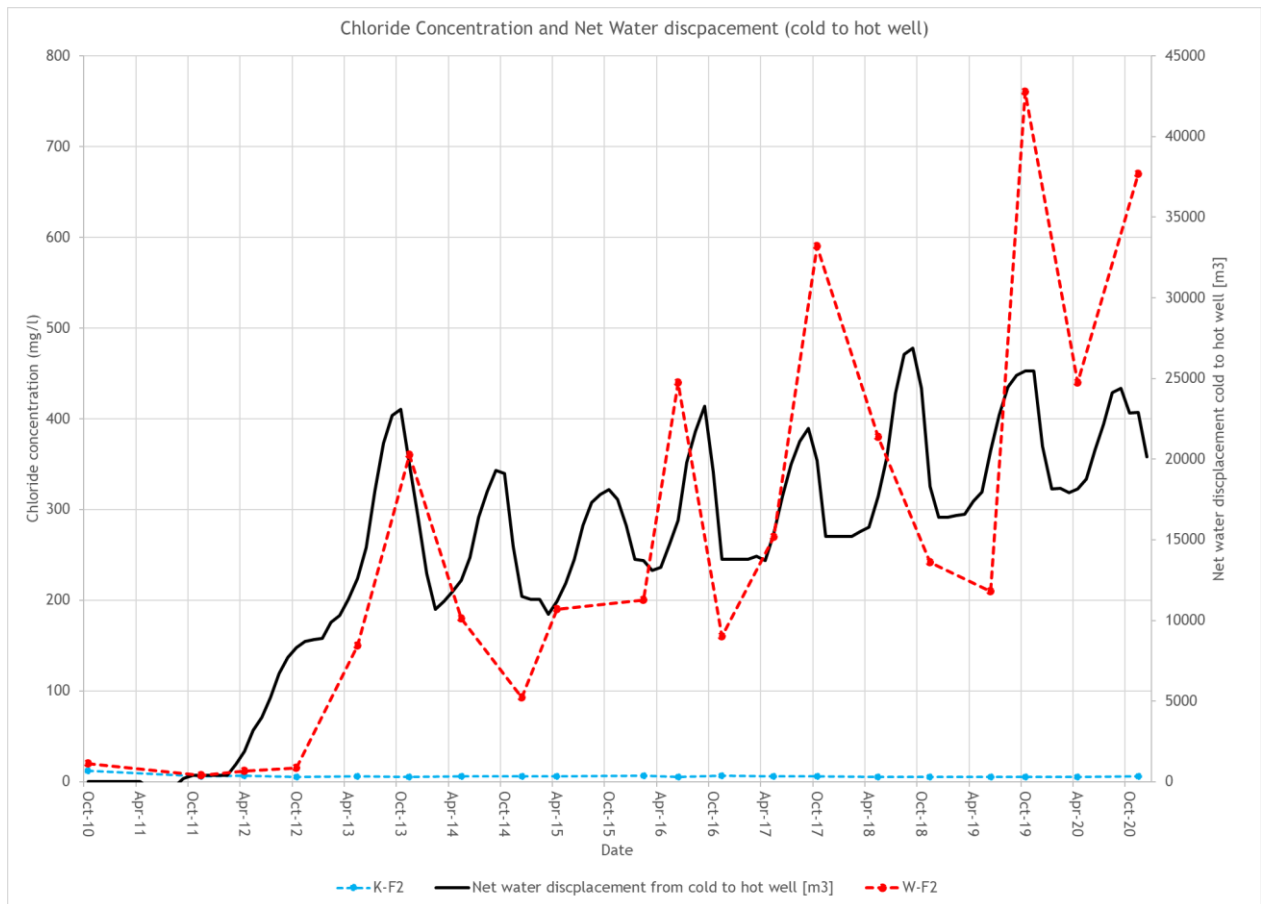


Figure 7-4. Chloride concentrations at a depth of 195 mbgs, as measured at W-F2 (red), and K-F2 (blue). Net water volume pumped from the cold to the hot well are shown in black.

K-F2 is located 25 m above the cold well screen and does not show any increase in chloride concentration with respect to the reference situation of 2010 (Table 7-1). Oppositely, W-F2, shows a clear increasing trend in chloride concentration. The explanation for this is found in the net water displacement between the wells. Between 2010 and 2019, a net water volume of nearly 20,000 m³ is pumped from the cold to the hot well. Because of the absence of the confining layer over the heat storage depth, the water injected in the hot well (at least 500 mg Cl/l) has been able to flow in upward direction, towards W-F2, increasing the concentration there.

Based on all the observations on chloride concentrations at the hot, cold and monitoring well between 2010 and 2020, the original and current location of the fresh-brackish interface (150 mg Cl/l) can be schematized, as shown in Figure 7-5.

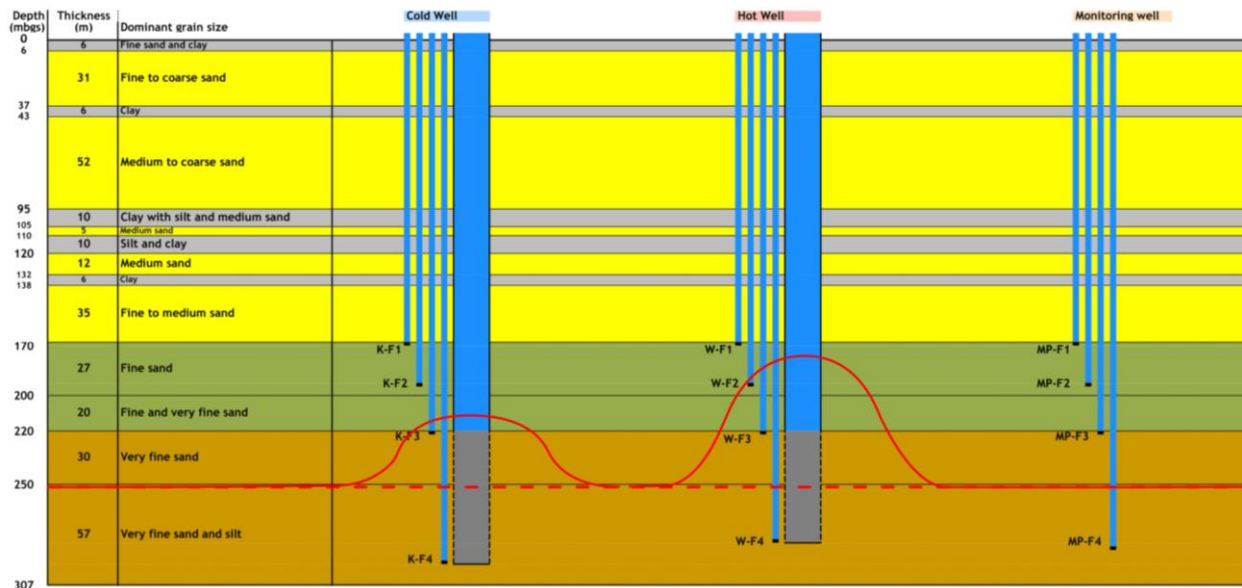


Figure 7-5. Original (dashed line) and expected current location (solid line) of the fresh-brackish groundwater interface (150 mg Cl/l), based on chloride concentration observations.

Processes causing upward transport of chloride

At W-F2, 25 m above the top of the hot well screens, chloride concentrations have clearly increased. This indicates that the mixed water injected in the hot well was transported upwards, bringing chloride with it. The upward transport of chloride at the hot well may be explained by several processes:

- Because of the absence of a clay layer above the hot well screen, part of the mixed water injected in the hot well is forced to flow upward, following the hydraulic gradients set by the pumping. This leads to advective transport of chloride to shallower regions. The actual chloride concentration is dependent of the net amount of mixed water injected at the hot well: the larger the volume of water stored in the hot well, the farther the mixed water will reach. Since water is continuously being injected in and recovered from the hot well, the boundary between the injected mixed water inside the hot bubble and the natural groundwater outside of it is constantly moving. This means that the timing of sampling influences the concentration that will be measured, which is reflected in the fact that two of the chloride peaks at W-F2 were measured at the end of a period in which a considerable net volume of water was injected at the hot well, displacing chloride-rich groundwater towards W-F2.

By assuming that 85% of the net amount of groundwater injected in the hot well at the end of the summer of 2020 was injected in the top 30m of the hot well screen, one can estimate from geometry that the vertical distance that a water and a chloride particle has travelled after injection is about 5 m (based on an anisotropy of 4).

- Density driven flow at the hot well has expectedly contributed continuously to the vertical movement of injected hot water, although the density differences between the injected hot water (45 °C, 500 mg Cl/l) and the cold, fresh water (< 150 mg/l) above the hot well screen are relatively small (< 1%).
- The process of hydraulic dispersion causes the interface between the injected brackish water and the natural fresh water (above the well screens) to be smeared out. This means that the chloride effects reach farther compared to a situation with a sharp chloride front.
- Furthermore, heterogeneities in the flow properties around the well promotes the relatively easier advective transport of chloride through zones with relatively high permeability. Thus, chloride will be transported farther from the well horizontally through relatively coarse sand layers.

Note that heterogeneities in the region above the well screens may also facilitate vertical transport of chloride to this region. Vertical flow may occur within the gravel pack of the borehole, alongside the formation. This is possible because the borehole gravelpack material contains coarse to very coarse sand (coarser than the formation). This may act as a shortcut route that facilitates enhanced vertical flow (hence advective transport of chloride) to shallower regions. If that is the case, the chloride concentrations measured at W-F2 and W-F1 are expectedly higher than the chloride concentration a couple of decimeters into the formation, at that same depth.

Conclusions

At NIOO, the interface between fresh and brackish water was originally located around 250 mbgs, and not at 200 mbgs, as was assumed before system realization. Since the well screens are placed between 220 mbgs and 283/295 mbgs for the hot/cold well respectively, the wells extract fresh water in the top part of the well screen and saline water in the bottom part of the well screen. As a consequence mixing of fresh and saline water occurs in the well pipes after extraction, and this process determines the chloride content of the injected water. In this way the chloride concentrations near the well screens are influenced by the HT-ATES system. Since a considerable net volume of groundwater has been pumped from the cold to the hot well in the 2010 – 2020 period and the chloride content after mixing is brackish, the fresh-brackish water interface has been displaced upwards at the hot well.

Changes in chloride concentrations were measured near the wells at and around heat storage depth, but no changes were observed at the monitoring well 60 m away from the hot storage. This underlines that the HT-ATES system only influences the groundwater composition close to the wells, for the range of water volume displaced over the past 10 years. Because of the absence of a clear confining layer overlying the storage depth, part of the injected water is forced to flow in upward direction, supplying mixed water (with a chloride concentration over 500 mg Cl/l) to shallower regions. Because at NIOO a considerable net volume of water was pumped from the cold to the hot well, the displacement of the fresh-saline water interface is largest at the hot well. It was found that the chloride concentration measured at W-F2 (25 m above the top of the hot well screen) is highly dependent on the timing of measurement: when samples were taken after a period of net water displacement from the cold to the hot well, the observed chloride concentrations consistently showed higher values. This means that the depth of the fresh-brackish water interface at the hot well is partly determined by the historical balance in water displacement between the wells of the doublet HT-ATES system. Other contributions to upward displacement of the interface may come from processes like density-driven flow, hydraulic dispersion and heterogeneities in the vertical flow properties around the well, like the short-cut flow of injected water through the coarse gravelpack material.

7.2 Other chemical parameters

In addition to chloride, other chemical parameters were measured on a regular basis at piezometers K-F3 and W-F3. Based on the measurement data, HT-ATES related processes like mixing, calcite precipitation and carbon mobilization are discussed.

7.2.1 Mixing

The chloride measurements have shown that mixing of deep, saline water from the depth interval of the bottom of the well screens with fresh water from depth interval of the the top of the well screens has been an important process controlling the groundwater composition around the wells, from the start of the HT-ATES operation. Figure 7-6 shows that the mixing process is not only reflected in the chloride measurements, but also in the regular measurements of Electrical Conductivity (EC), boron and bromide near the well screens (W-F3 and K-F3). These trends support that mixing is the primary process determining the concentrations of several chemical parameters near the well.

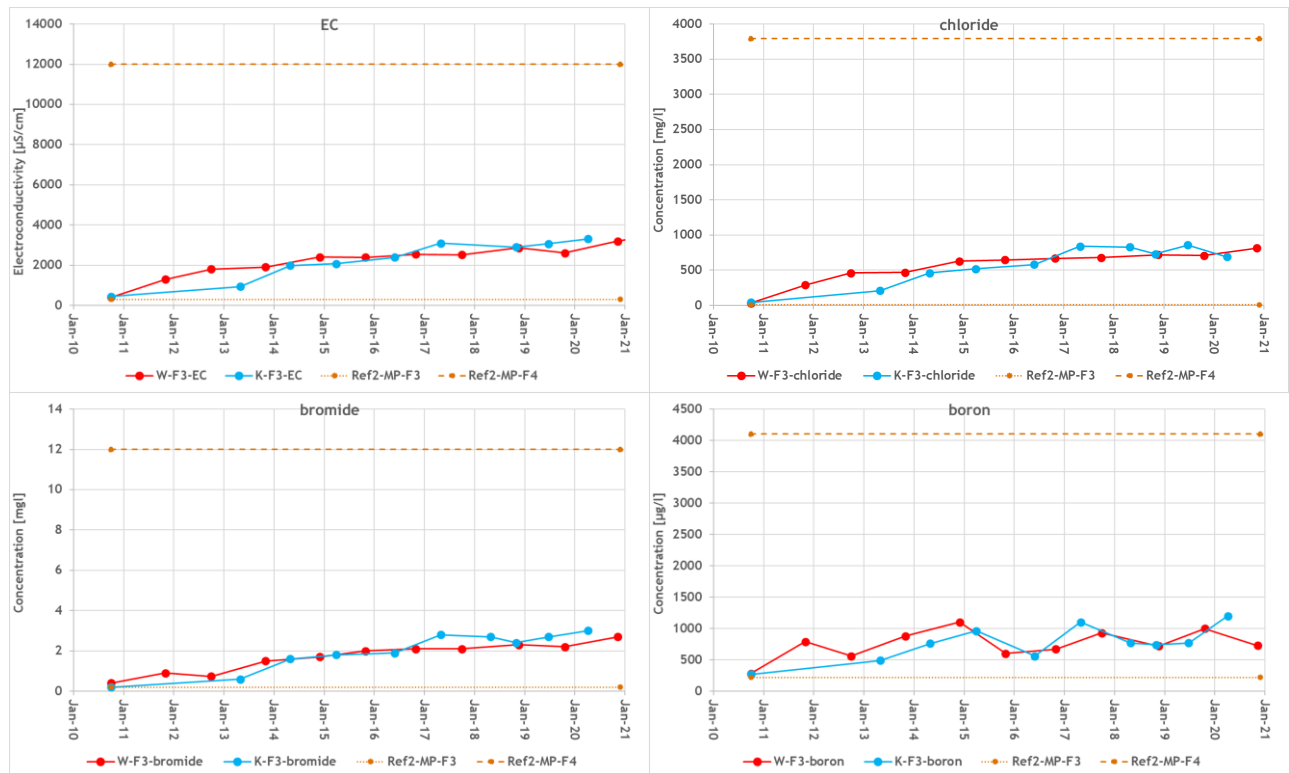


Figure 7-6. Trends of chloride, EC, boron and bromide concentrations with time. The native concentrations at the bottom and top of the well screens are shown as horizontal brown dashed lines. The red and blue lines represent the measured concentrations in groundwater that was sampled from the piezometers that were installed in the depth interval of the top part of the well screens of the hot well (W-F3) and cold well (K-F3) respectively.

7.2.2 Mineral equilibria: calcite precipitation and silicate dissolution

Calcite precipitation

Figure 7-7 shows the trends in several chemical parameters related to carbonates: calcium, magnesium, bicarbonate and pH. The calcium concentration of the mixed water, based on the mixing ratio of 85:15 for the top:bottom part of the well screen, would be around 15 mg/l, which is in line with the range of the measurements. One must keep in mind that mixing two types of groundwater that are saturated with respect to the calcite mineral, lead to a water mixture that is undersaturated with respect to calcite (Goldscheider et al., 2010), which may cause dissolution of calcite due to mixing, instead of calcite precipitation due to the increased temperatures. The only two bicarbonate measurements show an increase over time, which too seems close to the concentration as expected from the mixing ratio. pH shows relatively large deviations especially between 2011 – 2015, but shows a more steady trend over the last years, close to the pH of the original measurements.

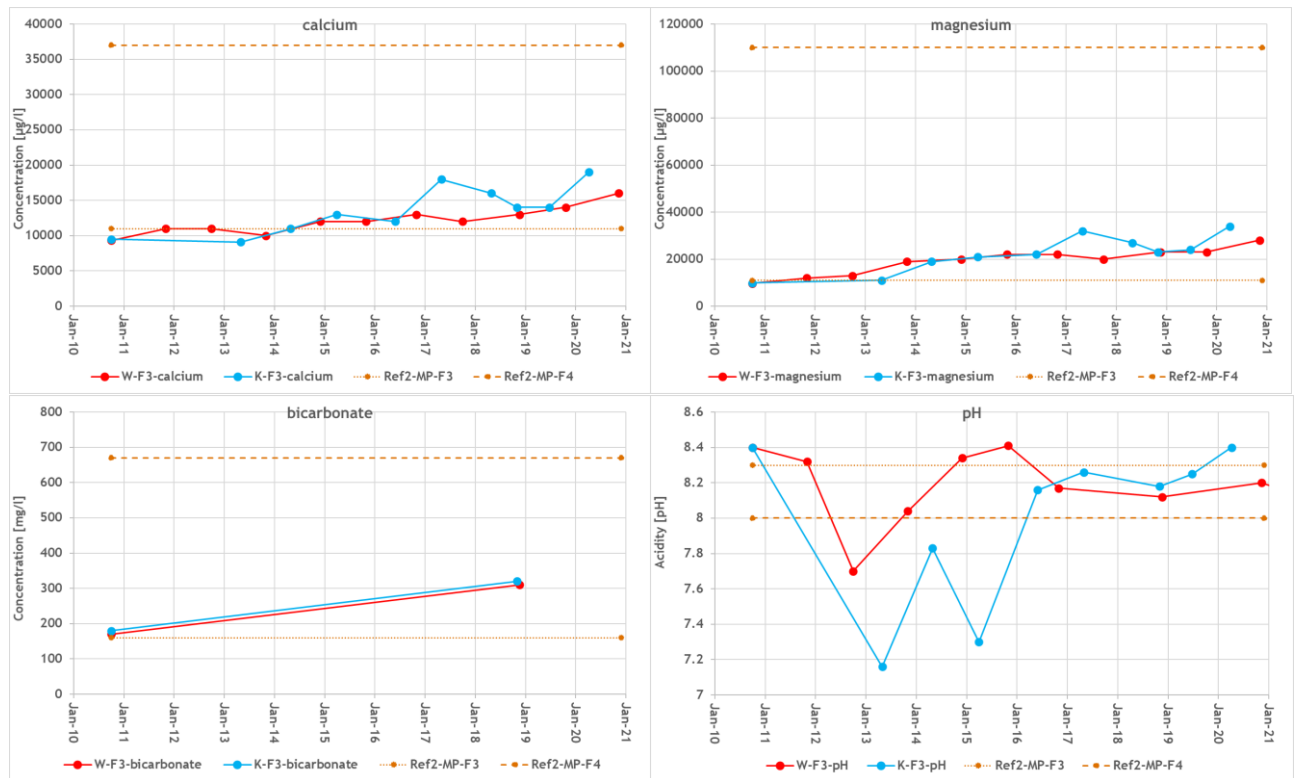


Figure 7-7. Trends in concentrations of calcium, magnesium, bicarbonate and pH over time. The reference concentrations at the bottom and top of the well screens (as measured in 2018) are shown as horizontal brown dashed lines. The red and blue lines represent the measured concentrations in groundwater that was sampled from the piezometers that were installed in the depth interval of the top part of the well screens of the hot well (W-F3) and cold well (K-F3) respectively. Note that pH was measured in the field.

It was expected that the original groundwater in the marine storage aquifer is saturated with respect to calcite, and that calcite is present in the sediment. Still, since storage temperatures are up to 45 °C, no significant precipitation of carbonate minerals like calcite was expected and hence no water treatment has been applied at NIOO. In January 2020, the well screens of the HT-ATES system were inspected by descending a camera into the well, but no calcite precipitates were observed on the well screens. Also, the calcium and magnesium concentrations follow the similar pattern as chloride, suggesting that changes in their concentrations are mainly related to mixing processes. These finding that no significant carbonate precipitation occurs is in line with the literature and with earlier research that showed that no considerable calcite precipitation occurs at these temperatures. The presence of natural inhibitors like phosphate and Dissolved Organic Carbon (DOC) may contribute to inhibiting calcite precipitation at the wells. The measurement data and the camera inspection results suggest that no calcite precipitation occurs at the HT-ATES system at 45 °C, at least not distinctly compared to the mixing effects occurring at the HT-ATES system of NIOO.

Silicate dissolution

Silicon concentrations seems to show a slight increase between 2010 and 2020 (see Figure 7-8), with the trend moving around the MP-F3 reference concentration. The trend may be explained by mixing, while the relatively high MP-F3 concentration compared to the trend may be ascribed to measurement error: reference measurements at K-F3, W-F3 and MP-F3 in 2010 show concentrations around 3,900 µg/l. Bonte (2013) performed column experiments at temperatures of 5, 11, 25 and 60 °C and only found increased silicon concentrations at 60 °C, which he linked to dissolution of silicates. At the NIOO HT-ATES system, the maximum temperature is 45 °C but the average temperature will be lower. The average temperatures well below 45 °C, combined with the mixing as dominant process controlling compositions, may explain why no significant si-increase was observed over the last decade.

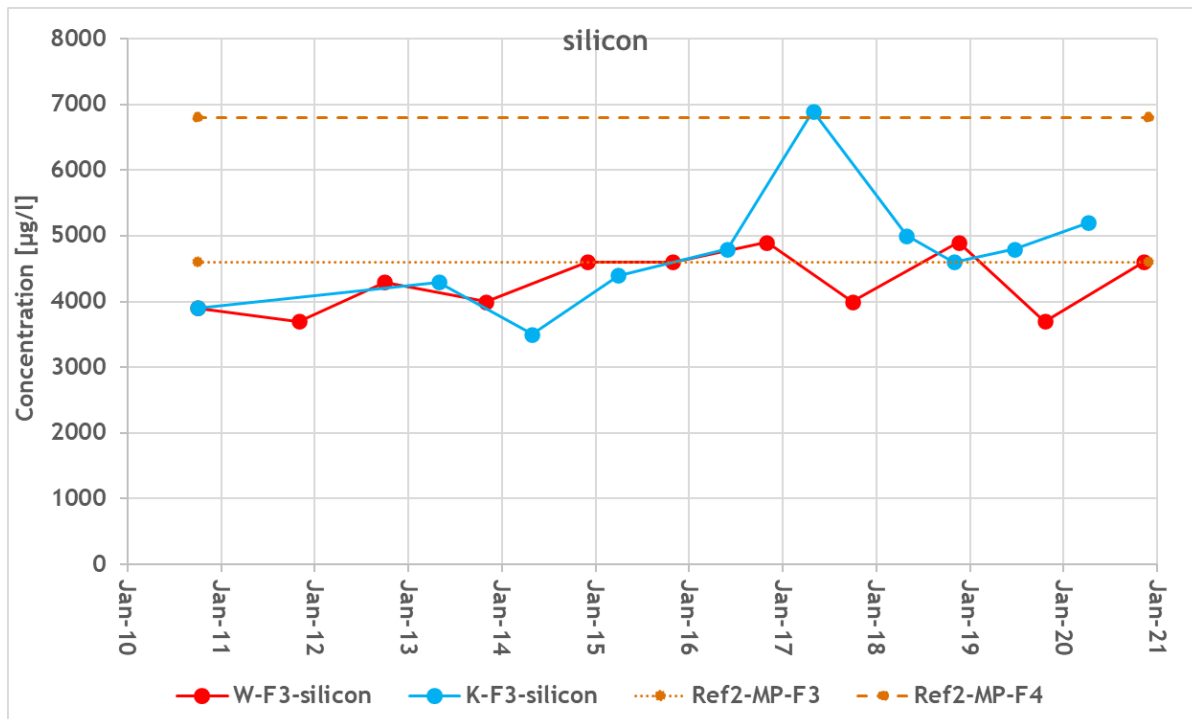


Figure 7-8. Silicon concentration measurements. The native concentrations at the bottom and top of the well screens are shown as horizontal brown dashed lines. The red and blue lines represent the measured concentrations at the top of the hot well (W-F3) and cold well (K-F3) respectively. The blue peak is expectedly caused by a measurement or analysis error.

7.2.3 Organic carbon mobilization

The Dissolved Organic Carbon (DOC) and sulphate concentrations are plotted in Figure 7-9. The concentrations measured in 2010-2012 were all below the detection limit of 5 mg/l and are not plotted. Since 2013, the detection limit was improved and results were more accurate. Literature sources state that DOC concentrations increase when temperatures rise (>40 °C) due to mobilization of organic matter from the solid (sediment) phase to the dissolved phase (Brons, 1992; Meer met Bodemenergie, 2012a, Meer met Bodemenergie, 2012b; Bonte, 2013). However, on average there seems to be a slight increase of DOC concentrations in the wells, which corresponds to the trend that is expected from the mixing process. This suggests that mixing is a more dominant process controlling DOC concentrations than mobilization. A high DOC concentration was measured in 2019 at the hot well (6.2mg/l), which may be attributed to an error in the measurement or in some way be related to the fact that the hot well pump stopped working in September 2019.

Another theory that may explain the absence of an increase in DOC, may be that DOC could be mobilized by the increased temperature whereafter it is consumed directly by microbes. In that way, no increase in DOC is measured. Such microbial respiration processes also require an electron acceptor like sulphate. However, sulphate decrease seems similar to the trend that could be expected from the mixing process (Figure 7-9), hinting that microbial processes may only occur on a non-dominant scale. The camera inspection of the wells in 2020 showed some brown-yellowish flocculent material, expectedly of organic nature. This suggests that microbes are indeed active in and around the wells. However, the groundwater composition data support that the influence of the microbial population on the groundwater composition is subordinate to the effects of the mixing of fresh with saline water. Additionally, the organic carbon content of the sediment is expected to be low, based on the borehole logs. Therefore, it was concluded that the processes of carbon mobilization and microbial respiration have had no considerable effect on the groundwater composition yet, compared to the mixing processes that occur. Note that the influence of microbial processes on the composition depends on the size and activity of the microbial community. This means that their influence may grow over time, but only if significant microbial growth is facilitated.

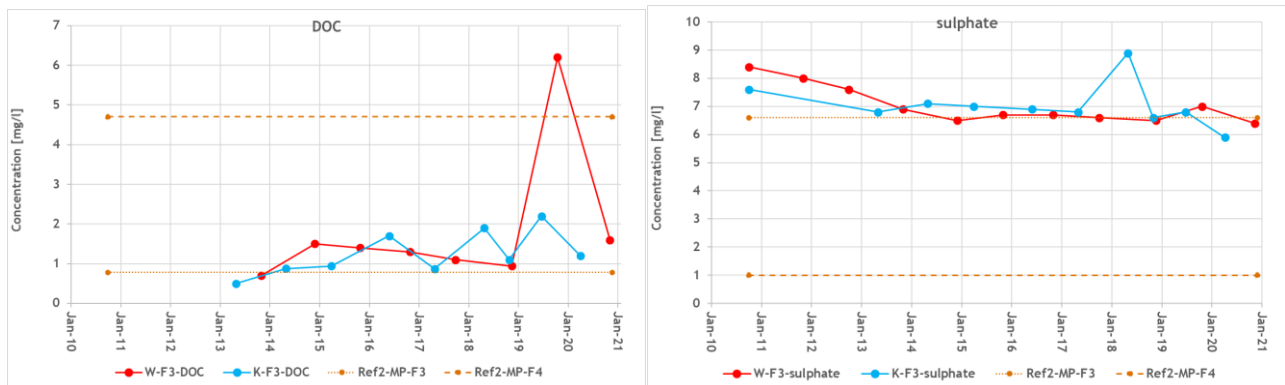


Figure 7-9. Concentrations of Dissolved Organic Carbon (DOC, left) and sulphate (right) over time. For DOC, the measurements between 2010 – 2012 have remained below the detection limit of 5 mg/l and are hence not shown. Since 2013, the detection limit was improved and results were more accurate. The sulphate concentrations remain close to the natural concentration at MP-F3.

7.2.4 Arsenic mobilization

In the literature, arsenic is repeatedly reported to be mobilized when temperatures of the sediment and the groundwater rise. In 2010, before the system was taken into operation, arsenic concentrations were measured at F2, F3 and F4 of the hot, cold and monitoring well to obtain an idea of the natural concentrations at several depths. To investigate whether arsenic concentrations have increased at NIOO, arsenic was measured more extensively in 2018 – 2020, at F2, F3 and F4 of the hot and cold well. The results are summarized in Table 7-2.

An increase in arsenic concentrations is observed at W-F2, at 25 m above the heat storage. Measurements at similar depth (at K-F2 and MP-F2) suggest that the natural groundwater has low arsenic concentrations (<5, 6.3 and 8.8 µg/l). The thermal measurements showed that temperatures around (or just below) W-F2 have increased due to the storage of heat. The heating may have resulted in the mobilization of arsenic from the sediment near W-F2. Or alternatively, the explanation may be that arsenic has been mobilized at the hot well of the HT-ATES system, where it is subsequently transported upwards by advective/convective transport. Bonte (2013) performed a chemical modelling study on arsenic mobilization around HT-ATES wells. He found that arsenic is mobilized (by either desorption or reductive dissolution of iron-oxides) near the heat storage and subsequently transported towards the outer parts of the heated zone, where the heated water cools down because of heat transfer to the cold sand grains and (part of) the arsenic can be sorbed again. Although sorption is not investigated at NIOO, the increased arsenic concentrations at W-F2 may be caused by subsequential mobilization at and transport away from the hot part of the storage. However, the arsenic concentrations measured at W-F3, at the hottest part of the heat storage, have never passed the detection limit of 5 µg/l so far. This may also suggest that the sediment layers around the depth of W-F3 have higher arsenic content, which may be mobilized into the fluid phase at W-F2 because of the locally increased temperatures.

It is suggested to continue the monitoring of arsenic concentrations, to obtain a clearer view of the arsenic concentrations around the HT-ATES system with time.

Table 7-2. Arsenic concentrations as measured at the HT-ATES system of NIOO between 2010 – 2020.

Piezometer	Depth (mbgs)	Concentration (µg/l)					
		Oct 2010 (REF)	Oct 2017	May 2018	Nov 2018	Jun 2019	Nov 2020
W-F1	170 - 172						20
W-F2	193 - 195	5.7			28	31	31
W-F3	220 - 222	<5	<5		<5	<5	<1
W-F4	280 - 282	0.2			<5	<5	<1
K-F1	170 - 172						14
K-F2	193 - 195	8.8			<5	<5	3.6
K-F3	220 - 222	<5		<5	<5	<5	1.1
K-F4	293 - 295	50			<5	<5	1.4
MP-F1	170 - 172	<5					
MP-F2	193 - 195	<5			6.3		
MP-F3	220 - 222	<5			<5		
MP-F4	285 - 287	<13			21		

8 Microbiology

Following the permit conditions, the monitoring aim is to track whether pathogenic microbial species can grow due to the higher temperatures, which might introduce risks for the shallower high quality fresh water aquifers. The 10-year trend of microbial measurement is presented first, followed by additional measurements performed in 2019 and 2021, offering insight in the monitoring of microbiology from another perspective.

8.1 Regular measurements

Microbial groundwater composition was measured twice a year: groundwater from K-F3 was sampled at the end of winter, and water from W-F3 at the end of each summer. The results of the general colony counts (performed at 22, 25 and 37 °C) show a similar pattern (see Figure 8-1 for 25 and 37 °C). An initial peak in general microbial activity can be observed in 2010, expectedly due to the drilling activities, after which general activity sharply drops and remains relatively low.

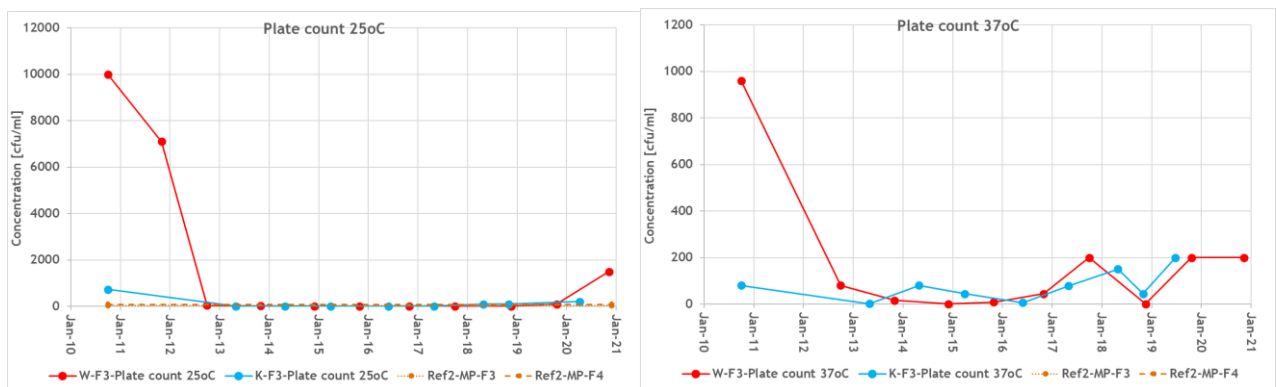


Figure 8-1. Results of the general colony counts performed on the groundwater samples at NIOO. Groundwater sampled from K-F3 and W-F3 were plated and subsequently contained under aerobic conditions, at a temperature of 25 °C (left) and 37 °C (right). The number of colony-forming units (CFU) per ml are indicated on the vertical axes.

Additionally, the groundwater was regularly tested on four pathogenic microbial species, using plating techniques: *Aeromonas*, *Coliforms* (37 °C), *E. Coli* (at 44 °C) and *Enterococci*. The results are consistently showing that <1 colony-forming unit was found per 100 ml sample (concentration below the detection limit), for all these species. Only for *Aeromonas*, the very first measurement (reference) shows a peak, probably caused by the drilling activities.

The data suggest that none of the analysed pathogen microbes (which all prefer aerobic and nutrient-rich (i.e. human body-like) conditions) can survive in the HT-ATES system, in which groundwater is anaerobic, saline and nutrient-poor. This is in line with earlier findings from the literature (Zaadnoordijk, Hornstra, & Bonte, 2013). Initial peaks in microbial presence suggests that the drilling activities create the opportunity for microbes to intrude and survive for some time, but not long-term. Sulphate reducing bacteria may survive, but these had no dominant control on the groundwater composition at NIOO since no considerable deviation of the sulphate concentration from the mixing trend was found.

8.2 Additional microbial analysis in 2019

Looking at the results (see section 8.1), none of the tested microbes were found in the samples and the general colony counts too demonstrated that microbial activity near the HT-ATES wells was relatively low. The standard technique used at NIOO for the microbiological measurements involved plating techniques. Replica plating (or: plate counting) is a way to quantify the relative abundance of a microbial species in a sample. Part of the sample is mixed with a nutrient-rich medium, and poured on a Petri plate so that it can grow. The number of colonies that is formed after a certain time is representative for the original number of cells that were present in the sample. However, this standard technique comes with a low sensitivity, as typically <10% of the microbes present are growing on the plates (so <10% of the microbes can be

measured) and the spread of the result is relatively high (Schiessl & Besmer, 2020). Therefore, alternative microbial analysis methods were used at NIOO, additional to the regular microbial monitoring.

8.2.1 Background: ATP and DNA-analysis

New DNA-based analysis techniques like Next Generation Sequencing (NGS) and quantitative Polymerase Chain Reaction (qPCR) have been developing over the past decade, offering new ways to research microbial populations, potentially with better results. Also, the literature advocates for AdenosineTriPhosphate (ATP) as a chemical parameter that is indicative for the activity of the biomass present in the sample (Zaadnoordijk et al., 2013).

Using Next Generation Sequencing (NGS), all organisms in a water sample can be characterized. This is done by analyzing all DNA that is present in a sample. Using existing genomic libraries on numerous species, the microbiological population of the sample can be characterized on a Genus level with this powerful analysis tool. The result of such an analysis offers a 'fingerprint' of the microbiological population in the sample.

Quantitative Polymerase Chain Reaction (qPCR) is another DNA-based analysis method which is used to identify a specific microbial species, by checking whether its characteristic DNA-sequence is found in a sample. This analysis is suitable when looking for a specific species of which the unique genomic sequence is known.

ATP is an energy-rich chemical substance that plays an important role in the metabolism of each living organism. Therefore, the concentration of ATP in a sample is representative for the (relative) activity of the biomass present. ATP is relatively affordable to analyze, and can hence be used as a signal parameter, signaling when biomass activity increases, for example when increasing temperatures have lead to conditions that are (more) favorable for microbial processes. When ATP concentrations start increasing considerably, more expensive DNA-based analysis methods may be considered to investigate how the population developed. Potentially, monitoring of the microbial population can provide valuable information that helps to better understand which processes occur. In this way, it is a addition to chemical monitoring. At the same time, microbiological monitoring is more complex and relatively expensive. As a consequence, microbial monitoring of ATEs systems is relatively scarce.

Based on the literature, a few pathogenic microbes may survive the anaerobic, saline and nutrient-poor conditions of the subsurface, like the protozoa *Acanthamoeba* and some pathogenic species of the *Vibrio* genus (KWR, 2011). Since the DNA-sequences of these specific microbes are known, they can be identified with qPCR or NGS.

The possible inaccuracy of the standard plating technique used at NIOO since 2010, as well as the potential discovery power of the more recently developed DNA-based analysis techniques, brought NIOO to perform additional measurements on microbiology using these newer methods. The objectives of the extra measurements were:

- to obtain insight in the general microbial activity of the groundwater by measuring ATP concentrations.
- to investigate whether specific pathogenic microbes (like *Acanthamoeba* and *Vibrio*), which may survive the subsurface conditions, are actually found in the subsurface;
- to compare the results of new DNA-based analysis techniques (NGS, qPCR) with the results of standard plating techniques;
- to obtain an image of the general microbial composition of the groundwater and the chemical processes they may help facilitate.

8.2.2 Methods: NGS, qPCR and ATP measurements at NIOO

In 2019, groundwater was sampled from the NIOO HT-ATES system at heat storage depth and NGS, qPCR and ATP-measurements were performed to obtain a deeper understanding of the microbial population living around the HT-ATES system. These analyses were performed using budget from the HEATSTORE project.

In September 2019, groundwater was sampled from the heat storage depth, at the hot well (W-F3) and the monitoring well (MP-F3). NGS was applied to both samples to obtain a genetic fingerprint of the microbial population at these two locations. Additionally, qPCR and ATP analyses were applied on the W-F3 sample: A number of species were looked for in the W-F3 sample, using qPCR:

- *Aeromonas* spp., *Enterococccen* EPA, *E.coli* HSP: three species that have been measured by plating techniques since 2010, following the permit instructions. It is to be checked whether the results from the qPCR method are in line with the long-term 'plating' trend.
- *Acanthamoeba*: this is a pathogen that is potentially capable of surviving in deep, anoxic, saline groundwater, as identified in a report on microbiological risks that was made for a study on HT-ATES in Brielle (KWR, 2011).

Another pathogen that may survive in the harsh environment around a HT-ATES is the *Vibrio* spp.. Since no qPCR analysis was available for this species, its presence in the W-F3 sample was analyzed using a plate count technique, performed by the RIVM institute (National Institute for Public Health and Environment) in the Netherlands. Also, the ATP concentration at W-F3 was measured to obtain a general insight in the activity of the biomass near the hot well.

It was expected that the activity and diversity of the microbial population around the HT-ATES is limited, because of the anaerobic, saline, relatively cold (under natural conditions) and nutrient-poor conditions. When expected microbe presence is low, the microbial composition of the samples is more sensitive to disturbance during sampling. Hence, it is important to illustrate the sampling method, to show where external microbes may intrude in the sample: Before the piezometer is sampled, three times the piezometer volume is extracted to ensure that groundwater from the storage aquifer has entered the piezometer. A small polyethylene (PE) sampling tube is lowered into the piezometer, up to a depth of 1 – 5 m below the water level, before pumping up a groundwater sample through the tube with a low flow rate. The sample is pumped in a bottle, stored under dark and cool conditions, and brought to the laboratory, where it is to be analyzed within 24 hours after sampling.

8.2.3 Results

The results of the analyses performed in September 2019, as described above, are shown in Table 8-1. The results of the regular microbial analysis using plating techniques (samples W-F3 taken in October 2019) are added for comparison.

Table 8-1. Measurement results for pathogenic microbes, as identified by the NGS, qPCR, plating and other microbiological analysis techniques. Sampling was performed in September-October 2019 at piezometers W-F3 and MP-F3.

NGS-analysis Samples taken 24-9-2019				qPCR-analysis Samples taken 24-9-2019				Plating (oct 2019) Samples taken 23-10-2019			
Pathogen name	Method	MP-F3	W-F3	Pathogen name	Method	W-F3	unit	Parameter name	Method	W-F3	unit
total Krona reads	NGS	59662	10154								
% of total DNA counts											
Burkholderia (Genus)	NGS	0.70%	2.00%								
Campylobacter (Genus)	NGS	0.10%	0.10%								
Pseudomonas (Genus)	NGS	1.00%	2.00%								
Enterobacteriales (Order-level)	NGS	0.80%	0.20%								
Enterococcus (Genus)	NGS	0.06%	not found	Enterococcus (EPA)	qPCR	<240	gene copies/l	Coliformen	filtration + plating	<1	cfu/100ml
Legionella (Genus)	NGS	0.20%	not found					Enterococccen	filtration + plating	<1	cfu/100ml
Aeromonas (Genus)	NGS	0.10%	0.10%	Aeromonas spp.	qPCR	<1200	gene copies/l	Aeromonas spp.		<1	cfu/100ml
Vibrio (Genus)	NGS	0.08%	not found								
Salmonella (Genus)	NGS	0.04%	not found								
Escherichia (Genus)	NGS	0.02%	not found	E. Coli (HSP)	qPCR	<240	gene copies/l	Escherichia coli (44C)	filtration + plating	<1	cfu/100ml
Stenotrophomonas (Genus)	NGS	0.10%	0.10%								
Total concentration of DNA found	µg/ml	0.252	0.281	Acanthamoeba	qPCR	3580	gene copies/l	sulfite-reducing clostridia traces	filtration + plating	<1	cfu/100ml
								Colony count (22C)	plating	88	cfu/ml
								Colony count (25C)	plating	92	cfu/ml
								Colony count (37C)	filtration + plating	>200	cfu/100ml

Other measurements taken from sampling well W-F3, at 24-9-2019			
Parameter name	Method	result	unit
Vibrio species (37C)	Plating	<1	MPN/l
ATP	n.a.	<1	pg/ml

The NGS-analysis showed DNA-concentrations of 252 ng/ml and 281 ng/ml in M-F3 and W-F3 respectively. In general, the NGS-analysis of both W-F3 and MP-F3 identified a microbial population with both aerobic, facultative anaerobic and strictly anaerobic metabolisms (a general view of the NGS-results is shown in Figure 8-2). Note that, based on the hydrogeological situation and the associated redox conditions in the subsurface, no oxygen or nitrate is present in the storage aquifer (which is also supported by the chemical monitoring results).

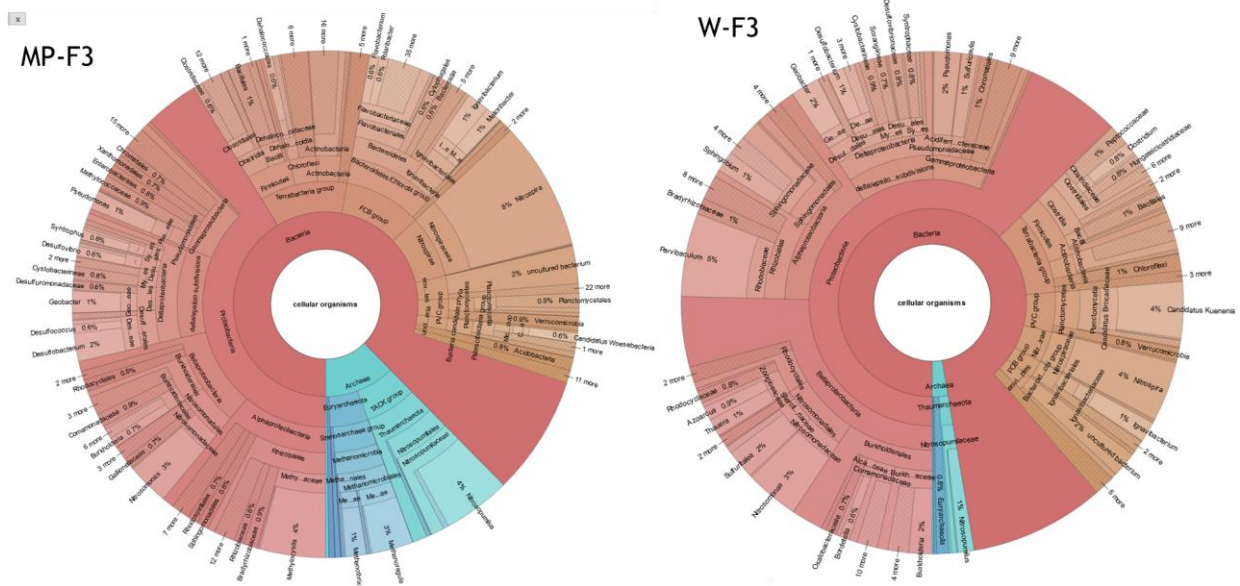


Figure 8-2. Pie charts with the genera found in 2019, at the storage depth, at the monitoring well (MP-F3) and the warm well (W-F3).

Focusing on the pathogenic species as identified in the report of KWR (2011), the following was found:

- Table 8-1 shows that no pathogenic microbes were found with the plating and qPCR techniques.
- ATP concentration in W-F3 is below detection limit (<1 pg/ml), indicating a low overall microbe activity.
- According to the NGS-analyses, DNA-concentrations of W-F3 and MP-F3 are similar.
- The most dominant genera found in the NGS-analyses are both anaerobic and aerobic.
- Following the NGS-results in the table, a minor relative abundance of some specific pathogens was found. The relative abundance of pathogens is higher for W-F3 (4,5%) compared to MP-F3 (3,2%) based on the counts, but the composition of pathogens varies (specifically for Burkholderia and Pseudomonas).
- Some microbial genera found with NGS in MP-F3 are not found in W-F3 (e.g. Enterococcus), but oppositely, some pathogens have higher relative abundance in W-F3 than in MP-F3 (like genera of Burkholderia and Pseudomonas).
- In both MP-F3 and W-F3, the (near) absence of *Enterococcus*, *Aeromonas* and *E. coli* in all of the NGS, qPCR and plating analyses (indicated in blue in Table 8-1) support that these pathogens are not likely to grow in subsurface conditions, even when temperatures increase. The finding that the genera of *Enterococcus*, *Legionella*, *Salmonella* and *Escherichia* are found at MP-F3, but not at W-F3, is in line with earlier findings in the literature that aerobic pathogens die off faster under the anaerobic conditions in the subsurface when temperatures increase (KWR, 2011).
- NGS and plating both showed that *Vibrio* is not present at W-F3, and a tiny amount of *Vibrio* was found with NGS at MP-F3. It is not distinguishable whether this *Vibrio* belongs to a pathogenic or harmless *Vibrio* species.
- qPCR-analysis of W-F3 showed that some *Acanthamoeba* is present in this piezometer or in the subsurface near the hot well. Note that qPCR cannot distinguish between DNA from living or dead organisms.
- The colony count (October 2019) suggest that some microbes are present. However, the activity of the microbes in the subsurface is very low, since it must be kept in mind that colonies are grown after a period of incubating the microbes on a nutrient-rich medium under warm and oxic conditions for some time: conditions not representative for the subsurface.

8.2.4 Discussion

In general, the results of the various types of analyses (NGS, qPCR, plating, ATP) in autumn 2019 are consistent with each other.

The NGS analysis results showed that both aerobic and (semi)anaerobic genera were found in the samples. From this, it was concluded that the regular sampling methodology provided a groundwater sample with both (anaerobic) microbes from the storage aquifer, and (semi-)aerobic microbes. The presence of (semi-)aerobic

microbes is striking, since these microbes grow under (semi-)aerobic conditions which are unlikely to occur in the storage aquifer. This suggests, that the results are not representative for the storage aquifer. In the top of the piezometer, where the sample was collected, (semi)aerobic conditions are more realistic. Note that the water level within W-F3 will respond to the injection/production at the hot well, periodically allowing oxygen to intrude in the upper part of the piezometer, which may then diffuse into the top meters of groundwater. This is in line with frequent observations of iron(hydr)oxide precipitates near the water level in camera inspections of ATES wells. This oxygen may facilitate the growth of aerobic microbes, potentially attached to the inside piezometer walls in biofilms. The regular sampling method samples groundwater at 2 – 5 m below the water level of the piezometer, so that parts of the biofilm may be sucked into the sampling tube during sampling. This advocates for a further investigation of the influence of the sampling methodology on the results and adjusting the procedure for the next sampling, which was planned in 2021 (see below).

Regarding the low representation of pathogenic microbes in all of the NGS, qPCR and plating analyses, it seems that the conditions in and around HT-ATES are not feasible for growth of pathogens. The measurement of *Acanthamoeba* at W-F3 requires attention, but it is hard to say if this concentration is higher than in the undisturbed groundwater (since *Acanthamoeba* was not measured in the monitoring well) and at what concentrations this pathogen actually starts being harmful. Moreover, the ATP-analysis indicates that the present biomass has a very low activity, hence that microbes will not grow easily, let alone flourish, in the harsh subsurface environment around the HT-ATES system. This 2019 measurement represents only one specific moment in time hence follow-up monitoring on these parameters is advised, which was performed in 2021 (see below).

8.3 Additional microbial analysis in 2021

The results of microbial analysis in 2019 hinted that the sampling methodology influenced the composition of the groundwater sample. (Bloemendal et al., 2020) too showed for the other Dutch HEATSTORE HT-ATES case study of Koppert-Cress that the sampling methodology has effect on the microbial analysis results: the sampling depth and the flow rate by which the water in the piezometer was extracted played a role.

A follow-up microbial sampling was performed at NIOO in July 2021. The aim was to address the following research questions:

- What is the effect of the groundwater sampling methodology on the microbial analysis results?
- What are the differences in microbial composition in MP-F3 and W-F3?
- How have the concentrations of ATP and of the pathogen species of *Acanthamoeba*, *Enterococccen* and *E.coli* changed in 2021 compared to 2019?

8.3.1 Methods

To research the microbial composition at storage depth, groundwater from storage depth was sampled at the hot well (piezometer W-F3) and the monitoring well (MP-F3). The samples from both piezometers were analyzed on the same set of parameters, facilitating comparison of the results:

- ATP concentration
- NGS-analysis
- qPCR-analysis on *E. coli*, *Enterococcus*, *Acanthamoeba*.

Additionally, to research the influence of sampling methodology on analyses results, the samples taken from each piezometer were gathered using both the 'regular' and a new sampling methodology, described below.

Regular sampling methodology

This methodology corresponds to the NEN5744 norm for sampling of groundwater. Before the piezometer is sampled, three times the piezometer volume is produced from the well to ensure that groundwater from the storage aquifer has entered the piezometer. The pump is removed from the piezometer and a small polyethylene (PE) sampling tube is lowered into the piezometer, up to a depth of 2 – 5 m below water level. Then, groundwater is pumped through the tube with a low flow rate and gathered in the bottle.

New sampling methodology

The new method aims to gather groundwater from the piezometer at greater depth, so that the sample better represents the groundwater of the piezometer well screen depth, with smaller atmospheric influences. Just like in the regular method, three piezometer volumes are discharged before sampling. The sampling occurs by descending a submersible pump into the piezometer, to a depth of 20 – 25 m bgs. At the NIOO

piezometers of W-F3 and MP-F3, no air has ever been present at this depth (the pump inlet is ~20mbgs in hot well), and atmospheric influence is considerably smaller compared to the top of the piezometer, because of the several meters of water above the intake depth. The water is pumped from this depth into the sampling bottle.

In both methodologies, after sampling, the bottle is stored under dark and cool conditions, is delivered to the laboratory on the same day and is to be analyzed within 24 hours after sampling.

For each piezometer (W-F3 and MP-F3), groundwater samples were gathered using the new method first, followed by the regular method. All NGS (2.4L per sample) and qPCR (1L per sample) samples were gathered in duplo.

8.3.2 Results

Field measurements are shown in Table 8-2. The results of the microbial analyses are shown in Table 8-3. The NGS analysis report with a more elaborate description of results and interpretations is attached in the appendix.

Table 8-2. Field measurements performed on the extracted groundwater, on the moment before the groundwater was put in the sampling bottles. Note oxygen in 'W-F3 Regular' is relatively high.

Field measurements					
Piezometer	Sampling method	EC	pH	O ₂	Temp
		μS/cm	-	mg/l	C
MP-F3	New	307	8.75	0.11	14.3
MP-F3	Regular	307	8.53	0.23	13.5
W-F3	New	3470	8.14	0.14	27.2
W-F3	Regular	3240	8.08	2.71	26.5

Field measurements show that the EC-values at MP-F3 have not changed significantly compared to reference measurements of 2010 (320 μS/cm) and 2018 (304 μS/cm). This suggests that no injected (mixed) water has reached the monitoring well yet. Oxygen concentration is relatively high in the W-F3 Regular sample. This means that either relatively oxic water is attracted from the top part of the piezometer where air can enter the tube, or it may be caused by a measurement error.

Table 8-3. Analysis results of microbial samples gathered on July 13th, 2021.

Piezometer	Sampling method	ATP-analysis	qPCR-analyses								NGS-analyses	
		pg/ml	gene copies/l								ng/ml	
		ATP	E.Coli	Duplo	Enterococcus	Duplo	Aeromonas	Duplo	Acanthamoeba	DNA conc	duplo	
MP-F3	New	<1	240	<200	<170	<200	<830	<980	11000	1270	1090	
MP-F3	Regular	13	400	<260	<250	260	4000	<1300	590000	29000	26200	
W-F3	New	3.3	<190	<190	<190	<190	29000	21000	43000	3520	3060	
W-F3	Regular	46	740	460	4700	8100	16000	9600	1100000	63000	56000	

Regular versus New sampling methodology:

After comparing the sample analysis results of the new and regular method for each piezometer, the following was observed:

- In many ways, the results of the regular method differ from the results of the new method.
- Comparing ATP concentrations, the regular method consistently shows higher concentrations.
- qPCR results show that the number of gene copies in the samples taken with the regular method is consistently higher compared to the new method, with one exception (*Aeromonas*).
- The qPCR results show that the duplos taken with the new method show consistent concentrations, while the duplos taken with the regular method shows larger differences in concentrations.
- NGS analyses show that the DNA-concentration is on average about 20 times higher for samples gathered using the regular method, compared to the sample from the same piezometer taken by the new method.

- The NGS analysis report (see appendix) shows that a small number of (mainly nitrifying) microbial genera is strongly dominating in the samples taken with the regular method. The samples taken with the new method show a more diverse composition of microbial genera.
- Based on the NGS-report, some samples taken with the regular method indicates that the sample may not be homogeneous, which may be related by the presence of sediments or biofilms in the sample.

Differences between W-F3 and MP-F3:

Addressing the analysis results from the two different piezometers, the following was observed:

- ATP is consistently lower in MP-F3, compared to W-F3
- For the qPCR results on the pathogens *E.Coli* and *Enterococcus*, the results are the same for both piezometers, when looking at the new method (near or below detection limit). Looking at the regular method, (sample taken from top of piezometer), the concentrations of *E. coli* is slightly higher and *Enterococcus* is significantly higher in W-F3.
- qPCR results for *Aeromonas* and *Acanthamoeba* show higher gene copy concentrations in W-F3 compared to MP-F3.
- The NGS analysis results show that DNA-concentrations are a factor 2-3 higher in W-F3 compared to MP-F3.
- Looking at the NGS results of the new method (described in the appendix), the monitoring well seems more anaerobic than the warm well piezometer. W-F3 is mainly dominated by aerobic, or facultatively anaerobic (such as nitrate reducing or iron reducing) microbial genera. The monitoring well is mainly dominated by strictly anaerobic microbial genera such as methanogens and sulphate reducing bacteria.
- Looking at the NGS results of the regular method, the differences between the two piezometers are not as clear and in general they both appear to contain mainly aerobic or facultatively anaerobic microbial genera. However, some dominant strictly anaerobic genera are present in the monitoring well, indicates that the sample contained inhomogeneities (like sediment or biofilm).

Comparing results of 2021 with 2019

The results at W-F3 of 2021 can be compared to the results of this same piezometer in 2019 (see Table 8-1). Note that in 2019, the samples were gathered using the regular method.

- ATP has increased in W-F3 from <1 pg/ml in 2019 to 46 pg/ml in 2021 (regular method). The new method in 2021 shows a concentration of 3.3 pg/ml.
- According to the qPCR analysis, all four measured pathogens have increased in concentration:
 - *Aeromonas* has significantly increased in W-F3 from <1200 copies/l (2019) to >9600 copies/l in 2021
 - *Acanthamoeba* has significantly increased in W-F3 from 3560 copies/l (2019) to >1 mln copies/l in 2021.
 - Although more moderate than *Aeromonas* and *Acanthamoeba*, the concentration of gene copies has also increased for *E.Coli* and *Enterococcus*.
- Taking the regular sampling method results of W-F3 in 2021, the NGS analysis shows that the DNA-concentration in W-F3 is considerably higher in 2021 (63000 ng/ml) compared to 2019 (252 ng/ml). Taking the 2021 DNA-concentration of the new method also shows a more than 10-fold increase in DNA-concentration (to 3000 – 3500 ng/ml) compared to 2019.
- The NGS results showed that a number of strictly anaerobic microbial genera are not dominant in 2021 that were in 2019, such as *Syntrophus* (1,217x higher in 2019) and the Anammox bacteria *Ca. Brocadia* (10x higher in 2019) and *Dehalococcoides* (not detected in 2021). Vice versa the only microbial group that is significantly more dominant in 2021 is aerobic ammonium oxidising bacterium *Nitrosopumilus* (average of duplicates is 48x higher than in 2019). Shortly, both DNA-concentration and the relative abundance of aerobic genera are significantly higher in 2021 compared to 2019.

8.3.3 Discussion

Regular versus New sampling methodology:

The hypothesis, based on the 2019 results, was that the microbial analysis of samples gathered using the regular method would show two types of microbes in one sample: one part of the microbes in the sample would be gathered from groundwater from the storage aquifer (low activity, limited amount of microbes), and another part would originate from the top part of the piezometer, where (semi)oxic conditions prevail and where aerobic microbes may grow in biofilms in greater numbers and in higher activity. By taking the

groundwater samples from the piezometer at a greater depth (i.e. using the new method), the relative contribution of water from the shallow (semi-oxic) part of the piezometer would be smaller.

This hypothesis is supported by the monitoring results of 2021: Both ATP and DNA concentrations of all analyses were consistently and considerably higher for samples taken with the regular method, compared to samples taken with the new method (except for *Aeromonas*).

Also, the NGS report indicated inhomogeneities only in the samples of the regular method, hinting to the collection of biofilm into the samples. The NGS analysis showed the relative abundance of nitrifying microbes in the samples taken with the regular method, which are expected to live near the top of the piezometer closest to the atmosphere.

Aeromonas forms one exception (in W-F3, its gene concentration was higher for the new method than for the regular method), but the high *Aeromonas* concentration in the qPCR analysis was put in perspective by the NGS-results, where *Aeromonas* genus was observed in very limited relative abundance (0.004 – 0.06% of observed cellular organisms). This shows that the relatively high number of *Aeromonas* gene copies (compared to other species) found in the qPCR-analysis may still represent only a fraction of the total abundance of microbes present in the sample.

Based on the results on the regular vs. new sampling method, the new sampling method should deliver a groundwater sample that is more representative for the groundwater in the subsurface compared to the regular method.

Differences between W-F3 and MP-F3:

Based on the findings above, the microbial composition of the groundwater in the storage aquifer can best be investigated using the new method, although with this method some material (water or biofilms) from the upper part of the piezometer may still be collected. By looking at the 2021 results of the new method, the following interpretation was derived from the observations:

- Both the ATP- and the DNA-concentrations are higher in the W-F3 samples compared to samples from MP-F3. Although this may hint to a higher activity and larger microbial biomass in the subsurface around W-F3 compared to MP-F3, it must be noted that, expectedly, part of this difference is caused by the fact that the conditions at the top of W-F3 are more feasible compared to the top of MP-F3, and at least some water from this shallow part will be collected in the new sampling method.
- Note that the feasibility for survival and growth of microbes is controlled by several factors:
 - nutrient availability
 - temperature: higher temperatures stimulate metabolic processes (temperatures ranged about 26-28 °C in July according to the field measurements)
 - availability of oxidators, facilitating respiratory processes.
- Although the temperature in the storage aquifer is increased by HT-ATES, the low amount of nutrients and the limited availability of oxidators in the subsurface still complicate large-scale microbial growth in the storage aquifer. So, although it cannot be ruled out that the elevated concentration and activity in W-F3 compared to MP-F3 is caused by the elevated temperatures in the storage aquifer, the collection of water from the top part of the piezometer has strong influence on the analysis result.
- This means that the challenge in researching the microbial effects in HT-ATES storage aquifers requires a reliable method to obtain samples representative for the groundwater in the aquifer. The improvement of sampling methods is needed in order to obtain representative groundwater samples from HT-ATES storage aquifers, which in turn facilitate the further research on microbial effects in the subsurface.

Comparing results of 2021 with 2019

The significantly higher ATP and DNA-concentration at W-F3 in 2021 compared to 2019 suggests that the microbial population near W-F3 in 2021 was generally larger compared to 2019. No ATP-measurements were done at MP-F3 in 2019, but here too the DNA-concentration in 2021 was significantly higher. The NGS-analysis showed that the microbial composition at both W-F3 and MP-F3 represented more aerobic species in 2021 compared to 2019. This would indicate that the conditions are more aerobic in the samples of 2021 than in the sample of 2019. This may be explained by the intake of relatively more biofilms in 2021, collected from the top of the piezometers. Also the sample gathered with the new method shows significantly higher DNA-concentrations compared to 2019 for both W-F3 and MP-F4. This may suggest that in general the microbial population has grown over the last two years, but it is not clear to what extent oscillation has occurred between 2019 and 2021. Possibly, the surface temperatures at the time of measurements being higher in 2021 (mid-July) compared to 2019 (end of September) may have played a role in the size and activity of the microbes at the top of the piezometer, and this may have influenced the sample composition.

Another explanation may be that, even using the new method, part of the sampled water originates from the top of the piezometer, where expectedly microbial activity and concentration is highest.

Note that because of the seasonal activity of the well, temperatures vary all the time and the composition of the groundwater extracted from the wells may be influenced by the moment at which a sample is taken. This means that the timing of the sampling may also influence the analysis results. Temperatures in W-F3 will be higher in July compared to September, because high temperature heat will be stored from May to August, heating the piezometer during these weeks. In September, pumping of heat is less frequent and the system may even be inactive for some days. Hence, the average temperature both at the bottom and top of the W-F3 piezometer will be lower, causing lower activity, and potentially even the decrease of biomass.

Whereas the DNA-concentrations were similar at W-F3 and MP-F3 in 2019, the concentrations at W-F3 were considerably higher than MP-F3 in 2021. This suggests that the factor of temperature cannot be ruled out in the explanation of this difference: the W-F3 piezometer will always have a higher temperature, both at the bottom (near the heat storage) and at the top (where heating occurs because its vicinity to the hot well pipe).

9 Modelling heat and solute transport

9.1 Introduction

The field data have provided insight in the temperatures and groundwater composition in the near vicinity (<0.5 m) of the HT-ATES wells. The temperature and chloride concentrations at the monitoring well show that no significant effects of HT-ATES have reached the monitoring well over the past decade. However, the question remains how temperatures and chloride concentrations have changed in the region between the wells and the monitoring well. Furthermore, the development of the chloride concentrations in the vertical direction is of interest considering the possible impact on the freshwater body in the third aquifer. In order to obtain more insight in this, a numerical model was built to simulate the heat and solute transport around the NIOO HT-ATES system. The software package Heat and Solute Transport 3D (HST3D) was used to reconstruct the changes in temperature and chloride concentrations around the HT-ATES system. The findings from the previous sections and registered data on injected and produced water temperatures and volumes were used as input for the model calculations. The results of the model calculations were compared to the results of the available field measurements. The main questions are if the observed changes in the chloride concentrations in the more shallow piezometers can be explained by the model calculations and if so: what are the predictions on how the impact in both the horizontal and the vertical direction will develop in the coming years?

9.2 Methods

9.2.1 HST3D Software

The HST3D (Heat and Solute Transport 3D) software of IF Technology is capable of simulating heat and solute transport in water-saturated groundwater systems (Kipp, 1997). The model numerically solves the fluid, heat and solute transport by the following equations. The flow equation of the model is formed by the conservation of total fluid mass and Darcy Law for porous media. The conservation of enthalpy for fluid and porous medium is used for the heat transport equation. For the solute transport, the conservation of mass of a solute species, which may decay or adsorb to the porous medium, is applied. The model includes dependency of fluid viscosity on temperature and solute concentration, as well as the dependency of fluid density on pressure, temperature and solute concentration. These latter properties are important to consider, specifically in HT-ATES systems, as temperature ranges are larger in comparison to ATES systems, resulting in significant variation in fluid viscosity and density, which in turn affect the flow.

9.2.2 Model input parameters

Spatial discretization

The horizontal extent of the model is 2 x 2 km, made up by 73 nodes in the X direction and 73 nodes in the Y direction. The model grid is relatively dense in the center of the model, where the wells are located, and decreases towards the edges of the model. The modelled depth interval is 305 m thick (from 95 to 400 mbgs), with 36 nodes. Vertical grid density is highest near the well screens and decreases towards the top and bottom of the model. With this spatial discretization, simulation results were not affected by the boundary conditions.

The locations (X,Y) and the screen depths of the wells and all the piezometers were put in the model, according to Table 3-1 and Table 3-2.

Hydrogeological and thermal properties

The hydrogeological and thermal properties applied to the model are static, i.e. constant in time. These properties are assumed to be laterally homogeneous but may vary with depth, as is shown in Table 9-1.

Table 9-1. Static properties of the model regions: Horizontal and vertical hydraulic conductivity (K_h and K_v), porosity (n), storativity (S) based on Van der Gun (1979), volumetric heat capacity of the grains ($C_{v,grains}$), bulk thermal conductivity (λ).

Layer	Depth mbgs	K_h m/d	K_h/K_v -	K_v m/d	n -	S -	$C_{v,grains}$ $MJ\ m^{-3}\ ^\circ C^{-1}$	λ $W\ m^{-1}\ ^\circ C^{-1}$
Aquitard 2	95 - 138	0.01	10	0.001				1.8
Aquifer 3	138 - 170	10	2	5	0.35	3.01E-04	2	2.4
HB1	170 - 200	8	4	2	0.35	2.55E-04	2	2.1
HB2	200 - 220	5	4	1.25	0.35	1.58E-04	2	2.1
Filter top	220 - 250	2.4	4	0.6	0.35	2.24E-04	2	2.2
Filter bottom	250 - 295	0.4	4	0.1	0.35	2.30E-04	2	2.2
HBbottom	295 - 400	0.01	10	0.001	0.35	1.49E-04	2	2.1

Fluid properties

A volumetric heat capacity of 4189 J/(kg °C) was applied for water. The density and viscosity of the groundwater is dependent on pressure, temperature and solute concentration.

Initial conditions

A pressure gradient of 3 Pa/m is superimposed on the hydrostatic pressure field to form the initial pressure field. The gradient represents the regional hydraulic gradient of 0.3 m/km in southwestern direction, as is applicable to the third aquifer. The input for the initial chloride concentration profile is based on the interpretation from the chloride data, as shown in Figure 7-3. The initial temperature profile put in the model was based on the reference temperature monitoring data of the wells (see Figure 6-3), which is 14 °C at storage depth.

Boundary conditions

Fixed pressure, temperature and solute concentration conditions were applied to the outer boundaries of the model, with values corresponding to the initial conditions.

Temporal discretization

The temporal discretization is based on the flow and temperature data at NIOO. Since the start of the HT-ATES operation in 2011, temperatures and volumes of the injected and produced water have been registered at 8 minute frequency, at each well. The monthly average injection/production volumes and the monthly average injection temperatures (Figure 4-1) were used as input for the HST3D-model. Especially during spring and autumn, both storage and recovery of heat occurs within the same month. To account for this, the model applies two periods each month: one for storage of heat and one for the recovery of heat.

9.3 Results and discussion

9.3.1 Chloride concentrations

The chloride concentrations that were calculated by the model for 2013, 2015, 2018 and 2019 are shown in Figure 9-1. Note that this is a cross-section through the hot and cold well, located 70 m apart. The monitoring well is located 56 m south of the hot well, i.e. 'behind' the hot well in the figure.

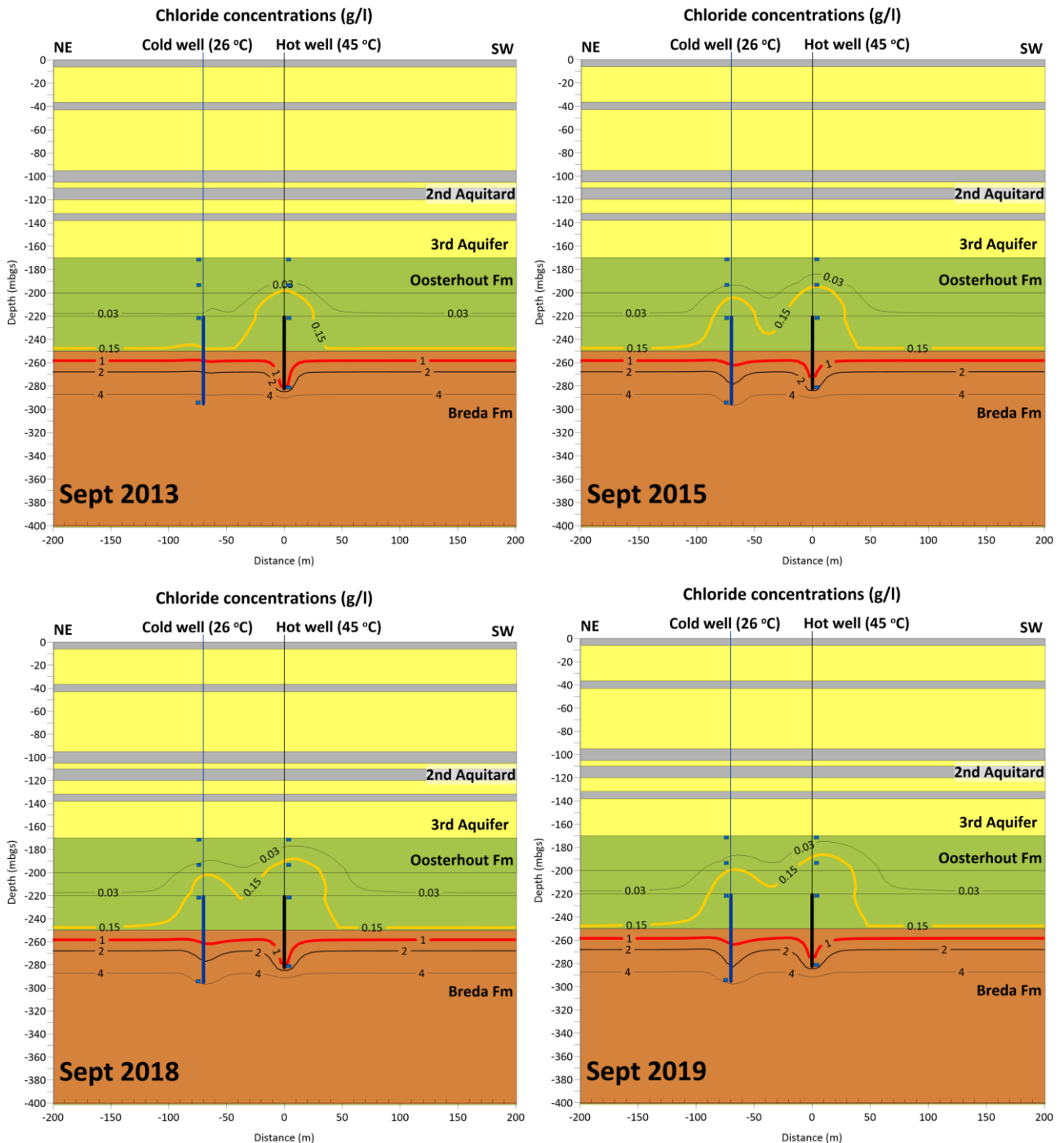


Figure 9-1. Chloride concentration contour lines (g/l) resulting from the HST3D-model, for September 2013, 2015, 2018 and 2019. The fresh-brackish water interface (0.15 g/l) is indicated by the yellow contour line, and the brackish-saline interface (1.0 g/l) is indicated by the red one. The cold well (blue) and the hot well (black) are shown as vertical lines, with their four piezometers represented by small squares.

Mixing of water with different chloride concentrations

- The original fresh-brackish water interface (0.15 g Cl/l) was located at 250 mbgs, and the brackish-saline water interface (1.0 g Cl/l) at around 260 mbgs. The HT-ATES well screens are positioned over these interfaces.
- The mixing of water with different salinity will occur in the extraction well when pumping starts and the mixed water is subsequently injected in the injection well. The hydraulic conductivity for the upper part of

the screen (220-250 mbgs) is higher than the bottom part (250-293 mbgs), so that the majority of the water volumes are produced by/injected in the upper part of the well screens. This also causes the mixed water composition to be primarily determined by the salinity of the groundwater in the upper part of the well screens. However, because of the relatively high salinity of the groundwater at larger depths, even a small contribution of deeper groundwater can result in a rising salinity of the pumped water.

- The mixed water has a chloride concentration of about 0.5 g/l. The mixed water pushes the fresh-brackish water interface upwards, while pushing the brackish-saline interface downward.

Upward movement of the fresh-brackish interface

- The fresh-brackish water interface has moved further upward at the hot well compared to the cold well, which is a direct effect of the net water displacement from the cold to the hot well.
- According to the model, the fresh-brackish interface has moved upward approximately 30 m in 2019, passing W-F2, but not yet passing W-F1. This model result is in line with the field measurements, which show concentrations >150 mg/l at W-F2, but no composition changes (yet) in W-F1. Above the cold well, the fresh-brackish interface has not yet reached K-F2, which too is in accordance with the field measurements, showing that K-F2 has not experienced an increase in chloride concentrations.

Horizontal movement of the fresh-brackish interface

- The horizontal distance at which chloride concentrations have changed is less than 50 m from the hot well in 2019. This is in line with the field measurements, as no indications of increased chloride concentrations or EC-values have yet been measured at the monitoring well at 56 m distance from the hot well.

The model used the subsurface properties as interpreted in the chapters above, and the stored/recovered volumes and temperatures as registered by the automatic flow and temperature sensors. The simulated location of the fresh-brackish water interface corresponds with the field data that was gathered at NIOO. This validates to some extent the flow properties assigned to the model, which determine the 3D distribution of the mixed water.

In case the net water displacement from the cold to the hot well continues, the chloride concentrations above the hot well screens will keep increasing. However, since only part of the injected mixed water flows upward, it takes a large net amount of water to be injected into the hot well, before chloride concentrations start increasing considerably at W-F1 (i.e. at the bottom of the 3rd aquifer). Whether this actually occurs depends on the future operation of the HT-ATES system. In any case, with the planned yearly chloride measurements at W-F1 at the end of each summer, a breakthrough of groundwater with higher chloride content at W-F1 is effectively monitored and will hence be noticed.

9.3.2 Temperature distribution

A topview of the simulated temperature distribution at 220 mbgs (top of heat storage) in September 2019 is shown in Figure 9-2.

In Figure 9-3, cross-sections are presented of the subsurface, providing a more detailed insight in the 3D simulated thermally impacted zone around the HT-ATES wells, at various moments in time.

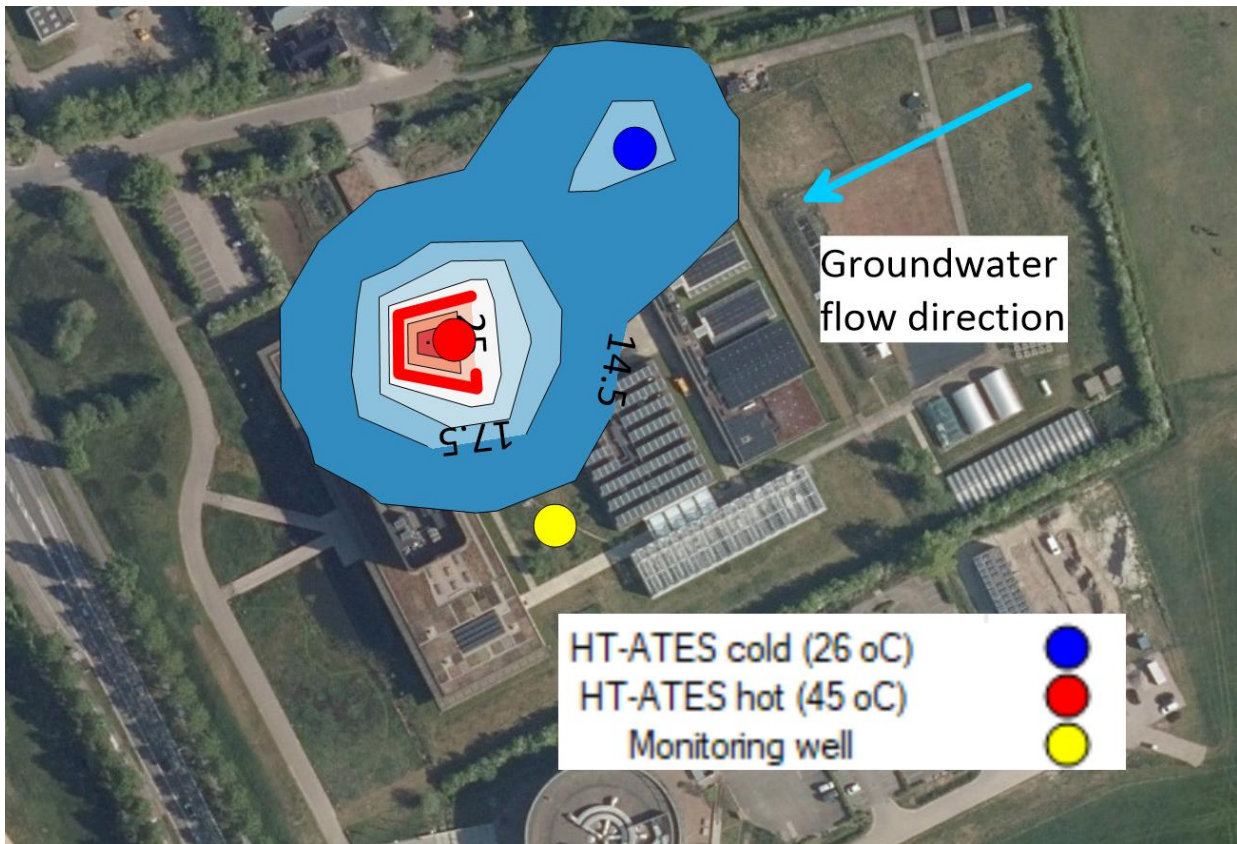


Figure 9-2. Topview of the subsurface temperatures at a depth of 220 mbgs (top of storage) at the end of the 9th hot season (September 2019)

The natural temperature in the storage aquifer at 220 mbgs is around 14 °C. The topview shows that no temperature changes (>0.5 °C) are simulated at the monitoring well at the end of 2019. This corresponds with the field data, where no temperature increments have so far been measured at the monitoring well (Figure 6-3). Should the yearly net water displacement from the cold to the hot well continue over the coming decade, the breakthrough of more saline and heated water may occur at the monitoring well. Timing of field measurements will determine whether this actually will be observed at the monitoring well, as salinity and temperatures will decrease again when water is produced from the hot well.

The cross-sections provide insight in the vertical extent of the thermally influenced zone. In September 2019, the 17,5 °C contour line directly over the hot well screen is located at a depth of approximately 195mbgs. This means that some temperature change can be expected near this depth, which coincides with the depth of the W-F2 piezometer. This is roughly in agreement with the temperature measurements (Figure 6-2), which show that temperatures start to steeply increase from about 190-200 mbgs, probably because these depths are heated from below by the effects of the heat storage.

The vertical extent of the thermally impacted area is considerably smaller at the cold well, because of the lower injection temperatures (max 26 °C) and the net water displacement to the hot well. Also, the cross-sections of Figure 9-3 show the temperature distribution in September, i.e. after a period of heat storage when the hot bubble is at its largest, and the bubble around the cold well is smallest. At the end of winter, after water has been produced from the hot well and injected in the cold well, the vertical extent of the thermally impacted zone above the cold well will be larger than is shown in the cross-sections. According to the measurements (Figure 6-1), the water injected in the cold well (26 °C) influences the subsurface between storage depth up to ~210 mbgs, in the first years already. But according to the simulation, the increased temperature reach a depth of 210 mbgs only after 9 years. Although the choice of the contour line values play a role in the visualization, it is noticeable that temperatures up to 210 mbgs have in reality increased sooner than was expected from the simulation below. However, note that the permeability above 200 mbgs is higher than below this depth, allowing for more heat from the 'cold' well casing to be transported away by

the groundwater flow. Another explanation may be that short-cut flow from the cold well screens through the coarse-grained gravelpack facilitates upward flow of injected water (26 °C).

Temperatures (°C)

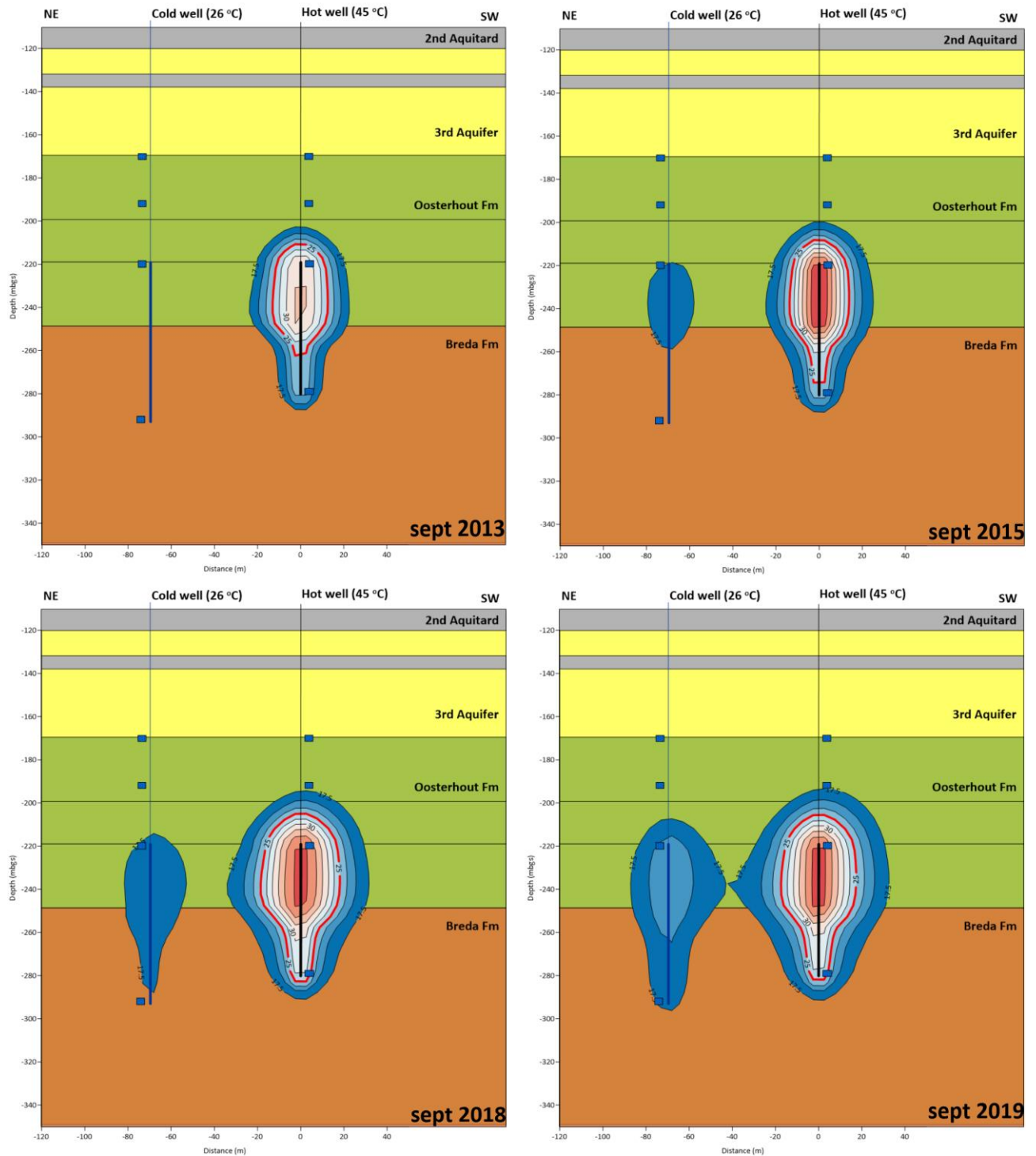


Figure 9-3. Cross-sections through the cold and hot well at NIOO, showing the temperature distributions as simulated by the model for September 2013, 2015, 2018 and 2019. The 25 °C isotherm is indicated in red. The cold well (220 – 293 mbgs, blue) and the hot well (220 – 285 mbgs, black) are shown as vertical lines, with their four piezometers represented by small squares.

10 Conclusions and recommendations

10.1 Conclusions

In the Netherlands, LT-ATES is applied successfully in unconsolidated sediments for over two decades and research on these systems has shown that the effects of LT-ATES on the groundwater quality are generally regarded limited and acceptable (Meer met Bodemenergie (2012), Bonte (2013), KWR (2019)). However, for HT-ATES (>25 °C), little research has been performed on the associated effects in field systems so far. Currently, the development and application of HT-ATES in the Netherlands focuses on the storage of heat (25 – 90 °C) in unconsolidated aquifers up to 500 mbgs. With natural temperatures at this depth ranging from 10 to 20 °C, the subsurface temperatures are considerably increased by HT-ATES. Higher temperatures influence (bio)chemical processes in the subsurface, which may lead to changes in the groundwater composition and impact groundwater quality. Since the initial geochemical composition of the subsurface (i.e. sediment and groundwater) is often uncertain, it remains challenging to quantitatively assess the effects of HT-ATES on groundwater composition and quality beforehand. This is important in order to secure the quality and safety of fresh groundwater aquifers, which are a valuable natural resource for drinking water production in a large part of the Netherlands. The insecurity about the effects has led to extensive and complex permitting processes for HT-ATES systems in the past, with no certainty on the outcome of the application. This in turn generates risks for investors and users of HT-ATES and is hence seen as an important barrier for its large-scale implementation in the Netherlands. Therefore, to advance HT-ATES and to benefit from its CO₂-emission reduction potential in the strive for a zero-emission European society, it is important to obtain more insight in the thermal, chemical and microbiological effects of HT-ATES on the subsurface.

The Netherlands Institute of Ecology (NIOO-KNAW or NIOO for short) is a scientific research institute which built a new sustainable headquarters in Wageningen in 2010. In order to create a sustainable climate system for the buildings, two ATES systems were realized: one for storage of low temperature heat and cold (LT-ATES, <25 °C) at 70 mbgs and one deeper system around 250 mbgs for the storage of solar and residual heat at higher temperatures up to 45 °C (HT-ATES). The results from the monitoring program prescribed in the NIOO permit were expanded by additional measurements within the HEATSTORE framework, resulting in a unique 10-year data series on temperature as well as the chemical and microbial groundwater composition around this HT-ATES system. Within the HEATSTORE context, the existing dataset was investigated and additional measurements were performed, allowing for an evaluation of the thermal, chemical and microbial effects of the NIOO HT-ATES system on the subsurface, as reported in this Case Study.

Hydrogeological setting and well configuration

In the subsurface at NIOO, alternating sand and clay deposits (glacial and fluvial) are found up to 140 mbgs, in which the well screens of the LT-ATES system were placed. The '3rd aquifer' is a valuable freshwater aquifer located at a depth of 140 – 170 mbgs containing medium grained sand, from which drinking water is produced in the region (but not near NIOO). Fine marine sands are found between 170 – 220 mbgs (M50 120 – 200 µm). Between 220 – 300 mbgs, the grainsizes further decrease to very fine marine sands up to 300 mbgs (M50 100 – 120µm). The well screens of the hot (45 °C) and 'cold' (26 °C) wells of the HT-ATES system are placed in these very fine marine sands, between 220 – 295 mbgs, as to limit heat losses due to buoyancy flow. The wells are 70 m apart. A monitoring well with four piezometers was installed at 56 m from the hot well to facilitate measurements in the horizontal direction. Well production tests combined with flowmeter tests have shown that the majority of the pumped water from the wells (>85%) is produced from the upper 30 m along the well screens (220 – 250 mbgs), which suggests that the permeability is significantly higher along this section, compared to the deeper part (250 – 295 mbgs). The permit prescribes that negative influences of the HT-ATES on the 3rd aquifer are not allowed, and accordingly all of the three boreholes were to be equipped with four piezometers between 170 and 295 mbgs, which facilitated the tracking of the propagation of thermal, chemical and microbial effects from the heat storage to the bottom of the 3rd aquifer.

Thermal effects

Temperature profiles were obtained by descending a probe in the deepest piezometers that are installed in the gravel pack of the wells, at approximately 20 cm from the well casing. The temperature measurements in the warm and the cold well are strongly influenced by the temperature of the water flowing through the well in

the days (and hours) before the measurement was performed, because of heat conduction losses through the well casing. Peaks and dips in the temperature profiles were observed in the 20 – 200 mbgs depth interval, which are attributed to variations in the horizontal groundwater velocity at different depths, carrying away the heat that is lost through the well casing. Below 200 mbgs the stronger deviations from the natural temperature suggest that temperatures are influenced by the heat storage directly above the hot well (and to a smaller extent also directly above the cold (26 °C) well). The monitoring well, located 56 m from the hot well, has not shown any temperature changes at the HT-ATES depth to date, but thermal influence of the LT-ATES system was observed around 50 – 90 mbgs. The stored water volumes are considerably smaller than designed for, which is caused by (1) a much lower hydraulic conductivity than expected, which has led to a reduction of the maximum flow rate of the system, (2) a smaller heat production capacity by the solar panels, reducing the amount of heat available for storage and (3) an increase in direct use of the solar heat by the NIOO facilities, further reducing the amount of heat available for storage. These factors have contributed to the fact that temperature changes at the monitoring well have not been observed yet.

Chemical effects

The chemical data gathered during the operation between 2010 and 2020 was analysed, and additional groundwater analyses were performed in 2018 – 2021. Before realization of the system, it was expected that the fresh-brackish water interface (150 mg Cl⁻/l) was located around 200 mbgs. Therefore, well screens were designed for a depth of 220 mbgs and deeper, as to limit the displacement of this interface. After installation of the wells and piezometers, a reference measurement was performed to investigate the natural groundwater compositions at four depths (i.e. at 170, 195, 220 and 285 mbgs). At the piezometers installed at the top of the well screens the natural groundwater was fresh (on average 35 mg Cl⁻/l), while the piezometers installed at the bottom of the storage depth showed that groundwater was saline (on average ~2,400 mg Cl⁻/l). Also the concentrations of other chemical species showed considerably different compositions at the top and bottom of the well screens. From the data it was interpreted that the original depth of the fresh-brackish interface was located around 250 mbgs (i.e. 50 m deeper than expected beforehand). Upon operation, groundwater was produced from both parts of the well screens and mixed in the well pipe circuit. Since ~85% of the produced water originates from the upper part of the well screens, the groundwater composition at that depth has a strong influence on the mixture composition. But on the other hand, adding only a small fraction of saline water from the bottom of the screens can lead to a significant increase in the salinity of the mixture.

Extensive measurements on chemical and microbial groundwater composition were carried out at the piezometer at the top of the hot well at the end of each summer, and at the piezometer at the top of the cold well at the end of each winter. At these moments, groundwater was also sampled from four other piezometers at the hot and cold wells, but these samples were only analysed for chloride. Chloride is a conservative chemical species which is not influenced by temperature-dependent chemical reactions induced by HT-ATES. The extensive chloride data has shown that mixing of water with various compositions occurs in and around the well screens of the HT-ATES system. The fact that a net volume of water was pumped from the cold to the hot well over the last decade, combined with the absence of a confining layer above the heat storage, has resulted in the upward displacement of the fresh-brackish interface. However, no change in chloride concentration has yet been observed in the piezometers at 170 mbgs (i.e. at the base of the 3rd aquifer). This means that some salinization occurs above the hot well, but this is limited to a vertical distance of about 30 m above the top of the hot well screens.

Also, it was observed that the chloride concentrations at the top of the well screens of the hot and cold wells keep increasing gradually over time. This is explained by the fact that a net volume of groundwater has been displaced from the cold to the hot well than vice versa, combined with the fact that the well screens of the cold well are located deeper (reaching up to 295 mbgs, in more saline water) compared to the hot well (reaching up to 283 mbgs), so that every year relatively saline water is introduced in the stored volume from the cold well. Another possible contribution to this gradual trend may be the process of density driven upward flow of the heated water near the well screens, leading to upconing of saline water below the warm well. Other chemical compounds like calcium, bromide and boron as well as electroconductivity (EC) have a pattern similar to that of chloride, showing that their concentrations too are dominated by the mixing process. No groundwater compositional changes have yet been observed at the monitoring well, meaning that both temperature and groundwater compositional effects of the HT-ATES have remained locally around the HT-ATES well screens.

Temperature-dependent chemical processes that were expected based on literature like carbon mobilization, calcite precipitation and silica dissolution were not distinguished from the monitoring data, although these may have been masked by the mixing process. Additional measurements showed that arsenic

concentrations had increased significantly at the piezometer located 30 m above the hot well, but not at the heat storage depth itself. This observation is in line with the findings of Bonte (2013) that arsenic may be mobilized near the heat storage and subsequently be transported (by advection) to the outer spheres of the heated zone, increasing its concentration there. However, more measurements are needed to further investigate this trend in the future, and this is also taken up in the renewed HT-ATES system permit for NIOO (since 2021).

Microbiology

In accordance with the HT-ATES permit, groundwater samples were taken from the piezometers with screens at the depth of the top of the hot and cold well screens (220 mbgs) twice a year, and analysed for a number of microbiological parameters. General standard plate counts (at 22, 25 and 37 °C) were used to get an indication of the general microbial concentrations of the sampled ground water. These results showed an initial peak in microbial concentrations in the first measurements, caused by the drilling activities. This was followed by significantly fewer counts in the years that followed, often below the detection limit, which can be explained by very low microbial concentration in the ambient groundwater, related to the absence of oxygen and a low nutrient availability at storage depth. The same groundwater samples were also tested on four pathogenic microbial species, using specific plating techniques: *Aeromonas*, *Coliforms* (37 °C), *E. Coli* (at 44 °C) and *Enterococcus*. The results of the last years show that these species were not detected or only in low concentrations. This is in line with earlier findings from the literature (KWR, 2011) and could be explained by the conditions around the HT-ATES being anoxic, nutrient-poor and saline, which are far from optimal for the growth of these pathogenic species. So, the pathogens seem not to be capable of competing with other species that are much better adapted to the conditions in the aquifer.

Additional measurements were performed in 2019, using different analysis methods like qPCR (quantitative Polymerase Chain Reaction) and NGS (Next Generation Sequencing). Samples were gathered from the piezometer with screens near the hot well screen and analysed for the three pathogenic species *Enterococcus*, *Aeromonas* and *E. Coli* using qPCR analysis method. Their gene concentrations were below the detection limit, and the NGS-analysis showed that these species were found in the NGS-analysis in very low relative abundance. Also, in the regular plating analyses (for the permit) performed one month later these pathogens were again not observed. Moreover, ATP-concentration at the hot well was below the detection limit (<1 pg/ml), indicating that the activity of the total microbial population present was very low. These findings supported the hypothesis that the risks associated with these pathogens are limited in the context of this HT-ATES system. Together with the existing data series, these data were the basis to remove the obligatory microbiological analyses from the permit in 2020. Based on the metabolisms of various pathogens as reported by KWR (2011), the pathogenic *Acanthamoeba* may survive in the anoxic conditions around the HT-ATES. Some of its DNA was found at the hot well, but the impact of HT-ATES on this species could not be quantified as no sample was available from the monitoring well.

The NGS analyses were applied to groundwater samples from storage depth, at both the hot and the monitoring well. The results showed that DNA concentrations were similar in both samples. Notably, the samples contained not only strictly anaerobic species (as was to be expected based on the chemistry of the groundwater), but also (strictly) aerobic species which were not expected to be capable of surviving the anoxic conditions in the storage aquifer. This suggested that (semi-)oxic water was collected in the sample, probably originating from the top of the piezometer where atmospheric influences have allowed for the growth of aerobic species which may potentially grow in biofilms at the inner walls of the piezometer.

In 2021, a more extensive microbiological measurement was performed with the aim (1) to find how the analyses results are influenced by the sampling methodology, (2) to see how the microbial conditions differed between the hot and monitoring well and (3) to investigate the changes compared to 2019:

(1) Groundwater samples were gathered from the piezometers at storage depth at the hot and monitoring well, using two different methods. Applying the regular method, at least 3 piezometer volumes are discharged before sampling and the sample is gathered from the top 5 m of the groundwater in the piezometer. The new method was similar, but samples were gathered at greater depths in the piezometer (~20 m below the water level). Hypothetically, the water collected using the new, deep sampling method would provide a sample which is more representative for the groundwater in the aquifer, compared to the sample gathered using the regular method. The hypothesis was confirmed by the analyses results, as the concentrations of DNA, ATP and genes (as identified by qPCR) were consistently considerably lower with the new method (with one exception for *Aeromonas*). In addition, applying the new method, the variation between measurements in duplo was smaller. Assuming anoxic conditions and considering the chemical

groundwater composition at NIOO, a low biomass and activity of microbes was expected. This means that groundwater originating from a more oxic location (like the top of the piezometer) may have a large influence on the total microbial composition of water samples. Because the groundwater in the piezometer originates from an anoxic aquifer, the introduction of oxygen at the depth of the water level in the piezometer creates relatively favorable conditions for microbes. Oxidizing components (oxygen) and reduced species (dissolved iron, ammonium, etc.) come together and result in (bio)chemical processes and associated microbial activity. Only a small percentage of water from the top of the piezometer may have a large impact on the microbial composition and concentration in the samples. Thus, in researching the microbial effects of HT-ATES using sensitive microbial analyses methods with a large discovery potential like NGS and qPCR, one must assess whether the sampling methodology will deliver a groundwater sample that is representative for the storage aquifer. This aspect was also found to be important at the other HEATSTORE Case Study of Koppert-Cress in Monster, the Netherlands. There, KWR used an adapted procedure for groundwater sampling in order to minimize these disturbing effects.

(2) The microbial compositions of water samples taken from the piezometers at the hot well (i.e. within the HT-ATES zone of influence) were compared to samples from the monitoring well (i.e. outside of this zone). The results consistently showed higher DNA-concentrations (NGS, qPCR) and activity (ATP) at the hot well. This suggests that more microbes can survive and live around the HT-ATES system. However, based on the data, it cannot be stated with certainty that the main cause for this difference with the monitoring well is the elevated temperature at the hot well: as described earlier, the water samples are probably influenced by groundwater originating from the top of the piezometers. At the hot well, the water level in the piezometer fluctuates frequently because of the variations in the pumping activities, so that the top of the piezometer is more intensively exposed to air, which may facilitate the growth of microbes. At the piezometer in the monitoring well, the fluctuations are considerably smaller (or may be absent), constraining microbial growth at the top of the piezometer. This explanation is supported by the NGS data, which showed that the majority of the identified microbes from the monitoring well were strictly anaerobic, while those at the hot well were mainly aerobic or nitrate-reducing. This may explain the difference in microbial results between the hot and monitoring well. Still, the piezometer at the hot well will be heated by the hot well casing, as the temperature data showed, and this may have stimulated microbial growth in the piezometer of the hot well. So, the data merely shows the differences in microbiological composition and activity in the piezometers, but the question remains to what extent this is representative for the situation in the storage aquifer.

(3) Comparing the results from 2021 with 2019, it becomes clear that the DNA-concentrations and the activity have increased significantly both at the monitoring well and the hot well piezometers with screens at storage depth. The NGS-analyses of the samples taken with the new method showed a relatively larger portion of aerobic species in 2021 compared to 2019. Using the old sampling method, this relative portion was still larger. This suggests that the increase of the DNA in 2021 compared to 2019 for both the piezometers at the monitoring and hot well may be explained by an increased size and activity at the top of the piezometer, rather than at storage depth. Moreover, at the piezometer with screens at storage depth in the monitoring well, no thermal and chemical changes have been observed yet, so the increase in microbial activity at this location is probably not caused by the HT-ATES effects but rather by improved conditions in the piezometer. At the hot well, the increased temperatures in the piezometer (due to heat losses) may have contributed to the increase, while the role of the heat storage itself on this finding remains subject to debate. Regarding pathogenicity, the qPCR analyses on samples taken with the new sampling methods (that are expected to be more reliable) showed that gene concentrations of *E. Coli* and *Enterococcus* were still close to the detection limit (similar to 2019), while the concentrations of *Aeromonas* and *Acanthamoeba* were both considerably higher. Still, the NGS results showed a limited relative presence of *Aeromonas*, as the relative number of counts are < 0.06% of the total. This suggests that, although the absolute number of *Aeromonas* gene found in the qPCR analysis of 2021 was higher compared to 2019, the relative presence of this species remains low. Also, in DNA-based analysis methods, there is no distinction between DNA of living and dead organisms. This may explain why these pathogens were not found with the plating techniques, from which only living species are derived that are able to grow under the plating conditions.

Overall, regarding the microbial effects at NIOO, the 10-year data series has shown a peak in general cell counts in the first months, related to disturbances caused by the drilling activities, followed by considerably lower numbers in the years that followed. The 10-year data series on microbial species suggests that the risk of growth of considerable amounts of pathogens in the anoxic and nutrient-poor subsurface circumstances is limited, which is in line with findings from the literature (KWR, 2011). Additional analyses showed that DNA-concentrations were about 20x higher when samples were gathered from the top 5 m of the piezometer

compared to samples taken from greater depth (~20 m), because the top part of the piezometer is exposed to atmospheric influences which provide better conditions for microbial growth than the deep, anoxic and nutrient-poor groundwater. This shows that sampling methodologies need to be optimized in order to research microbial effects of HT-ATES in the subsurface. DNA-concentrations at both the hot and monitoring well were higher in 2021 compared to 2019, but as no thermal and geochemical changes were observed yet at storage depth of the monitoring well, this finding suggests that these trends are caused by changes in microbial conditions at the top of the piezometer rather than the thermal effects of the HT-ATES. DNA concentrations were higher at the piezometer at the hot well compared to the piezometer at the monitoring well, but this may be explained by the fact that the piezometer at the hot well is heated by the well casing, rather than by the possibility of improved conditions at storage depth due to HT-ATES application.

Heat and Solute Transport Simulations

The software package Heat and Solute Transport 3D (HST3D) of IF Technology was used to reconstruct the changes in temperature and chloride concentrations around the HT-ATES system. The hydrogeology of the subsurface and the registered data on injected and produced water temperatures and volumes were used as input for the model calculations. The results of the model calculations were compared to the results of the available field measurements. The model results on salinity agree with the field data, as in 2019 it too shows that the fresh-brackish interface was located between the upper two piezometers above the hot well (i.e. between 170 – 193 mbgs), and between the middle two piezometers above the cold well (i.e. between 193 and 220 mbgs), and that no effects were observed at the monitoring well. Also, thermal simulation results fit the field observations in that the heated zone above the hot well reaches up to ~ 200 mbgs (i.e. about 20 m above the hot well), and that no temperature change was observed at the monitoring well. No future simulation was performed for the HT-ATES at NIOO, but if the net water displacement from the cold to the hot well is continued over the following years, it may be expected that both chloride concentrations and temperatures will keep increasing directly above the hot well, and thermal and compositional effects may occur at the bottom of the 3rd aquifer on the long term.

10.2 Recommendations

Two sets of recommendations are presented, for the system at NIOO specifically, and for HT-ATES systems in general, based on the data and the experiences acquired at NIOO from 2009 to date.

Regarding the HT-ATES system at NIOO:

- Set forth the regular monitoring of chloride in and around the HT-ATES system, since this is a good indicator of the effect of mixing in and around the HT-ATES system. It also facilitates the tracking of the fresh-brackish interface displacement and the salinization risks for the 3rd aquifer, which is relevant for the permit.
- Perform regular measurements on arsenic concentration in and around the heat storage to extent the current dataset on this chemical species, which has been proven sensitive to mobilization upon heating. A more extended data series may contribute to a better understanding of the mobilization and transportation processes of this parameter in the field, and specifically in the NIOO context.
- Ensure that future monitoring activities are performed following the same measurement methodologies as applied in the last decade in order to continue the existing data series and its consistency. For microbial sampling, an improved methodology as tested in 2021 may be applied.
- Although the microbiological data acquired at NIOO was interpreted within the Case Study, it is advised to continue a more in-depth analysis and interpretation of the microbiological data in future years by experts in this field. Interesting species for future research are *Acanthamoeba* and *Aeromonas*.
- Communicate the findings at NIOO with the HT-ATES licensing authorities. This practical NIOO case may contribute to a better understanding of the subsurface effects of HT-ATES up to 45 °C, and the lessons learned from the permit application (and the change of the permit in 2019-2020) may be helpful in resolving legal obstacles for future HT-ATES projects.

Regarding HT-ATES in general:

- Perform a test drilling before designing and realizing a HT-ATES system. This allows for a detailed image of the subsurface, a successful design and a good well performance during operation.
- A confining layer above the well screens is of huge importance to a successful HT-ATES system. Not only does it improve the recovery efficiency, it also considerably limits both thermal and groundwater

compositional changes to shallower layers, which is typically a major assessment criterium during the permitting process.

- It is recommended to perform an extensive reference measurement on the subsurface temperatures and chemical and microbial composition of the groundwater at the storage depth (and directly above), before the system is taken into operation. The temperature effects of HT-ATES on the groundwater composition is still subject to debate, and for the interpretation of later measurements it is of vital importance to have a good reference to compare the results with. NGS is suggested as an analysis technique with large microbial discovery potential, suitable for reference measurements regarding microbiology, with additional ATP-concentration measurements for a reference on the activity of the biomass. In cases where specific pathogens are of particular interest, qPCR can be considered as an addition. It has to be taken into account that the microbial results of samples taken relatively shortly after realization of the wells, may be affected by the effects of the drilling and construction process (temporarily increased microbial activity).
- At the same time, the monitoring activities performed during the operational phase should be confined, since the sampling and analysis activities (including its preparations) are expensive, especially when microbial analyses are performed. It is advised to clearly formulate the research questions at a HT-ATES system, and then select the parameters that most effectively address them.
- In the Netherlands, changing the Water permit for the HT-ATES system is a relatively extensive legal process. This means that the permit application (or changing it) takes a lot of time and effort. Therefore, it is advised not to include the subsurface monitoring activities directly into the permit requirements, but rather in a separate document that can be changed with less legal complexity, based on new insights.
- Regarding the chemical effects of HT-ATES systems on ground water quality in areas with both fresh groundwater and saline groundwater, both modelling and in-situ chloride measurements are recommended to predict and where necessary monitor potential salinization processes.
- If HT-ATES effects may propagate to subsurface areas with fresh groundwater that may potentially be used for drinking water, monitoring of arsenic is recommended.
- Regarding microbial measurements, this case study yields evidence that Next Generation Sequencing analysis combined with qPCR and ATP analysis provide a better and more in-depth insight than standard microbial plating techniques. Based on the experiences, NGS analyses have provided most information and are hence interesting to perform also during the operational phase, but as costs for this analysis is high it should be applied effectively. It is especially important to make an effort to ensure that the samples are representative for the groundwater in the storage aquifer.
- For better insight on microbial effects further research and experience is needed. This research should include a.o. topics as the reliability of various sampling methodologies and potential sources of contamination (e.g. biofilms in piezometers), the reliability of various DNA-based and not DNA-based analyses in samples with low DNA concentrations, streamlining of the interpretation of various types of data, and quantification of the risk of pathogenicity based on DNA-concentrations or relative abundance.

11 References

- BAM. (2010a). *Boorstaat HTO Koude bron*.
- BAM. (2010b). *Boorstaat HTO Warme bron* (p. 11). p. 11.
- Bloemendal, M., Beernink, S., van Bel, N., Hockin, A., & Schout, G. (2020). *Transitie open bodemenergiesysteem Koppert-Cress naar verhoogde opslagtemperatuur Evaluatie van energiebesparingen en*. (December).
- Bolton, A. J., Maltman, A. J., & Fisher, Q. (2000). Anisotropic permeability and bimodal pore-size distributions of fine-grained marine sediments. *Marine and Petroleum Geology*, 17(6), 657–672. [https://doi.org/10.1016/S0264-8172\(00\)00019-2](https://doi.org/10.1016/S0264-8172(00)00019-2)
- Bonte, M. (2013). *Impacts of shallow geothermal energy on groundwater quality - A hydrochemical and geomicrobial study of the effects of ground source heat pumps and aquifer thermal energy storage*.
- Brons, H. (1992). *Biogeochemical aspects of aquifers*.
- GEBO. (2010). *Boorstaat HTO Meetput*. Dessel, Belgium.
- Goldscheider, N., Mádl-Szönyi, J., Eröss, A., & Schill, E. (2010). Review: Thermal water resources in carbonate rock aquifers. *Hydrogeology Journal*, 18(6), 1303–1318. <https://doi.org/10.1007/s10040-010-0611-3>
- Hemker, K., & Randall, J. (2010). *Modeling with MLU. Applying the multilayer approach to aquifer test analysis. Tutorial*. (January), 66.
- IF Technology. (2009a). *Ontwerp grondwatersysteem - Warmteopslag NIOO te Wageningen*. Arnhem.
- IF Technology. (2009b). *Pilotproject Warmteopslag NIOO te Wageningen - Effectenstudie*. Arnhem.
- IF Technology. (2010). *Doorontwikkelen bronnen*. Arnhem.
- IF Technology. (2011). *HT warmteopslag NIOO Wageningen - Referentierapport hoge temperatuur warmteopslag*. Arnhem.
- IF Technology. (2012). *Bodemanalyse filtertraject; verklaring flowverdeling*. Arnhem.
- IF Technology. (2013). *Monitoringsrapportage NIOO HTO 2012*.
- IF Technology. (2014). *Monitoringsrapportage NIOO HTO 2013*. Arnhem.
- IF Technology. (2015). *Monitoringsrapportage NIOO HTO 2014*. Arnhem.
- IF Technology. (2016). *Monitoringsrapportage NIOO HTO 2015*. Arnhem.
- IF Technology. (2017). *Monitoringsrapportage NIOO HTO 2016*. Arnhem.
- IF Technology. (2018). *Monitoringsrapportage NIOO HTO 2017*. Arnhem.
- IF Technology. (2019). *Monitoringsrapportage NIOO HTO 2018*. Arnhem.
- IF Technology. (2020). *Monitoringsrapportage NIOO HTO 2019*. Arnhem.
- IF Technology. (2021). *Monitoringsrapportage NIOO HTO 2020*. Arnhem.
- Kipp, K. L. (1997). Guide to the revised heat and solute transport simulator: HST3D- Version 2. *U.S. Geological Survey Water-Resources Investigations*, 97–4157, 1–158.
- KWR. (2011). *Microbiologische risico's van een Hoge Temperatuuropslag GeoMEC Vierpolders (Brielle)*. (September).
- Masad, E., Martys, N., & Muhunthan, B. (2000). Simulation of fluid flow and permeability in cohesionless soils. *Water Resources Research*, 36(4), 851–864.
- Meer met Bodemenergie. (2012a). *Meer met Bodemenergie Rapport 3-4: Effecten op de ondergrond*.
- Meer met Bodemenergie. (2012b). *Meer met Bodemenergie Rapport 6: Hogetemperatuuropslag*.
- Okagbue, C. O. (1995). Permeability of stratified sands. *Geotechnical and Geological Engineering*, 13(3), 157–168. <https://doi.org/10.1007/BF00456715>
- Provincie Gelderland. *Vergunning Grondwaterwet tbv een pilotproject warmteopslag te Wageningen*. , (2010).
- Provincie Gelderland. *Wijzigingsvergunning 29 januari 2021*. , (2021).
- Schiessl, K., & Besmer, M. (2020). *Microbial Monitoring with flow cytometry*.
- Shepherd, R. G. (1989). Correlations of Permeability and Grain Size. *Groundwater*, 27(5).
- TNO. (2013). *DINOloket - Data en Informatie van de Nederlandse Ondergrond*. Retrieved from www.dinoloket.nl
- van den Berg, E. H. (2003). *The Impact of Primary Sedimentary Structures on Groundwater Flow*.
- Zaadnoordijk, W. J., Hornstra, L. M., & Bonte, M. (2013). *Grondwaterbescherming en hoge-temperatuur opslagsystemen*. Nieuwegein.

12 Appendix

NGS Analysis report of the microbial measurements performed in summer 2021.

ORVIdcode NGS analyses of eight groundwater samples – an interpretation of results

Client NIOO KNAW

Date: 27 July 2021

Project code: P756

Document type Report

Author(s): Aleida Hommes-de Vos van Steenwijk

1. Introduction

Orvion was asked by NIOO KNAW to perform ORVIdcode NGS biodiversity analyses on two groundwater samples as part of their HEATSOURCE project. An ORVIdcode analysis is used to elucidate and visualise the entire microbial biodiversity (Bacteria and Archaea) in a sample.

The following eight samples were provided by NIOO KNAW for analysis:

Sample name	Code used in report	Description
W-F-3-N NGS1	WN1	Groundwater samples (200-220 m-mv) from warm (W) well sampled using a new (N) method. Samples were taken in duplicate (NGS1 and NGS2)
W-F-3-N NGS2	WN2	
MP-F-3-N NGS1	MPN1	Groundwater samples (200-220 m-mv) from measuring well (MP) sampled using a new (N) method. Samples were taken in duplicate (NGS1 and NGS2)
MP-F-3-N NGS2	MPN2	
W-F-3-Reg NGS1	WR1	Groundwater samples (200-220 m-mv) from warm (W) well sampled using the regular (Reg) method. Samples were taken in duplicate (NGS1 and NGS2)
W-F-3-Reg NGS2	WR2	
MP-F-3-Reg NGS1	MPR1	Groundwater samples (200-220 m-mv) from measuring well (MP) well sampled using the regular (Reg) method. Samples were taken in duplicate (NGS1 and NGS2)
MP-F-3-Reg NGS2	MPR2	

In 2019 both wells were also analysed using ORVIdcode (see info in table below). This previous biodiversity data was updated using Orvion's most recent identification database (December 2020) and included in the interpretation.

Sample name	Code used in report	Description
W-F-3 NGS (220-222)	WR2019	Groundwater samples (200-220 m-mv) from warm (W) well sampled using the regular (Reg) method. Sampled and analysed in 2019.
MP-F-3 NGS (220-222)	MPR2019	Groundwater samples (200-220 m-mv) from measuring well (MP) well sampled using the regular (Reg) method. Sampled and analysed in 2019.

In this report a concise interpretation is made of the ORVIdcode NGS biodiversity results. The analysis results per sample and the corresponding interactive files were provided by email at the same time as this report. The ORVIdcode analysis certificate is included in APPENDIX A.

In this report the focus lies mainly on comparing the biodiversity between the two sample types: Warm well and Measuring well. The comparison is discussed separately for the different sampling methods (new and regular). The following points are discussed in the report:

- Which microbial groups are dominant in the Warm well, but not in the Measuring well (and vice versa). For the regular sampling method the results of 2019 are also included.
- Of the most dominant, or otherwise notable microbial groups, a short description of their general metabolism or other significant traits is provided (if known/possible). Because ORVIdecode identifies to the genus level, the information should not be considered to be all-encompassing as some species within the genus may deviate.
- The client has indicated that there is a specific interest in sulphate reducing bacteria (SRB), iron reducing bacteria (IRB) and (strictly) aerobic micro-organisms. Where relevant this information is included, however, it lies beyond the scope of this interpretation to determine this for all 1,305 identified microbial genera.
- There is also specific interest in the presence of potential pathogens. To this end the data of all the samples is filtered for microbial genera known to contain (potential) pathogenic species. It must be noted that these microbial genera are not necessarily pathogenic, but contain certain (sub)species that are. Also the pathogen data filter does not include an exhaustive list of all known (potential) pathogens, this is merely included to provide some indication of the presence of well-known potential pathogens. For more specific and quantitative data on pathogens it would be necessary to analyse the samples using a different method, such as for example qPCR.

When interpreting ORVIdecode results it is important to consider that the results are in relative abundances (percentages) and are not quantitative. To obtain quantitative data on (specific) micro-organisms a qPCR analysis should be used.

Some DNA in the samples cannot be identified to the level of 'genus' because it cannot be discriminated from other known microbial groups (is not distinctive enough) or because the organism is simply not (yet) known and therefore not included in the identification DNA database. These groups are categorised as 'undefined' in the results but are not included in the interpretation of the results in this report.

2. Comparison Warm and Measuring well

2.1. Sampled using the new “N” method

The identified biodiversity in the four samples (WN1&2 and MPN1&2) was filtered for microbial groups that are dominant (>2%) in the Measuring well samples (MP), but not dominant in the Warm well (W). The result is visualised in figure 1.

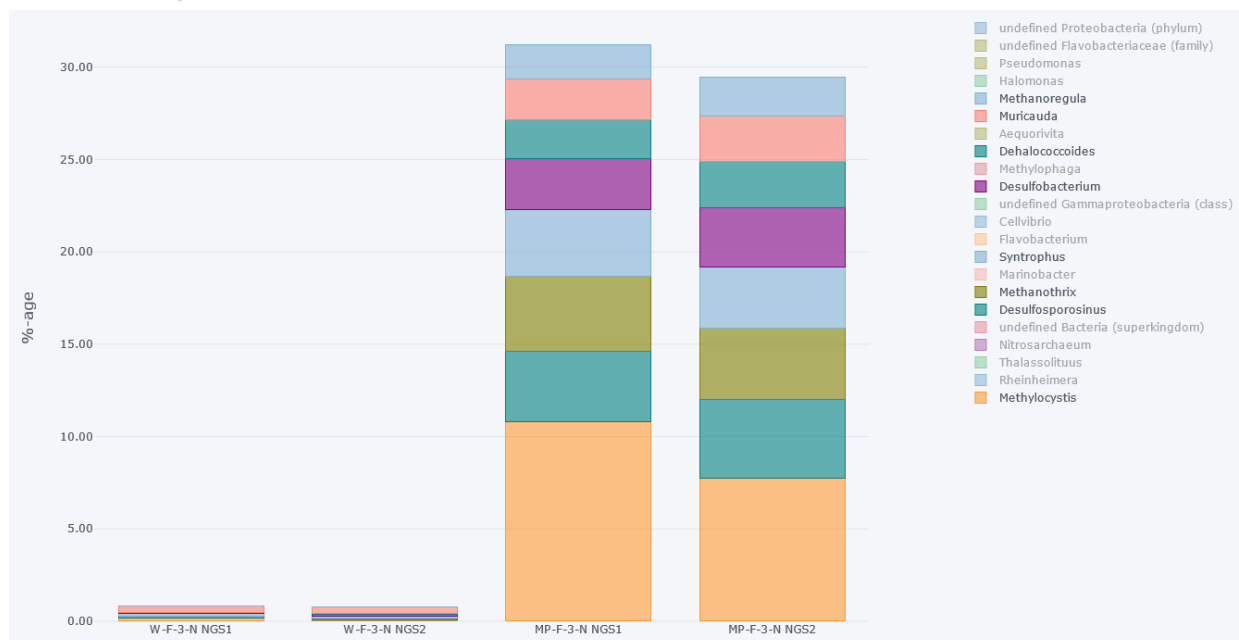


Figure 1. microbial genera dominant (>2%) in the Measuring well (MP-F-N), but not dominant in the Warm well (W-F-3) - (new sampling method)

The filtered genera are shown in table form below and a brief description is provided of their general metabolism or other relevant traits.

Table 1. microbial genera dominant (>2%) in the Measuring (MP) well, but not dominant in the Warm (W) well (new sampling method), with brief description of general metabolism.

Microbial genus	WN1	WN2	MPN1	MPN2	General metabolism
Methylocystis	0.19	0.08	10.8	7.8	Methylotrophic, aerobic / microaerophilic. Some species anaerobic.
Desulfosporosinus	0.06	0.07	3.9	4.3	Sulphate reducing, strictly anaerobic
Methanothrix	0.01	0.01	4.0	3.8	Methanogen (methane producing), strictly anaerobic (might tolerant some oxygen)
Syntrophus	0.15	0.12	3.7	3.4	Strictly anaerobic, requires a symbiotic partner
Desulfobacterium	0.04	0.07	2.7	3.2	Sulphate reducing, strictly anaerobic
Dehalococcoides	0.04	0.06	2.1	2.5	Reductive dehalogenation, strictly anaerobic
Muricauda	0.32	0.36	2.2	2.5	Fermentative, facultatively anaerobic or strictly aerobic, marine micro-organism(?).
Methanoregula	n.d.	0.01	1.9	2.1	Methanogen (methane producing), strictly anaerobic

n.d. not detected

The identified biodiversity of the four samples (WN1&2 and MPN1&2) was filtered for microbial groups that are dominant (>2%) in the Warm well (W) samples, but not dominant in the Measuring well (MP) samples. The result is visualised in figure 2.

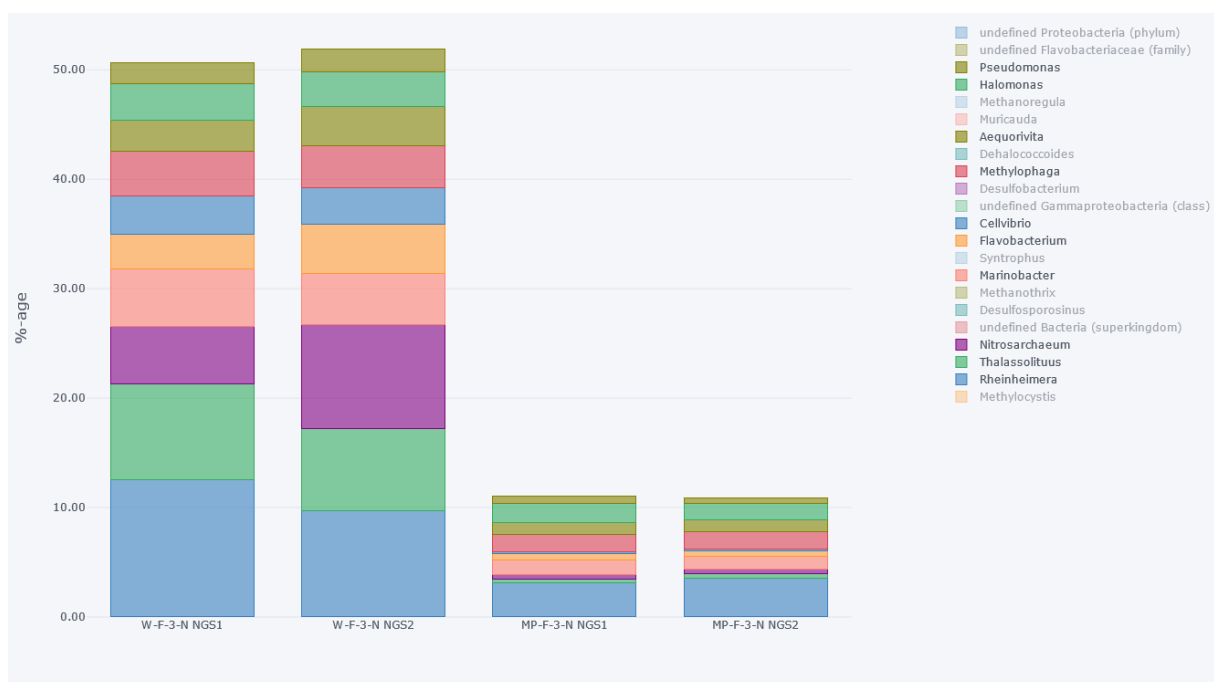


Figure 2. microbial genera dominant (>2%) in the Warm well (W-F-N), but not dominant in the Measuring well (MP-F-3) - (new sampling method)

The filtered genera are shown in table form below and a brief description is provided of their general metabolism or other relevant traits.

Table 2. microbial genera dominant (>2%) in the Warm (W) well , but not dominant in the Measuring (MP) well (new sampling method), with brief description of general metabolism.

Microbial genus	WN1	WN2	MPN1	MPN2	General metabolism
Rheinheimera					
Thalassolitus	8.8	7.5	0.4	0.4	Obligate hydrocarbonoclastic, well-known for oil degradation, aerobic
Nitrosarchaeum	5.2	9.6	0.44	0.46	Ammonia-oxidising archaeon, aerobic
Marinobacter	5.3	4.6	1.3	1.1	Aerobic, can grow anaerobically by denitrification, halophilic (saltwater)
Flavobacterium	3.2	4.5	0.60	0.57	Mostly aerobic (some species microaerophilic or anaerobic).
Cellvibrio	3.4	3.3	0.18	0.16	Aerobic, associated with degradation of polysaccharides (e.g. cellulose)
Methylophaga	4.1	3.6	1.6	1.6	Methylotrophic, halophilic (saltwater), aerobic or nitrate reducing
Aequorivita	2.9	3.6	1.1	1.1	Aerobic, halophilic (saltwater)
Halomonas	3.3	3.2	1.7	1.48	Strictly aerobic or facultatively anaerobic, halophilic (saltwater)
Pseudomonas	1.9	2.0	0.71	0.55	Aerobic, some nitrate reducing, very divers
Shewanella	1.9	2.0	0.23	0.22	Facultatively anaerobic, among others iron reducing & nitrate reducing.

From these results it seems that the conditions in the Warm well samples were more aerobic than in the Measuring well samples. This is most clearly seen in the significantly higher percentage (average of the duplicates) of **aerobic** microbial genera in the Warm well (only including groups more than 10x higher):

- Thalassolitus (22x higher)
- Nitrosarchaeum (16x higher)
- Cellvibrio (20x higher)

And a significantly higher percentage (average of the duplicates) of strictly **anaerobic** microbial genera in the Measuring well (only including groups more than 10x higher than the Warm well):

- Methylocystis (69x higher)
- Desulfosporosinus (62x higher)
- Methanotherix (393x higher)
- Syntrophus (26x higher)
- Desulfobacterium (53x higher)
- Dehalococcoides (46x higher)
- Methanoregula (not detected in the Warm well)

The data was furthermore filtered for potential pathogens (as described in the introduction) that were found to be present for 0.1% or more in at least one of the four samples.

Table 3. potential pathogens identified more than 0.1% in the at least one of the four samples (new sampling method).

Name	WN1 (%)	WN2 (%)	MPN1 (%)	MPN2 (%)
Citrobacter	0.14	0.11	n.d.	n.d.
Clostridium	0.02	0.03	0.20	0.24
Bacillus	0.09	0.12	0.18	0.17

n.d. not detected

2.2. Sampled using the regular “Reg” method

Microbial genera that were found to be dominant (>2%) in at least one of the four samples sampled with the regular (Reg) method are visualised in figure 3.

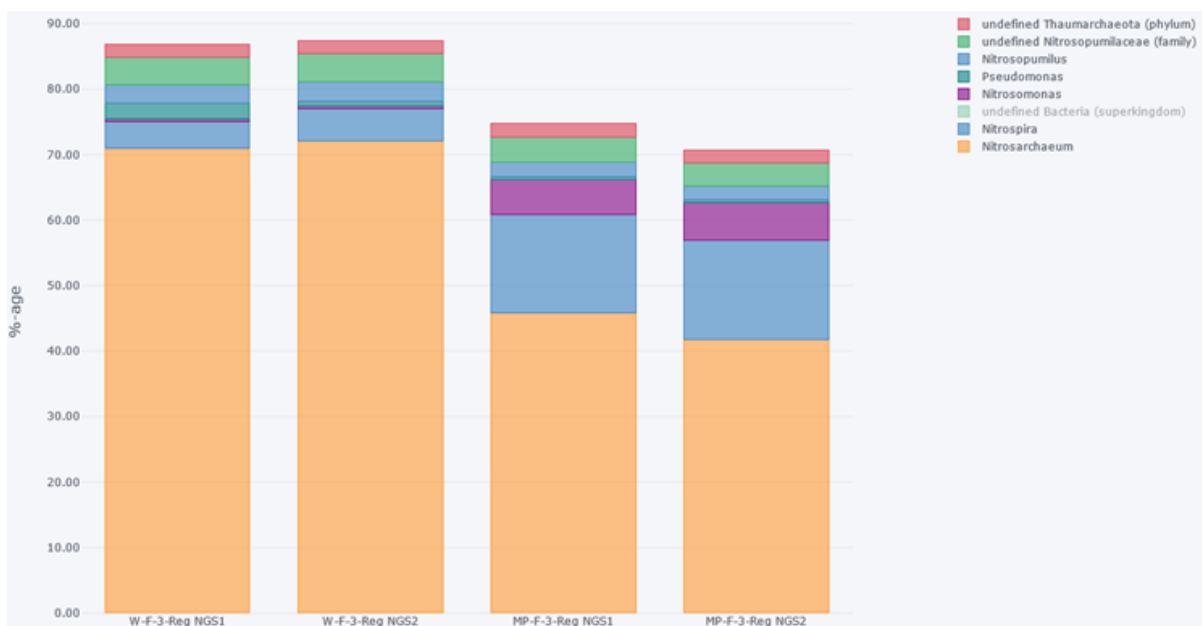


Figure 3. Microbial genera dominant (>2%) in at least one of the four samples (regular sampling method).

The dominant microbial genera are shown in table form below and a brief description is provided of their general metabolism or other relevant traits.

Table 4. Microbial genera dominant (>1%) in at least one of the four samples (regular sampling method), with a brief description of general metabolism.

Microbial genus	WR1 (%)	WR2 (%)	MPR1 (%)	MPR2 (%)	General metabolism
Nitrosarchaeum	71	72	46	42	Ammonia-oxidising archaea, aerobic
Nitrospira	4.0	4.9	15	15	Nitrite oxidising bacteria, aerobic
Nitrosopumilus	2.8	2.9	2.3	2.2	Ammonium oxidising bacteria, aerobic
Pseudomonas	2.5	0.76	0.43	0.42	Aerobic, some nitrate reducing, very divers
Methylocystis	0.55	1.2	0.81	0.87	Methylotrophic, aerobic / microaerophilic. Some species anaerobic.
Desulfosporosinus	0.11	0.12	1.9	1.9	Sulphate reducing, strictly anaerobic
Nitrosomonas	0.45	0.46	5.2	5.7	Ammonium oxidising bacteria, aerobic
Methylobacter	0.36	0.42	0.77	1.2	Methanotroph, aerobic

It is immediately apparent from these results that the sampling method has a significant effect on the microbial biodiversity in the analysed samples. Whereas the samples taken with the New method are relatively biodiverse, the samples taken with the Regular method are dominated by just a few microbial genera belonging mainly to the group of aerobic nitrifiers (ammonium and nitrite oxidising bacteria). Most notable is the ammonium oxidising Archaea Nitrosarchaeum.

Because of this dominance of just a few microbial genera, it is more difficult to make a comparison between the two sample types as the differences become less obvious. Therefore in the table the microbial genera that are at least >1% dominant (instead of 2% previously) have been included.

The only two microbial genera of those listed in table 4 that show a significant (more than 10x) difference between the two sample types are the aerobic ammonium oxidising bacteria *Nitrosomonas* (12x higher in MP well) and the anaerobic sulphate reducing bacteria *Desulfosporosinus* (17x higher in MP well). Both of these are more dominant in the Measuring (MP) well which might seem odd as the one requires oxygen and the other requires its absence. This usually indicates the sample is not homogenous, for example because there is sediment or growth in biofilms – the micro-organisms at the surface will be in contact with oxygen, but the deeper-lying micro-organisms are not (oxygen is depleted) – enabling them to coexist despite their different requirements.

The data was filtered for potential pathogens (as described in the introduction) that were found to be present for 0.1% or more in at least one of the four samples.

Table 5. potential pathogens identified more than 0.1% in the at least one of the four samples (regular sampling method).

Name	WR1 (%)	WR2 (%)	MPR1 (%)	MPR2 (%)
Bacillus	0.10	0.10	0.05	0.06

2.3. Comparison with samples of 2019

As mentioned previously, both wells were also sampled in 2019 (25th September 2019) and analysed with ORVidecode NGS. The DNA data that was generated from the 2019 samples were re-identified using the most recent Orvion identification database. A brief comparison between these samples and those of 2021 is made in this paragraph. Because the 2019 sample were also sampled with the regular sampling method, the comparison is made with these results for the 2021 samples. The two sample types are discussed separately.

Warm (W) well with Regular (Reg) sampling method

Dominant microbial genera (>1%) from 2019 that are no longer dominant in 2021 are visualised below and vice versa are shown in figure 5.



Figure 4. Visualisation of microbial genera dominant in the sample of the Warm (W) well in 2019 (>1%) but not dominant in the samples of 2021.

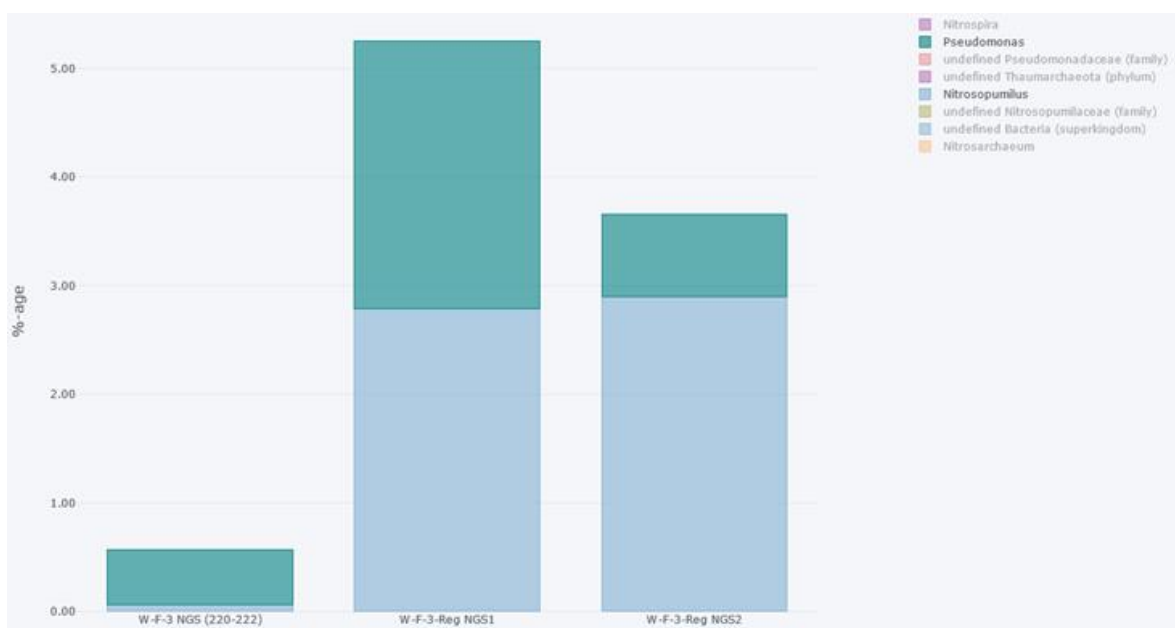


Figure 5. Visualisation of microbial genera dominant in the samples of the Warm well (W) in 2021 (>1%) but not dominant in the sample of 2019.

Microbial genus	WR 2019 (%)	WR1 (%)	WR2 (%)	General metabolism
Syntrophus	5.6	0.005	0.005	Strictly anaerobic, requires a symbiotic partner
Parvibaculum	4.7	0.004	0.003	Aerobic, associated with oil (hydrocarbon) degradation
Petrocella	3.8	0.01	0.01	Little known, fermentative, strictly anaerobic (marine?)
Nitrosomonas	3.1	0.45	0.46	Ammonium oxidising bacteria, aerobic
Candidatus Kuenenia	2.2	0.56	0.66	Anaerobic ammonium oxidising (Anammox), anaerobic
Candidatus Brocadia	2.2	0.22	0.23	Anaerobic ammonium oxidising (Anammox), anaerobic
Desulfobacterium	1.4	0.01	0.00	Sulphate reducing bacteria (SRB), anaerobic
Dehalococcoides	1.3	0	0	Reductive dehalogenation, anaerobic
Ignavibacterium	1.2	0.002	0.002	Fermentative, facultatively anaerobic
Thermodesulfovibrio	1.1	0.01	0.01	Sulphate reducing bacteria (SRB), anaerobic
Geobacter	1.1	0.02	0.02	Iron reducing bacteria (IRB), anaerobic
Nitrosopumilus	0.06	2.8	2.9	Ammonium oxidising bacteria, aerobic
Methylocystis	0.43	0.55	1.2	Methylotrophic, aerobic / microaerophilic. Some species anaerobic.
Pseudomonas	0.51	2.5	0.76	Aerobic, some nitrate reducing, very divers

These results show that a number of strictly anaerobic microbial genera are not dominant in 2021 that were in 2019, such as Syntrophus (1,217x higher in 2019) and the Anammox bacteria Ca. Brocadia (10x higher in 2019) and Dehalococcoides (not detected in 2021). Vice versa the only microbial group that is significantly more dominant in 2021 is aerobic ammonium oxidising bacterium Nitrosopumilus (average of duplicates is 48x higher than in 2019).

This would indicate that the conditions are more aerobic in the samples of 2021 than in the sample of 2019, although some aerobic genera (such as Nitrosarchaeum) are also dominant in 2019. As discussed previously this is possible in sample with heterogenous composition such as in sediments or biofilms.

Measuring (MP) well with Regular (Reg) sampling method

Dominant microbial genera (>1%) from 2019 that are no longer dominant in 2021 are visualised below and vica versa are shown in figure 7.

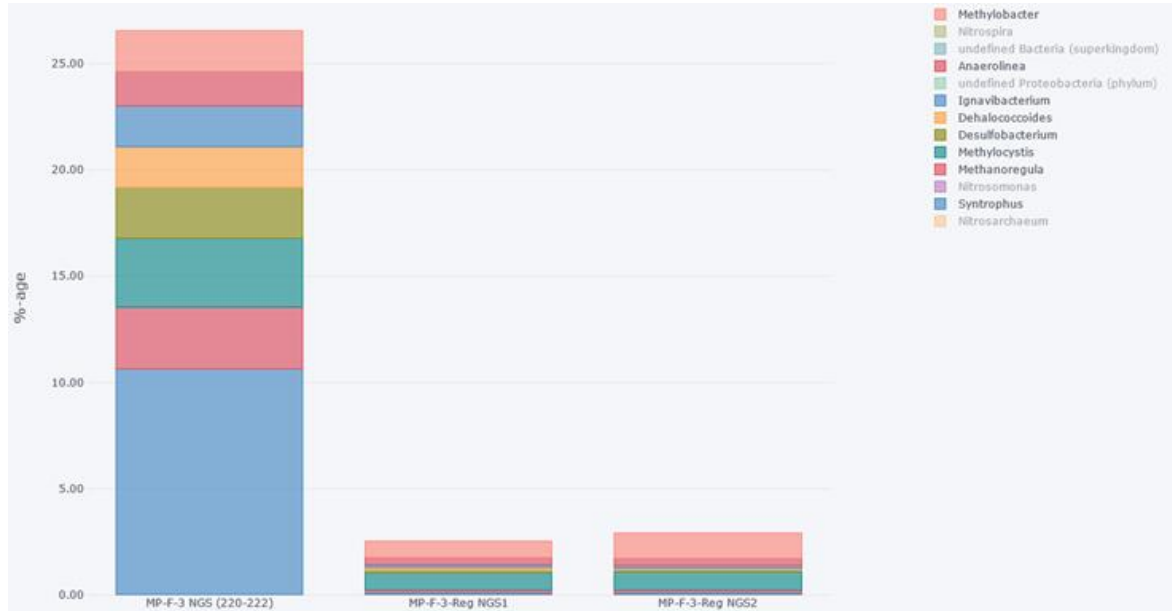


Figure 6. Visualisation of microbial genera dominant in the sample of the Measuring (MP) well in 2019 (>1%) but not dominant in the samples of 2021.

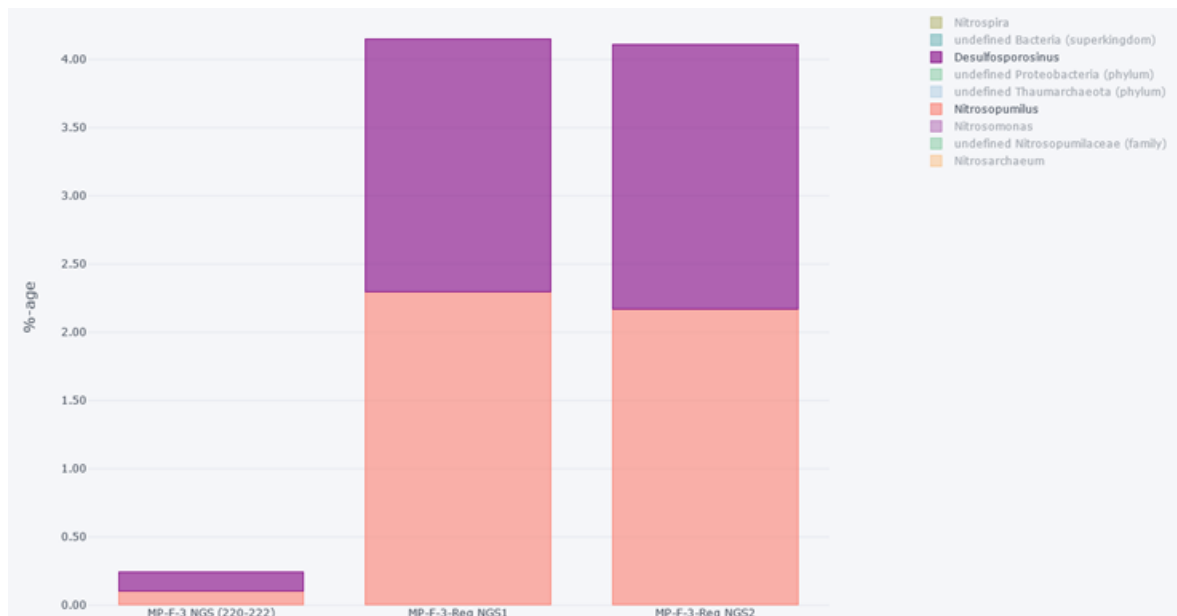


Figure 7. Visualisation of microbial genera dominant in the samples of the Measuring well (MP) in 2021 (>1%) but not dominant in the sample of 2019.

Microbial genus	WR 2019 (%)	WR1 (%)	WR2 (%)	General metabolism
Syntrophus	11	0.11	0.11	Strictly anaerobic, requires a symbiotic partner
Methylocystis	3.2	0.81	0.87	Methylotrophic, aerobic / microaerophilic. Some species anaerobic.
Methanoregula	2.9	0.13	0.10	Methanogen (methane producing), strictly anaerobic
Desulfobacterium	2.4	0.13	0.10	Sulphate reducing bacteria (SRB), anaerobic
Ignavibacterium	1.9	0.14	0.12	Fermentative, facultatively anaerobic
Dehalococcoides	1.9	0.12	0.09	Reductive dehalogenation, anaerobic
Methylobacter	1.9	0.77	1.16	Methanotroph, aerobic
Anaerolinea	1.6	0.35	0.35	Fermentative (?), strictly anaerobic
Nitrosopumilus	0.10	2.3	2.2	Ammonium oxidising bacteria, aerobic
Desulfosporosinus	0.14	1.9	1.9	Sulphate reducing bacteria (SRB), anaerobic

There is a significant (>10x) lower percentage in 2021 when compared to 2019 of a number of, mainly strictly anaerobic, species such as Syntrophus (94x higher in 2019), Methanoregula (25x higher in 2019) and Dehalococcoides (19x higher in 2019).

Vice versa, there is a higher percentage (>10x) in 2021 when compared to 2019 of the aerobic ammonium oxidiser Nitrosopumilus (22x higher in 2021) and the anaerobic sulphate reducing Desulfosporosinus (14x higher in 2021).

3. Brief evaluation duplicate samples

A brief analysis of the differences between the two duplicates was made. In general these were found to show no or very little significant variations in the microbial groups or percentages identified. Almost all variations can be considered small (e.g. <5x difference between the duplicates) and/or are a result of low abundances (e.g. <0.01%). The more notable differences that were found in the over 1,300 different microbial genera or 'undefined' groups identified are listed below.

Table 6. overview of microbial groups that were found to vary more than a factor of 5 between the duplicates or were only identified in one of the duplicates with more than 0.1%.

Sample	MPR1 (%)	MPR2 (%)	factor difference
Frankia	0.08	0.56	7.0
Desulfovibrio	0.02	0.11	6.9
Labilibacter	0.02	0.15	6.2
Xylella	0.01	0.04	6.2
Neptunomonas	0.00	0.02	5.5
Pantoea	0.04	0.20	4.7
Sample	WR1 (%)	WR2 (%)	factor difference
undefined Pseudomonadaceae (family)	1.9	n.d.	

These identified variations between duplicates have no effect on the interpretation of the results and may still be an effect mainly of the sample type (not homogenous) or sampling method. Any significant differences between samples that is mentioned in this report can be attributed to the differences in microbial biodiversity or sampling method and not variations in the analysis method itself.

4. Summary of main observations

- The sampling method has a great effect on the microbial biodiversity identified in the samples. The samples taken with the regular method show a great dominance of a small number of (mainly nitrifying) microbial genera. The samples taken with the new method show a more biodiverse composition of microbial genera.
- For the samples taken with the new (N) method: The measuring well seem more anaerobic than the warm well. The Warm is mainly dominated by aerobic, or facultatively anaerobic (such as nitrate reducing or iron reducing) microbial genera. The Measuring well is mainly dominated by strictly anaerobic microbial genera such as methanogens and sulphate reducing bacteria.
- For the samples taken with the regular (Reg) method: The differences between the two samples (MP and W) are not as clear and in general they both appear to contain mainly aerobic or facultatively anaerobic microbial genera. The presence of some dominant strictly anaerobic genera in the MP well indicates that the sample may not be homogenous (e.g. be of sediment or biofilm).
- The comparison of the samples taken with the regular method from 2019 and 2021 seem to indicate that mostly strictly anaerobic microbial genera are no longer dominant in the samples of 2021.
- The duplicate samples demonstrate that the analysis method (sample to result) is consistent and that differences observed are owing to changes in biodiversity or the sampling method and not the analysis method.

BIJLAGE A. ORVidecode analysis certificate (Dutch)